



**Universitat de les  
Illes Balears**

**Instituto Mediterráneo de Estudios Avanzados  
IMEDEA (CSIC-UIB)**

Departamento de Ecología y Recursos Marinos  
Departamento de Tecnologías Marinas, Oceanografía Operacional y  
Sostenibilidad

---

# **Wave hydrodynamic effects on marine macrophytes**

**Tesis Doctoral**

---

Memoria presentada para optar al título de doctor  
Departamento de Biología  
Universitat de les Illes Balears

por

**Eduardo Infantes Oanes**

Directores:

**Dr. Jorge Terrados Muñoz Dr. Alejandro Orfila Förster**

Ponente:

**Dr. Misericòrdia Ramón Juanpere**

Universitat de les Illes Balears, 2011



To my parents and family...



# Abstract

This doctoral Thesis was developed to explore interactions between benthic marine macrophytes, substratum type and fluid dynamics. Quantitative knowledge as well as a predictive capacity is obtained to estimate the presence of a seagrass meadow, two species of invasive macroalgae and two species of seagrass seedlings in response to near-bottom orbital velocities, drag forces, root anchoring capacity and substratum type. Additionally, the effect of a seagrass meadow on wave propagation under natural conditions is also evaluated. In order to get a deeper knowledge on these processes, data from different sources such as numerical models, aerial photographs, field experiments and flume measurements are combined.

Light and temperature are considered as the main determinants for the spatial distribution of marine macrophytes but hydrodynamic conditions and substratum type are also key factors limiting the distribution of marine vegetation. Wave hydrodynamic effects on macrophytes have been studied in three ways: i) The near-bottom orbital velocities that set the upper limit of a *Posidonia oceanica* seagrass meadow are obtained by correlating hydrodynamics and the spatial distribution of the meadow. ii) The role of hydrodynamics in the establishment of *P. oceanica* and *Cymodocea nodosa* seagrass seedlings is evaluated. Drag forces and root anchoring capacity of seedlings are studied in a biological flume while seedling survival is addressed under natural conditions. iii) Substratum type plays an important role on the spatial settlement and distribution of marine macrophytes. Substratum cover of the invasive macroalgae *Caulerpa taxifolia* and *Caulerpa racemosa* indicates that these species are more abundant in rocks with photophilic algae and in the dead matte of seagrass *P. oceanica* than in sand or inside the *P. oceanica* meadow. Correlative evidence shows that *C. taxifolia* and *C. racemosa* tolerate near-bottom orbital velocities below 15 cm s<sup>-1</sup> and that *C. taxifolia* cover declines at velocities above that value.

Wave damping induced by a seagrass meadow of *P. oceanica* is evaluated under natural conditions using data from bottom mounted acoustic doppler velocimeters. The bottom roughness is calculated for the meadow as 0.42 m using flow velocities above the seagrass. Wave friction factor has been related to the drag coefficient on the plant and obtained for two storms so as to compute the damping along a transect. Drag coefficient values ranged from 0.1 to 0.4 during both storms. The expected wave decay coefficient for different seagrass shoot densities and leaf lengths are also predicted.

A relation between fluid dynamics and benthic macrophytes is shown. High near-bottom orbital velocities have an effect on the spatial distribution, growth and colonisation processes of seagrass and macroalgae species. The influence of a seagrass meadow on wave propagation is also apparent, with potential impact on sediment stability and coastal erosion. Predicted and measured quantitative results are provided such as near-bottom orbital velocities and drag coefficients that could be tested and compared to other benthic marine macrophytes species on other locations.

This Thesis is in the intersection between Ecology and Fluid dynamics a research area characterized by strong nonlinear interactions. To get a deep insight on the processes involved a bench of mathematical tools are used in order to apply physical principles to understand and predict the behaviour of marine macrophytes in the Mediterranean Sea. Besides, experiments to validate the theories have been developed under both controlled and natural conditions.

# Resumen

Esta Tesis doctoral ha sido desarrollada para entender las interacciones entre el oleaje, los macrófitos bentónicos marinos y el tipo de sustrato. Se han obtenido datos cuantitativos y predicciones para estimar la presencia de una pradera de fanerógamas marinas, dos especies de macroalgas invasoras y dos especies de fanerógamas. Estas especies han sido relacionadas con las velocidades orbitales en el fondo, las fuerzas de resistencia, la capacidad de anclaje de las raíces y el tipo de sustrato. Además, se ha evaluado el efecto de una pradera de fanerógamas en la propagación del oleaje en condiciones naturales. Con el fin de obtener un conocimiento más profundo de estos procesos, se han combinado datos de diferentes fuentes tales como modelos numéricos, fotografías aéreas, experimentos de campo y medidas en canal de ensayo.

La luz y la temperatura están considerados como los principales determinantes de la distribución espacial de macrófitos marinos, pero las condiciones hidrodinámicas y el tipo de sustrato son también factores clave que limitan la distribución de la vegetación marina. Los efectos del oleaje en la distribución espacial de macrófitos se han estudiado de tres formas. i) La velocidad orbital en el fondo que establece el límite superior de una pradera de la fanerógama marina *Posidonia oceanica*. ii) Se han evaluado los efectos del hidrodinamismo en el establecimiento de plántulas de *P. oceanica* y *Cymodocea nodosa*. Las fuerzas de resistencia y la capacidad de anclaje de las raíces de las plántulas se han medido en un canal de ensayos, mientras que la supervivencia de plántulas se ha estudiado en condiciones naturales. iii) El tipo de sustrato juega un papel importante en la colonización y en la distribución espacial de los macrófitos. La cobertura del tipo de sustrato que colonizan las macroalgas invasoras *Caulerpa taxifolia* y *Caulerpa racemosa* indica que estas especies son más abundantes en rocas con algas fotófilas y en la mata muerta de *P. oceanica* que en arena o en el interior de praderas de *P. oceanica*. Los datos experimentales confirmaron que

la cobertura de ambas macroalgas es mayor sobre mata muerta de *P. oceanica* que sobre arena.

La atenuación del oleaje inducida por una pradera de *P. oceanica* en condiciones naturales se ha estudiado utilizando velocímetros acústicos doppler fondeados en la pradera. Se ha calculado la rugosidad de la pradera utilizando velocidades de flujo por encima del dosel folial. El factor de fricción se ha relacionado con el coeficiente de resistencia durante dos tormentas con el fin de calcular la atenuación del oleaje. Los coeficientes de resistencia varían desde 0.1 hasta 0.4 en ambas tormentas. Se han realizado predicciones de los coeficientes de atenuación de onda esperados para diferentes densidades de plantas y longitudes de hojas.

Las altas velocidades orbitales en el fondo tienen un efecto sobre los procesos de distribución espacial, el crecimiento y la colonización de fanerógamas y macroalgas. La influencia de una pradera de *P. oceanica* en la propagación del oleaje es también evidente, con un impacto potencial sobre la estabilidad de los sedimentos y la erosión costera. Las predicciones y los resultados cuantitativos obtenidos de las velocidades orbitales en el fondo y los coeficientes de resistencia, pueden ser testados y comparados con otras especies de macrófitos bentónicos en otros lugares.

Esta Tesis se encuentra en la intersección entre la ecología y la dinámica de fluidos, un área de investigación que se caracteriza por fuertes interacciones no lineales. Para profundizar en los procesos hidrodinámicos se utilizan un abanico de herramientas matemáticas con el fin de aplicar los principios físicos para comprender y predecir el comportamiento de los macrófitos marinos en el Mar Mediterráneo. Además, los experimentos para validar las hipótesis de estudio se han desarrollado tanto en condiciones controladas como naturales.



# Acknowledgements

Foremost, I would like to thank my parents and family who always supported me with love and care during good and difficult moments. I also deeply thank them for always giving me the education that they thought was best. I hope to do as well with my children as they did with me.

I would like to thank the support of my two Ph.D advisors Dr. Jorge Terrados Muñoz and Dr. Alejandro Orfila Förster for motivating me from the beginning. Thanks for their always availability to discuss, comment and solve problems with a constructive feedbacks over the last years. To Jorge, for introducing me into the amazing world of seagrass ecology, showing me the importance of scientific knowledge and experimental design to understand the marine ecosystem. I will remember the conversations over hundreds of SCUBA-dives and during field trips. To Alejandro, for showing me the importance of coastal dynamics and for his patience in teaching me the numerical aspects of fluid dynamics. Thanks for the time you spent answering all my questions, and pushing me towards the end of the Thesis, thanks for your continuous support, great advice and friendship.

Thanks to the Ministerio de Educación y Ciencia for the FPI grant BES2006-12850 linked to the project CTM2005-01434 for giving me funding for the PhD work, but specially for giving me the opportunity to visit other Universities and research institutes such as the Massachusetts Institute of Technology (USA), the Netherlands Institute voor Ecologie (Netherlands) and the Horn Point Laboratory (USA). These visits opened the opportunity for collaborations and future working perspectives.

Thanks to Professor Heidi Nepf and Mitul Luhar for hosting me at the Massachusetts Institute of Technology (MIT), Boston, US. Heidi great expertise and

wave flume let me look in detail at hydrodynamical effects of seagrasses on the waves and currents where I became interested in wave attenuation caused by seagrasses. It was inspiring to compare my field-base knowledge with a model-base perspective. During my visit to the MIT Mitul became interested in working with seagrass in the field and he came to Mallorca to work on wave attenuation in the field with the seagrass *Posidonia oceanica*.

Thanks to Dr. Tjeerd Bouma for hosting me at the Nederlands Institute voor Ecologie, (NIOO). Tjeerd ideas, endless energy and always great advice contributed to my interest in drag forces under unidirectional and oscillatory flows as well as to root anchoring capacity of seedlings and sediment erosion. The excellent biological flume at the NIOO let me work with seedlings of *Posidonia oceanica* and *Cymodocea nodosa*.

Thanks to Professor Evamaria Koch and Dale Booth for hosting me at the Maryland Environmental Center, Horn Point Laboratory (USA). Evamaria shared with me her enthusiasm and expertise in seagrass research linking seagrass, hydrodynamic and sediment. Thanks to Dale for her great hospitality during the three months and for showing excellent logistics and organisation skills during field trips.

Thanks to my working colleagues Francisco Medina-Pons, Ines Castejón Silvo, Fiona Tomas Nash and Marta Domínguez for sharing their time helping setting field experiment using SCUBA and for the good moments shared outside work. Other people that I would like to express my gratitude and support during these years are Pablo Fernández Méndez, Francisco Sancha Bermejo and Constanza Celedón Neghme. Thanks to my flatmates Albert Fernández Chacón, Patricia Puertas, Ylva Olsen, Susana Chamorro, Lorena Basso and Mikko Vihatakari who make my life happier after work.

I would like to thank Puertos del Estado for the HIPOCAS and WANA wave climate data. To the Marina of Cala D'Or (Santanyi), Club Náutico de S'Arenal and Club Náutico de Cala Bona which kindly made available its harbour facilities for executing the field work.

Eduardo Infantes Oanes

# Contents

<b>Abstract</b>	<b>v</b>
<b>Resumen</b>	<b>vii</b>
<b>Acknowledgements</b>	<b>ix</b>
<b>Contents</b>	<b>xi</b>
<b>List of Figures</b>	<b>xv</b>
<b>List of Tables</b>	<b>xxi</b>
<b>List of Symbols</b>	<b>xxiii</b>
<b>1 Introduction</b>	<b>1</b>
1.1 Upper limit distribution of macrophytes . . . . .	4
1.2 Hydrodynamics and seedling survival . . . . .	5
1.3 Substratum type and invasive species . . . . .	7
1.4 Wave damping by macrophytes . . . . .	8
1.5 Aims and motivations . . . . .	9
<b>2 Wave energy and the upper depth limit of <i>P. oceanica</i></b>	<b>13</b>
2.1 Summary . . . . .	13
2.2 Material and methods . . . . .	14
2.2.1 Study Area and Regional Settings . . . . .	14
2.2.2 HIPOCAS database (1958 - 2001) and deep water wave characterization . . . . .	15
2.2.3 Shallow-water wave conditions . . . . .	17
2.2.4 Bottom typology and bathymetry . . . . .	18

2.3	Results . . . . .	19
2.4	Discussion . . . . .	22
<b>3</b>	<b>Seedling tolerance to wave exposure</b>	<b>27</b>
3.1	Summary . . . . .	27
3.2	Methods . . . . .	28
3.2.1	Drag forces and drag coefficient . . . . .	28
3.2.2	Critical erosion depth and minimum rooting length . . . . .	30
3.2.3	Field study . . . . .	31
3.2.4	Statistical analysis . . . . .	33
3.3	Results . . . . .	34
3.4	Discussion . . . . .	39
<b>4</b>	<b>Substratum effect on invasive <i>Caulerpa</i> species</b>	<b>45</b>
4.1	Summary . . . . .	45
4.2	Methods . . . . .	46
4.2.1	Study Sites . . . . .	46
4.2.2	Presence of <i>Caulerpa</i> over different substrata . . . . .	46
4.2.3	Short-term experiment evaluating substratum effect on <i>Caulerpa</i> persistence . . . . .	47
4.2.4	Wave climate and modelling at the short-term experimen- tal sites . . . . .	49
4.2.5	Field wave measurements and velocity profiles . . . . .	50
4.2.6	Statistical Analysis . . . . .	51
4.3	Results . . . . .	52
4.4	Discussion . . . . .	56
<b>5</b>	<b>Effect of a seagrass meadow on wave propagation</b>	<b>63</b>
5.1	Summary . . . . .	63
5.2	Theory . . . . .	64
5.3	Material and Methods . . . . .	67
5.3.1	Determination of Nikuradse roughness length . . . . .	69
5.3.2	Determination of drag coefficient . . . . .	71
5.4	Results . . . . .	71
5.5	Discussion . . . . .	75
<b>6</b>	<b>General discussion and conclusions</b>	<b>81</b>
<b>7</b>	<b>Recomendations for future work</b>	<b>87</b>

<b>A Background review on fluid dynamics</b>	<b>89</b>
A.1 Waves . . . . .	89
A.2 Wave propagation . . . . .	93
A.3 Boundary Layers . . . . .	94
<b>Bibliography</b>	<b>97</b>
<b>Curriculum Vitae</b>	<b>113</b>



# List of Figures

1.1	Schematic diagram of the approach presented. . . . .	10
2.1	(a) Location of Mallorca in the Mediterranean Sea. (b) Location of the study area of Cala Millor in Majorca. The asterisk (*) indicates HIPOCAS node 1433. (c) Bathymetry of Cala Millor with isobaths (in meters). . . . .	15
2.2	Directional wave histogram for HIPOCAS node 1433 10 km from Cala Millor . . . . .	16
2.3	Bottom typology off Cala Millor (Mallorca, western Mediterranean Sea). . . . .	20
2.4	(a) Distribution of wave heights (m) at the beach derived from mean wave conditions ( $11.25^\circ$ , $H_m = 1.53$ m, $T_p = 7.30$ s). (b) Distribution of near-bottom orbital velocities ( $u_b$ , $\text{m s}^{-1}$ ) at the beach and cover of the <i>P. oceanica</i> meadow (gray) and dead rhizomes (dark gray). . . . .	22
2.5	Percent coverage of the different bottom types in each of the near-bottom orbital velocity ( $u_b$ ) intervals established in Cala Millor. . . . .	23
2.6	Mean near-bottom orbital velocity above each bottom type in Cala Millor. Different capital letters indicate significant differences between bottom types (post-hoc multiple pairwise comparison of mean ranks, $p < 0.05$ ). Error bars show 95 % confidence intervals. n-values indicate the number of points selected randomly in each bottom type. Differences in n-values between bottom types are driven by the differences in percentage covers of each bottom type in the study area. . . . .	23

3.1	Sketch of the flume experimental set-up showing the critical erosion depth and minimum rooting length ( $L_d$ ) of seedlings. (a) Seedling in the flume, (b) seedling before dislodging from the sediment after the discs addition. Critical erosion depth is equivalent to the total height of discs added when the seedling is dislodged. Not drawn to scale . . . . .	30
3.2	(a) Location of Mallorca Island in the Mediterranean Sea. (b) Location of study area and WANA node. (c) Location of the experimental sites, Cap Enderrocat (triangles) and Cala Blava (circles). Bathymetric contours in meters. . . . .	32
3.3	Experimental plots with a) <i>Posidonia oceanica</i> and b) <i>Cymodocea nodosa</i> seedlings at the beginning of the field experiment. . . . .	32
3.4	Drag forces acting on seedlings in (a) unidirectional flow and (b) oscillatory flow. (mean, SE, $n = 5$ ). . . . .	34
3.5	Drag forces acting on individual seedlings of different surface area in (a) unidirectional flow and (b) oscillatory flow. Flow velocity of $16 \text{ cm s}^{-1}$ . . . . .	35
3.6	Drag coefficient versus Reynolds number for <i>Posidonia oceanica</i> and <i>Cymodocea nodosa</i> under unidirectional and oscillatory flow. Experimental data under uniform flow for <i>P. oceanica</i> seedlings (triangles) and for <i>C. nodosa</i> (squares). For oscillatory flow <i>P. oceanica</i> seedlings (circles), and <i>C. nodosa</i> (crosses). Solid lines are the linear fitting for the different flow conditions. . . . .	36
3.7	(a) Critical erosion depth and (b) Minimum rooting length of <i>Posidonia oceanica</i> and <i>Cymodocea nodosa</i> exposed to two orbital velocities ( $u = 5$ and $10 \text{ cm s}^{-1}$ ). . . . .	38
3.8	Seedling survival on the experimental plots in Mallorca, August 2009 to February 2010. (a) <i>Posidonia oceanica</i> , (b) <i>Cymodocea nodosa</i> , and (c) wave heights in deep water (WANA node) shown in grey line and propagated wave heights in Cala Blava at 12 m depth shown in black line. Gaps in propagated $H_s$ corresponds to wave directions other than Southwest to Southeast no affecting the study area. . . . .	41



4.1	Location of the study areas. (a) Mallorca Island in the Mediterranean Sea. (b) Location of the four study areas and deep water wave data (WANA nodes). (c) Bathymetry of Cala D'Or with location of WANA node. (d) Bathymetry of Sant Elm. Experimental plots, WANA nodes and ADCP location in Cala D'Or. . . . .	47
4.2	Photographs of the experimental set up for <i>Caulerpa taxifolia</i> in (a) natural sandy bottom and (b) the model of dead matte of the seagrass <i>Posidonia oceanica</i> . (c) Illustration of <i>Caulerpa</i> fragments fixed to the plots using pickets. . . . .	48
4.3	Percent cover of (a) <i>Caulerpa taxifolia</i> and (b) <i>Caulerpa racemosa</i> in the different types of substratum during two consecutive years. . . . .	53
4.4	Relative frequency of total substratum surveyed and of the presence of <i>Caulerpa taxifolia</i> and <i>Caulerpa racemosa</i> on each substratum. Low presence of rocks was recorded at the <i>C. taxifolia</i> site. Rocky bottom with photophilic algae is indicated as Rocks. . . . .	54
4.5	(a) <i>Caulerpa taxifolia</i> cover (normalised means $\pm$ SE, $n = 3$ ). (b) Water temperature at the experimental site, hours of light per day and near-bottom orbital velocities, $u_b$ (means $\pm$ SD). Cover area on each sampling date (A) in $\text{cm}^2$ normalised by initial cover area (A0). Dotted square indicates the period used for the statistical analysis ANOVA, Table 4.3. . . . .	57
4.6	(a) <i>Caulerpa racemosa</i> cover (normalised means $\pm$ SE, $n = 3$ ). (b) Water temperature at the experimental site, hours of light per day and near-bottom orbital velocities, $u_b$ (means $\pm$ SD). Cover area on each sampling date (A) in $\text{cm}^2$ normalised by initial cover area (A0). . . . .	58
4.7	Vertical profiles of velocity (means $\pm$ 95 % CL). For convenience only the 40 cm above the bottom is shown. . . . .	59
5.1	(a) Location of Mallorca Island in the Mediterranean Sea. (b) Location of the study area. (c) Location of the transect and deployment sites in Cala Millor. (d) Bathymetric profile and distance between the deployment sites. . . . .	68
5.2	Acoustic doppler velocimeter (ADV) deployed in the <i>Posidonia oceanica</i> seagrass meadow. . . . .	69

5.3	Top panel: Significant wave height at 16.5 m depth (solid), at 12.5 m depth (dotted), at 10 m depth (dash-dotted) and at 6.5 m depth (dashed). Grey areas indicate the three storms. Bottom panel: near bottom orbital velocities at the same locations (depths and lines are the same as the top panel). . . . .	70
5.4	Normalized significant wave height (by incident) along nondimensional distance (by wave length) for the first storm. The first panel corresponds to conditions on July 13th at 4am and sequence are elapsed 2 hours. The solid black line displays the computed normalized significant wave height including the dissipation due to <i>P. oceanica</i> meadow. The grey line corresponds to the $H_s$ assuming no dissipation by the seagrass. Dashed lines displays the predictions for wave decay for a 15 % error in the measurement of initial wave height and wave period. . . . .	73
5.5	Normalized significant wave height (by incident) along nondimensional distance (by wavelength) for the second storm. The first panel correspond to conditions on July 18th at 12am and sequence are elapsed 2 hours. The solid black line displays the computed normalized significant wave height including the dissipation due to <i>P. oceanica</i> meadow. The grey line corresponds to the $H_s$ assuming no dissipation by the seagrass. Dashed lines displays the predictions for wave decay for a 15 % error in the measurement of initial wave height and wave period. . . . .	74
5.6	Wave damping $H/H_0$ along the transect for different conditions of shoot density. Initial wave height is $H_{s,0} = 1.56$ m, $\omega = 1.38$ s <sup>-1</sup> and $C_D = 0.41$ . . . . .	75
5.7	Decay coefficient ( $K_d$ ) versus seagrass shoot density (N) and leaf length ( $l_v$ ) for an incident wave $H_{s,0} = 1.56$ m, $\omega = 1.38$ s <sup>-1</sup> and $C_D = 0.41$ propagating over constant depth $h = 5$ m (top), $h = 10$ m (middle) and $h = 15$ m (bottom). Units in m <sup>-2</sup> . . . . .	76
5.8	Drag coefficient versus Keulegan-Carpenter number for experimental data -crosses-, for Sánchez-González et al. (2011) -black solid-, Kobayashi et al. (1993) -black dashed- and for Méndez and Losada (2004) -grey-. . . . .	78
A.1	Diagram of a shoaling wave approaching to shore. Variable names are defined in the text. . . . .	91
A.2	Relative depth and asymptotes to hyperbolic functions. . . . .	92

A.3 Vertical profile of velocity. Top, weak currents (black line) and fast currents (dashed line). Bottom, velocity reduction due to benthic macrophytes. . . . . 95



# List of Tables

2.1	Percent cover of bottom type at different depths. The total area of coverage of each bottom type is presented in the last row. . . .	21
3.1	Two-factor way ANOVA testing differences between species and orbital velocities and minimum rooting length. Significant differences are expressed in bold as, *** $p < 0.001$ , and ns = not significant. Cochran's C-test no significant. df = degrees of freedom and MS = mean square. . . . .	37
3.2	Morphological characteristics of seedlings at the beginning of the field experiment (mean $\pm$ SE, n = 144). . . . .	37
3.3	Computed near-bottom orbital velocities (cm s <sup>-1</sup> ) at the experimental locations during the sampling periods (mean $\pm$ SD). . . .	39
3.4	Results of three-factor way ANOVA of seedling survival percentage in October 2009. Significant differences are expressed in bold as ** $p < 0.01$ , *** $p < 0.001$ , and (ns) not significant. Cochran's C-test no significant. df = degrees of freedom and MS = mean square . . . . .	40
4.1	Wave heights from model outputs and field measurements in Cala D'Or (means $\pm$ 95 % CL). . . . .	50
4.2	Chi-square ( $\chi^2$ ) test of observed <i>Caulerpa</i> cover on different substrata. <i>Caulerpa taxifolia</i> has a critical $\chi^2$ $p=0.001^{***}$ , 2df = 13.81 and <i>Caulerpa racemosa</i> has a critical $\chi^2$ $p=0.001^{***}$ , 3df = 16.26. <i>C. taxifolia</i> was not found on rock substratum in enough quantities for the test. The type of contribution was classified as more than expected (M) or less than expected (L). . . . .	55

4.3 Results of repeated measures of ANOVA performed to evaluate if the cover of *Caulerpa taxifolia* and *Caulerpa racemosa* was different between a model of dead matte of *Posidonia oceanica* and a sandy substratum. \*p < 0.05, \*\*\*p < 0.001, ns = not significant. Cochran tests were not significant. . . . . 56

# List of Symbols

$a$	=	wave amplitude
$a_b$	=	orbital wave excursion
$a_v$	=	plant surface area
$a'_v$	=	plant surface area per unit height
$c_g$	=	group velocity
$C_D$	=	drag coefficient
$E$	=	wave energy
$F_x$	=	force acting on the plant
$f_w$	=	wave friction factor
$g$	=	acceleration of gravity
$h$	=	water depth
$H_s$	=	significant wave height
$H_{s,0}$	=	incident significant wave height
$k$	=	wave number
$k_s$	=	bottom roughness
$K_d$	=	wave decay coefficient
$L$	=	wave length
$L_d$	=	minimum rooting length
$l_v$	=	vegetation length
$l_*$	=	characteristic length
$N$	=	number of shoots per unit area
$Re$	=	Reynolds number
$T_p$	=	wave peak period
$u$	=	fluid velocity
$u_b$	=	near-bottom orbital velocity
$u_c$	=	characteristic velocity outside of the boundary layer
$x$	=	horizontal distance
$\varepsilon$	=	relative roughness

$\epsilon =$	non linear parameter
$\epsilon_D =$	rate of energy dissipation
$\delta =$	boundary layer
$\rho =$	seawater density
$\tau_b =$	bottom shear stress
$\Theta =$	wave direction
$\nu =$	kinematic viscosity of water
$\nu_T =$	eddy viscosity
$\omega =$	wave angular frequency



# Chapter 1

## Introduction

Coastal marine ecosystems are home to a host of different species ranging from microscopic planktonic organisms that comprise the base of the marine food web (i.e., phytoplankton and zooplankton) to large marine mammals like whales. Coastal habitats alone account for approximately 1/3 of all marine biological productivity and those dominated by macrophytes (salt marshes, seagrasses, mangrove forests) are among the most productive regions on the planet. Coastal zones provide humans with a wide variety of goods and services including foods, recreational opportunities, and transportation corridors. Despite the importance of marine ecosystems, increased human activities such as overfishing, coastal development, pollution, and the introduction of invasive species have caused significant damage and pose a serious threat to marine biodiversity.

Coastal zones are continually changing because of the dynamic interaction between the oceans and the land. Waves, currents and winds along the coast are both eroding rock and depositing sediment on a continuous basis, and rates of erosion and deposition vary considerably from day to day along such zones. Other sediment inputs in the coastal zone are from river runoffs, glaciers and the inorganic remains of dead organisms. The energy reaching the coast can become high during storms, and such high energies make coastal zones areas of continuous morphological evolution (Gómez-Pujol et al. 2011).

The shallow areas of the coastal zone (from 0 m to  $\sim 50$  m depth) are inhabited by benthic marine macrophytes. Macrophytes are large aquatic plants that grow in/or near water and are either emergent, submergent, or floating

namely mangroves, marshes, seagrasses and macroalgae. These aquatic plants play an important role in coastal environments providing many ecological services (Costanza et al. 1997). Macrophytes are primary producers that supply oxygen and food, stabilize the seabed, provide nursery grounds, attenuate wave heights and current velocities preventing coastal erosion.

Since water is the medium in which macrophytes exist, any physical disturbance of it would be expected to influence them. Benthic macrophytes in nature are exposed to fluid motion where inertial forces are more important than viscous forces. Hydrodynamics affects almost all biological and chemical processes of macrophytes along their entire life cycle in many different ways such as spatial distribution (Frederiksen et al. 2004), nutrient uptake (Thomas et al. 2000, Cornelisen and Thomas 2004), pollen dispersion (Ackerman 1986), seed and seedlings transport (Koch et al. 2010), seedling survival (Rivers et al. 2011), etc. Hydrodynamics also drives sediment dynamics causing macrophytes to become buried or eroded during storm events (Fonseca et al. 1996, Cabaco et al. 2008). On the other hand, macrophytes are a source of drag which reduces flow velocities along the portion of the water column where vegetation it is present (Nepf and Vivoni 2002, Luhar et al. 2010). The presence of macrophytes reduces sediment re-suspension in the water column (Ward et al. 1984, Short and Short 1984, Terrados and Duarte 2000, Gacia and Duarte 2001). Macrophytes have also shown to attenuate waves under laboratory (Fonseca and Cahalan 1996, Méndez and Losada 2004, Bouma et al. 2010) and natural conditions (Newell and Koch 2004, Bradley and Houser 2009).

Wave energy can have both positive and negative impacts on seagrass physiology, productivity and distribution. The periodic motion of the blades may enhance the water exchange between the seagrass meadow and overlying water column (Koch and Gust 1999). Nutrient uptake is enhanced in a seagrass meadow during wave conditions (Thomas and Cornelisen 2003). Stevens and Hurd (1997) suggest that the enhanced water flux derives from a periodic stripping of the diffusive boundary layer by the wave motion. Wave-induced motion can also detach epiphytes from seagrass blades (Kendrick and Burt 1997). Waves can also have a negative effect on seagrass communities, by mobilizing sediment that can bury, erode and dislodge plant fragments (Marbà and Duarte 1994, Paling et al. 2003, Frederiksen et al. 2004). Because of these negative influences, the spatial distribution of wave energy is believed to control, at least in

---

part, the spatial distribution of seagrasses (Koch and Beer 1996, Koch 2001, Frederiksen et al. 2004, Koch et al. 2006).

Some macrophytes populations show extensive spatial and temporal fluctuations and landscapes are under continuous transformation due to disturbances (Fonseca and Bell 1998). Physical disturbances are considered one of the main extrinsic factors controlling the spatial structure and species diversity of seagrass meadows (Clarke and Kirkman 1989, Duarte et al. 1997). Wind-generated wave dynamics and tidal currents create sediment movement, which may either bury plants, expose roots and rhizomes or during heavy storms even uproot entire plants (Kirkman and Kuo 1990, Preen et al. 1995). Depending on the degree of wave exposure, seagrass communities form characteristic landscapes ranging from highly fragmented to almost continuous meadows covering extensive areas (Frederiksen et al. 2004). In sheltered areas with calm hydrodynamic conditions, seagrass patches have been observed to be predominantly circular, while if the area is exposed to wave action and tidal currents, seagrass patches are more elongated (Den Hartog 1971). These patterns are not only present in seagrass communities but also on some coral reefs, freshwater plants and mussels (Den Hartog 1971).

When a seagrass meadow is disturbed, gaps are formed presenting new unoccupied sites that are potentially available for colonization. These new sites encompass several substrata including rock, sand and dead matte. Seagrass seedlings and invasive macroalgae are known to colonize these areas depending on the substratum type (Balestri et al. 1998, Hill et al. 1998, Rivers et al. 2011). Assuming that physical dislodgement is the primary mechanism for macrophytes failure, a favourable area would be one that reduces physical disturbance or enhances anchoring ability. Also, macrophytes morphology and rooting capacity will determine their success during physical disturbances. Despite all these evidences, to date there has been little effort to correlate wave and current energy with the spatial distribution and growth of seagrass meadows, seagrass seedlings and invasive macroalgae.

Gaps in knowledge of marine macrophytes are to date still evident. For instance, the effects of wave energy on the distribution at a landscape scale of plants in many cases are based on qualitative evidence. Besides, the tolerance of seedlings to wave energy and the capacity of seedlings to colonise a specific

---

coastal environment are very scarce. The importance of the Mediterranean seagrass *P. oceanica* on coastal protection as well as a reservoir of biogenic sediments has not been established quantitatively. In this Thesis, it is investigated the interaction between the wave induced hydrodynamics and some of the above mentioned points.

## 1.1 Upper limit distribution of macrophytes

The study of the light requirements for macrophytes growth has been a major focus of research in marine ecology and different quantitative models provide predictions of the lower depth limit of the distribution of seagrasses (Dennison 1985, Dennison 1987, Duarte 1991, Kenworthy and Fonseca 1996, Koch and Beer 1996, Greve and Krause-Jensen 2005). Seagrasses can thrive up to depths where the irradiance at the top of the leaf canopy is higher than 11 % of surface irradiance (Duarte 1991) or where the number of hours with values of irradiance higher than those that saturate the photosynthesis rate is higher than 6-8 hours (Dennison 1985). The upper depth limit of distribution of seagrasses has been related to their tolerance to desiccation at low tide (Koch and Beer 1996) and to ice scour (Robertson and Mann 1984). In seas with low tidal range and no ice formation like the Mediterranean, the upper depth limit of seagrasses will be determined mainly by their tolerance to wave energy (Koch et al. 2006). However, quantitative estimates of the wave energy that sets the upper depth limit of seagrasses are to date still scarce.

Conceptual models have been proposed to explain the differences in shape, bottom relief, and cover of seagrass meadows (Fonseca et al. 1983, Fonseca and Kenworthy 1987) or the depth distribution of intertidal seagrass (van Katwijk et al. 2000) as a function of wave energy and/or current velocity. Local hydrodynamics (indirectly estimated from the weight loss of clod cards) has been related to depth and seagrass presence and used to identify the habitat requirements of South Australian seagrass species (Shepherd and Womersley 1981). Keddy (1984) developed a relative wave exposure index (REI) in order to quantify the degree of wave exposure by using wind speed, direction and fetch measurements. REI values have been correlated to different attributes of seagrass meadows such as the content of silt-clay and organic matter of the sediment, seagrass cover, shoot density (Fonseca and Bell 1998, Fonseca 2002, Krause-Jensen 2003, Frederiksen et al. 2004) and biomass (Hovel 2002). Shallow seagrass popula-

---

tions tend to be spatially more fragmented in wave-exposed environments than in wave-sheltered ones (Fonseca and Bell 1998, Frederiksen et al. 2004) and temporal changes of seagrass cover are also higher at the most wave-exposed sites (Frederiksen et al. 2004). Plaster clod cards and REI provide only semi-quantitative idiosyncratic estimates of current and/or wave energy and, therefore, comparison between studies is difficult. Additionally, REI estimates do not consider the influence of depth on wave damping (but see van Katwijk and Hermus 2000). Direct quantitative measurements of the energy of waves and currents impinging on seagrasses are necessary to elucidate its effects on them, to identify their habitat requirements, to predict their spatial distribution and their response to both natural (i.e., storms, hurricanes, etc) and anthropogenic (i.e., dredging and beach nourishment, coastal development, etc) disturbances.

*Posidonia oceanica* (L.) Delile, an endemic seagrass species of the Mediterranean Sea, grows between the depths of 0.5 m and 45 m (Procaccini et al. 2003) and covers an estimated surface area between 2.5 and 5 million hectares, about 1-2 % of the 0-50 m depth zone (Pasqualini et al. 1998). *P. oceanica* is included in the Red List of marine threatened species of the Mediterranean (Boudouresque et al. 1990) and meadows are defined as priority natural habitats on the EC Directive 92/43/EEC on the Conservation of Natural Habitats and of Wild Fauna and Flora (EEC, 1992). Fundamental knowledge of these seagrasses species in nature is required to understand their interactions with hydrodynamics such as the maximum flow velocities that are able to stand. Some studies have look at the effect of *P. oceanica* on flow and the horizontal spatial distribution of plants with depth (Granata et al. 2001) but little is known about the influence of hydrodynamics on *P. oceanica* distribution.

## 1.2 Hydrodynamics and seedling survival

Seagrass seedlings are the elements that form new meadows and their survival in nature contributes to seagrass population dynamics. Reproduction strategies of seagrasses are diverse, for example buoyant fruits of *P. oceanica* will be dispersed by wind and currents while *C. nodosa* fruits will remain buried next to the parent plants (Orth et al. 2006). Waves and currents can strongly influence the spatial distribution of meadows (Fonseca and Bell 1998, Frederiksen et al. 2004), suggesting that hydrodynamics may be also important for seed dispersal

---

and seedling establishment (Koch et al. 2010). Measurements showing higher seedling survival rates at deeper locations suggest the same (Piazzi et al. 1999). Moreover, it has been shown that hydrodynamics can directly affect the survival of seagrass seedlings transplants (van Katwijk and Hermus 2000, Rivers et al. 2011). The effect of waves and currents on seedling establishment is expected to be through sediment movement, as this can cause burial or dislodgment of small seagrass plants.

Seagrass capacity to withstand sediment burial is strongly dependent on size and morphology (Idestam-Almquist and Kautsky 1995, Cabaco et al. 2008). The effect of sediment erosion on survival could be determined by the root capacity to remain anchored to the substratum (Madsen et al. 2001). Hence, seedlings may be expected to be highly vulnerable to sediment movement compared to adult seagrasses, as seedling roots will penetrate less deeply into the sediment. Although the effect of sediment burial on seagrasses has been reviewed (Cabaco et al. 2008), to our knowledge, little work has been devoted to the effect of sediment dynamics, in particular the effect of sediment erosion and root anchoring capacity on seedling survival. In this Thesis this question is addressed for the two most common seagrass species in the Mediterranean Sea (Green and Short 2003) that both strongly declined during the 20th century (Boudouresque 2009): *Posidonia oceanica* and *Cymodocea nodosa*.

Both species have morphological differences that could affect their interaction with hydrodynamics and their survival capacity. *P. oceanica* leaves are longer and wider than *C. nodosa* leaves (Buia and Mazzella 1991, Guidetti 2002). These differences will affect the drag force exerted on the leaves and thus the anchoring capacity of the roots. Wicks et al. (2009) suggested that *Zostera marina* seedlings with the same root length but higher leaf area would have less chance to survive by being dislodged from the sediment than seedlings with lower leaf area. As *P. oceanica* has a higher total leaf surface area than *C. nodosa* (Guidetti 2002), the drag experienced on the leaves will be higher in *P. oceanica* than in *C. nodosa*. The assessment of the capacity of seedlings to remain anchored to the substrata under different hydrodynamic conditions is necessary to get a fundamental understanding of seedling survival in nature.

---

### 1.3 Substratum type and invasive species

Consolidated substrata (i.e., rocks) offer a stable, non-mobile surface where macroalgae and some seagrass species attach effectively. Unconsolidated substrata (i.e., sand, mud) are unstable, mobile and only seagrasses and macroalgae with root-like structures can colonize them. Waves and currents can mobilise sediment particles producing sediment erosion and accretion that may affect seagrasses negatively through uprooting and burial (Fonseca and Kenworthy 1987, Williams 1988, Terrados 1997, Cabaco et al. 2008). Thresholds of maximum wave energy tolerated by some seagrasses species have been determined (Fonseca and Bell 1998, van Katwijk and Hermus 2000, Koch 2001) as well as the relationship between wave exposure and temporal variability of seagrass coverage in shallow sands (Fonseca et al. 1983, Fonseca and Bell 1998, Frederiksen et al. 2004). In contrast, information about the wave energy levels that macroalgae tolerate is limited, especially in unconsolidated substrata (D'Amours and Scheibling 2007, Scheibling and Melady 2008).

Most marine macroalgae grow over consolidated substrata such as rocks or over other macrophytes but a few Chlorophyta species of the order Caulerpaales are also able to grow on unconsolidated substrata (Taylor 1960). The thallus of *Caulerpa* species is composed of a creeping portion, the stolon, that it is attached to the substrata by root-like structures, the rhizoids, and an erect portion, the fronds that have different shapes depending on the species (Taylor 1960, Bold and Wynne 1978). The rhizoids of *Caulerpa* are able to bind sediment particles (Chisholm and Moulin 2003) and anchor the plant in sandy sediments or other unconsolidated substrata, and to attach to rocks and other macrophytes (Taylor 1960, Meinesz and Hesse 1991, Klein and Verlaque 2008). Hence *Caulerpa* species may be present both in wave exposed, rocky bottoms and sheltered, sandy-muddy sediments (Thibaut et al. 2004).

Macroalgae have been introduced to non-native locations around the world through human activities including aquaculture, shellfish farming, aquariums, shipping (ballast water and hull fouling), fishing gear and as less-than-ideal immigrants (migration through the Suez Canal) (Ruíz et al. 2000). Decline of seagrass meadows within the Mediterranean Sea often results in the replacement of seagrasses by opportunistic green macroalgae of the *Caulerpa* family. *Caulerpa taxifolia* and *Caulerpa racemosa* have been introduced in the Mediterranean Sea within the last 25 years showing an invasive behaviour (Meinesz and Hesse 1991,

Boudouresque and Verlaque 2002, Klein and Verlaque 2008). Both *Caulerpa* species are strong competitors which tend to eliminate native species forming monospecific beds (Verlaque and Fritayre 1994, Piazzzi et al. 2001). *C. racemosa* is able to overgrow other macroalgal species, reaching virtually 100 % cover in invaded areas (Piazzzi et al. 2001, Balata et al. 2004).

Initial observations of *C. taxifolia* invasion suggested that rocks and dead matte of *P. oceanica* were appropriate for the establishment of this species but sandy or muddy sediments in sheltered conditions were also colonized by it (Hill et al. 1998). A short-term experiment showed that algal turfs were more favourable for the establishment of *C. taxifolia* and *C. racemosa* than other macroalgal communities on rocky bottoms (Ceccherelli et al. 2002). Both *Caulerpa* species seem to tolerate a certain level of sediment deposition and burial (Glasby et al. 2005, Piazzzi et al. 2005) a feature that likely facilitates their development in sandy sediments. Elucidation of the factors influencing the establishment and spread of introduced *Caulerpa* species is essential to identify benthic communities susceptible of being invaded and to have scientific tools to predict future invasions.

## 1.4 Wave damping by macrophytes

Submerged plants increase bottom roughness and extract momentum from water resulting in flow velocity reduction and less energy for sediment transport (Koch et al. 2006). In addition to the effect of leaf, canopies on water flow, seagrass rhizomes and roots extend inside sediment contribute to its stabilization (Fonseca 1996). Flume and in situ measurements have shown that water velocity is reduced inside seagrasses. In sparse canopies, turbulent stress remains elevated within the canopy while in dense canopies turbulent stress is reduced by canopy drag near the bed (Luhar et al. 2008). The reduction in velocity due to seagrass canopies is lower for wave-induced flows compared to unidirectional flows because the inertial term can be larger or comparable to the drag term in oscillatory flow (Lowe et al. 2005, Luhar et al. 2010). Except for intertidal systems, where currents are dominant, most seagrass meadows are in wave-dominated habitats. Interaction between seagrass canopies and oscillatory flow has been, however, much less studied than that with currents. Nearbed turbulence inside seagrass canopies are lower than those on sands under wave-generated oscillatory flows (Granata et al. 2001). Wave energy and sediment

---



resuspension are also reduced by seagrasses (Terrados and Duarte 2000, Verduin and Backhaus 2000, Gacia and Duarte 2001), but water exchange between inside and outside the canopy increases (Koch and Gust 1999).

Wave attenuation by macrophytes has been studied in the laboratory (Fonseca and Cahalan 1992, Kobayashi et al. 1993, Augustin et al. 2009), in the field (Knuston et al. 1982, Newell and Koch 2004, Bradley and Houser 2009), and using analytical methods or numerical models (Kobayashi et al. 1993, Méndez et al. 1999, Méndez and Losada 2004, Chen et al. 2007). Wave attenuation by seagrass canopies has been detected only in shallow systems where canopies occupy a large fraction of the water column (Fonseca and Cahalan 1992, Koch 1996, Chen et al. 2007, Bradley and Houser 2009). *Posidonia oceanica* is the dominant seagrass species in the Mediterranean Sea, where it forms extensive meadows in depths up to 45 m (Procaccini et al. 2003) and canopy occupies less than 20 % of water column height. Although commonly assumed (Luque and Templado 2004, Boudouresque et al. 2006), wave attenuation by *P. oceanica* meadows has never been accurately assessed in the field.

## 1.5 Aims and motivations

The aim of this Thesis is to obtain quantitative knowledge as well as a predictive capacity about the responses of seagrasses and macroalgae to near-bottom orbital velocities. First, the role of near-bottom orbital velocities on the spatial distribution of a *P. oceanica* meadow, and on the survival of *P. oceanica* and *C. nodosa* seedlings are evaluated. Second, the importance of substratum type and hydrodynamics on the distribution and persistence of two marine invasive macroalgae, *Caulerpa taxifolia* and *Caulerpa racemosa* is explored. Finally, the wave damping effect of a seagrass meadow of *P. oceanica* on wave propagation under natural conditions is quantified and a relationship between the wave friction factor which integrates the seagrass landscape and drag coefficient exerted on individual plants is derived.

The wave energy impinging on seagrass meadows is assessed in a pilot area and presented in Chapter 2. Following a methodology that combines numerical modelling and geographical information systems, GIS, (Fig. 1.1) a quantitative and testable relationship between wave energy and the upper depth limit

---

of the Mediterranean seagrass *P. oceanica* is obtained. Wave energy estimation is obtained by means of the analysis of forty-four years of wave data. We considered that long-term historical wave data, rather than present-day wave measurements, are more appropriate to link wave energy to the presence of *P. oceanica* given the low rates of vegetative growth and space occupation of this seagrass species (Marbà and Duarte 1998). Aerial photographs and bathymetric data are used for an accurate mapping of the meadow as well as to delimitate the upper depth limit of *P. oceanica*.

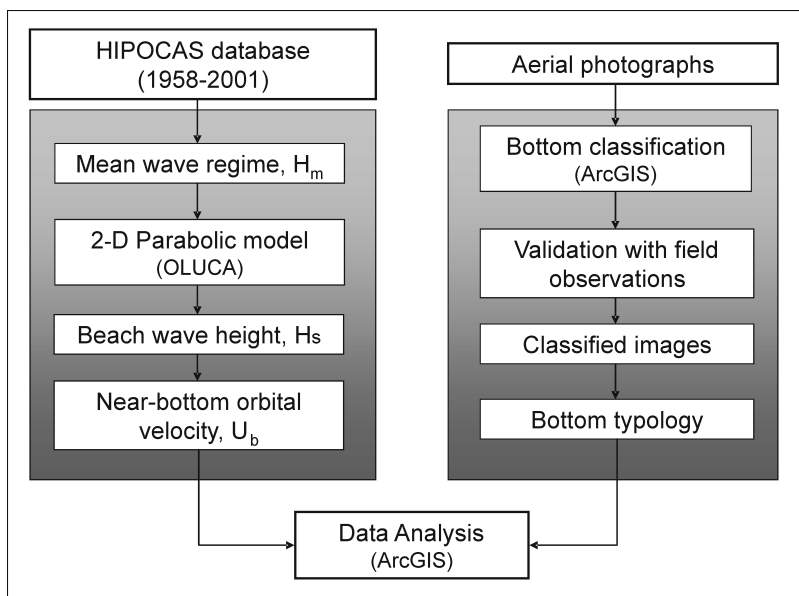


Figure 1.1: Schematic diagram of the approach presented.

The capacity of seedlings of *P. oceanica* and *C. nodosa* to remain anchored to the substrata under different hydrodynamic conditions is evaluated in Chapter 3. The underlying mechanisms that can affect seedling survival are studied in a biological flume. Drag measurements are carried out to obtain the effective drag forces acting on the seedlings and compute the drag coefficient under unidirectional and oscillatory flows. Further, the minimum root lengths necessary to remain anchored to the sediment are measured under different wave conditions on the flume. Additionally, a replicated short-term field experiment is carried out to compare the survival of seedlings at two depths (18 m and 12 m) to assess the effect of exposure to hydrodynamics on the survival of *P. oceanica* and *C.*

*nodosa* seedlings.

The effect of substratum on the persistence of two invasive *Caulerpa* species is evaluated in Chapter 4. First, the presence of *C. taxifolia* and *C. racemosa* is quantified in different types of substrata during two consecutive years testing if their presence was independent of the type of substratum. Then, a short-term experiment is performed where fragments of *C. taxifolia* and *C. racemosa* are established in a model of dead matte of *Posidonia oceanica* and in sand. The cover of both *Caulerpa* species is correlated to near-bottom orbital velocities and friction coefficients over sand and the model dead matte are computed.

The effect of a seagrass meadow on wave propagation under natural conditions is evaluated in Chapter 5 by a novel approach that relates individual plant parameters with meadow parameters. First, wave heights and orbital velocities in a *P. oceanica* meadow are measured during three storms. Data for one of the three storms measured are used to obtain the roughness length for the meadow. The friction factor for the two other events are then calculated and the drag coefficient related with meadow parameters. Most coastal models, introduce bottom effects through the roughness length and therefore it is worthwhile to obtain such magnitude for *P. oceanica*. Finally, the wave decay for different seagrass meadow densities and leaf lengths is predicted.

For completeness, a background review of fluid dynamics is presented in the Appendix A, where the basic concepts of linear wave theory, wave propagation and benthic boundary layers are summarised.



## Chapter 2

# Wave energy and the upper depth limit distribution of *Posidonia oceanica*

Parts of this chapter has been published as an article on *Botanica Marina*, Special Issue on Mediterranean Seagrasses<sup>1</sup>.

### 2.1 Summary

It is widely accepted that the availability of light sets the lower limit of the bathymetric distribution of seagrasses while the upper limit depends on the level of disturbance driven by currents and waves. The establishment of light requirements for seagrass growth has been a major focus of the research in marine ecology and therefore different quantitative models provide predictions of the lower depth limit of the distribution of seagrasses. In contrast, the study of the influence of energy levels on the establishment, growth and maintenance of seagrasses have received less attention and to date there are no quantitative models predicting the evolution of seagrasses as a function of the hydrodynamics

---

<sup>1</sup>Infantes E, Terrados J, Orfila A, Cañellas B, Álvarez-Ellacuaría A (2009) Wave energy and the upper depth limit distribution of *Posidonia oceanica*. *Botanica Marina* 52: 419-427.

at large scales. Hence it is not possible to predict either the upper depth limit of the distribution of seagrasses or the effects that different energy regimes will have on them. The aim of this Chapter is to provide a comprehensible methodology to obtain quantitative knowledge as well as predictive capacity to estimate the upper depth limit of the bathymetric distribution of seagrasses as a response of the wave energy disposed at the seabed. The methodology has been applied using forty-four years of wave data from 1958 to 2001 in order to obtain the mean wave climate at deep water in front of an open sandy beach in the Balearic Islands, Western Mediterranean where the seagrass *Posidonia oceanica* forms an extensive meadow. Mean wave conditions were propagated to the shore using a 2D parabolic model over the detailed bathymetry. The resulting hydrodynamics has been correlated with bottom type and the distribution of *P. oceanica*. Results showed a predicted near-bottom orbital velocity determining the *P. oceanica* upper depth limit between 38 - 42 cm s<sup>-1</sup>. This Chapter shows the importance of the interdisciplinary effort in ecological modelling and in particular the need of hydrodynamical studies to elucidate the distribution of seagrasses at shallow depths. Besides, the use of predictive models would permit the evaluation of the effects of coastal activities (construction of ports, artificial reefs, beach nourishments, dredging) on the benthic ecosystems.

## 2.2 Material and methods

### 2.2.1 Study Area and Regional Settings

The analysis was carried out in Cala Millor, located on the northeast coast of Mallorca Island (Fig. 2.1a,b). The beach is in an open bay with an area of ca. 14 km<sup>2</sup>. Near the coast to 8 m depth, there is a regular slope indented with sand bars near the shore (Fig. 2.1c), these bars migrate from offshore to onshore between periods of gentle wave conditions. At depths from 6 m to 35 m, the seabed is covered by a meadow of *P. oceanica*. This area was chosen for this study because of the availability of data from previous studies. The tidal regime is microtidal, with a spring range of less than 0.25 m (Gómez-Pujol et al. 2007). The bay is located on the east coast of the island of Mallorca and it is therefore exposed to incoming wind and waves from NE to ESE directions. According to the criteria of Wright and Short (1983), Cala Millor is an intermediate barred sandy beach formed by biogenic sediments with median grain values ranging between 0.28 and 0.38 mm at the beach front (L. Gómez-Pujol et al. 2007).

---

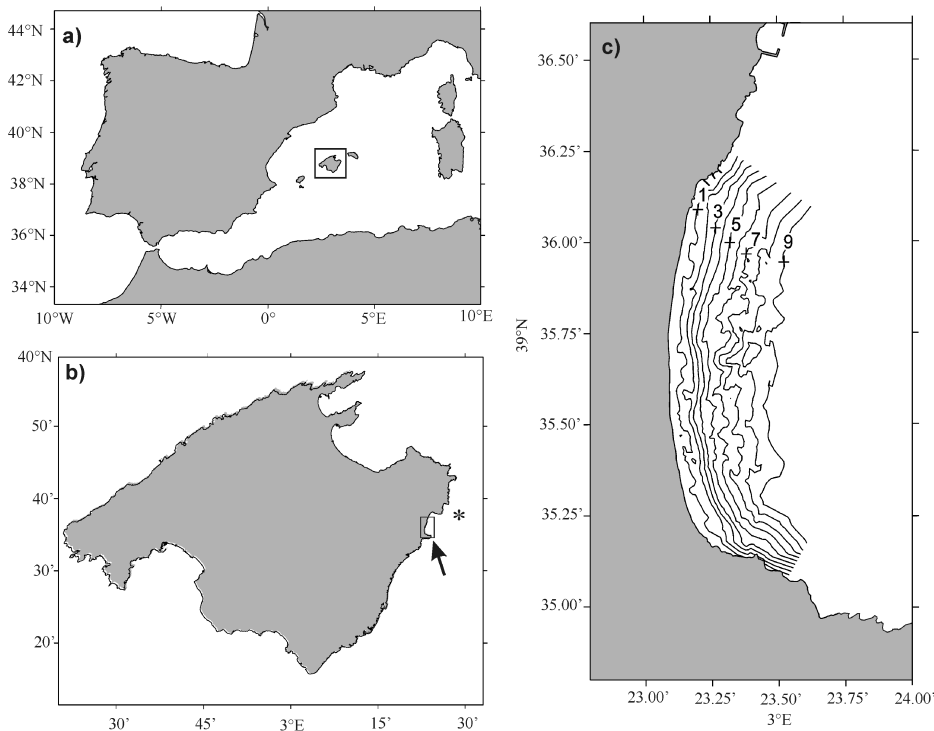


Figure 2.1: (a) Location of Mallorca in the Mediterranean Sea. (b) Location of the study area of Cala Millor in Majorca. The asterisk (\*) indicates HIPOCAS node 1433. (c) Bathymetry of Cala Millor with isobaths (in meters).

### 2.2.2 HIPOCAS database (1958 - 2001) and deep water wave characterization

Wave data used are part of the Hindcast of Dynamic Processes of the Ocean and Coastal Areas of Europe (HIPOCAS) project. This database consists of a high resolution, spatial and temporal, long-term hindcast dataset (Soares et al. 2002, Ratsimandresy et al. 2008). The HIPOCAS data were collected hourly for the period 1958 to 2001, providing 44 years of wave data with a 0.125 spatial resolution. This is the most complete wave data base currently available for the Mediterranean Sea. These hindcast models have become powerful tools, not only for engineering or predictive purposes, but also for long-term climate studies (Cañellas et al. 2007). These data were produced by the Spanish Harbor Authority by dynamical downscaling from the National Center for Environ-

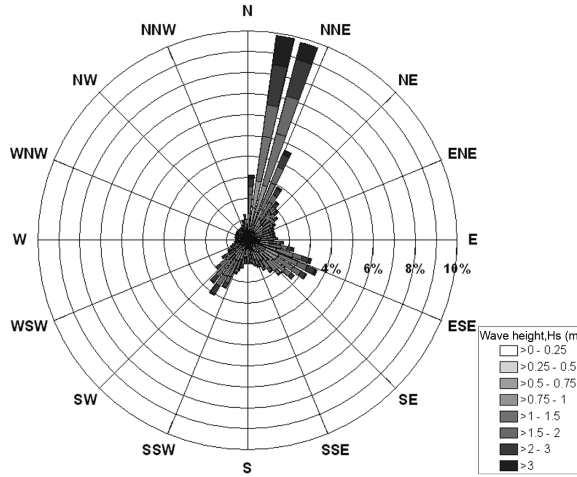


Figure 2.2: Directional wave histogram for HIPOCAS node 1433 10 km from Cala Millor

mental Prediction (NCEP) and the National Center for Atmospheric Research (NCAR) global reanalysis using the regional atmospheric model REMO. Data from HIPOCAS node 1433 (see Fig. 2.1) located 10 km offshore at 50 m depth, which is the closest HIPOCAS node to Cala Millor was used. The long-term distribution of significant wave height and wave direction at this node (Fig. 2.2) shows that the most energetic waves usually come from N-NNE. These wave directions are also the most frequent during the 44-year dataset.

Data contained in the HIPOCAS node consist of a set of sea states (one per hour) defined by their significant wave height, spectral peak period, and direction. An estimation of the long-term distribution of the mean significant wave height ( $H_m$ ) and its standard deviation was carried out making use of the lognormal probability distribution (Castillo et al. 2005). The long-term probability distribution identifies the most probable sea state for the 44-year period. Before estimation of this wave regime, data were preselected taking into account their incoming directions. Only sea states directed towards the beach were included in the analysis. Mean wave climate for HIPOCAS node 1433 provides an  $H_m$  value of  $1.53 \text{ m} \pm 0.96 \text{ m}$  ( $\pm 1 \text{ SD}$ ), a peak period of 7.3 s, and a direction of 11.258. This mean (most probable) wave climate was propagated to the shore using a parabolic model.



### 2.2.3 Shallow-water wave conditions

As water waves propagate from the region where they are generated to the coast, both wave amplitude and wavelength are modified. The surf zone is a highly dynamic area where energy from waves is partially dissipated through turbulence in the boundary layer and transformed into short and long waves, mean sea level variations, and currents (Dean and Dalrymple 2002). In the present work, waves were propagated using a gentle slope parabolic model (OLUCA-MC), which includes refraction-diffraction effects as well as energy losses due to wave breaking (Kirby and Dalrymple 1983, GIOC 2003). Detailed bathymetry obtained with echo-sounding was used to generate the numerical mesh. The model solves continuity and momentum equations assuming a smooth bottom (e.g., variations of the bottom negligible within a wave length) and converting the hyperbolic system to a parabolic system (e.g., with wave propagation in one direction).

Two grids were generated: the external grid (122 x 81 nodes), which covers the deeper area with 75 m resolution between nodes, and the internal grid (140 x 311 nodes), which covers the shallow area with 15 m resolution. The model output provides the wave field (significant wave height and direction of the mean flux energy) in the whole grid.

Maximum near-bottom orbital amplitudes  $a_b$  were calculated following the linear wave theory (see Appendix A):

$$a_b = \frac{H_s}{2\sinh(2\pi h/L)} \quad (2.1)$$

where  $h$  is the water depth and  $L$  is the wave length calculated iteratively as:

$$L = \frac{T_p^2}{2\pi} \tanh\left(\frac{2\pi h}{L}\right) \quad (2.2)$$

where  $T_p$  is the peak period and  $g$  is the acceleration of gravity. The maximum near-bottom orbital velocity ( $u_b$ ) is:

$$u_b = 2\pi a_b / T_p \quad (2.3)$$

## 2.2.4 Bottom typology and bathymetry

Remote sensing of the seabed from air or space is commonly used for mapping seagrass habitats over a wide range of spatial scales (McKenzie et al. 2001). Satellite spectral images from Ikonos are suitable for the detection and mapping of the upper depth limit of seagrass distribution in shallow clear waters (Fornes et al. 2006). Aerial color photographs have been used in some studies to describe temporal changes in the distribution of seagrasses (Hine et al. 1987), to evaluate the effect of wave exposure (Frederiksen et al. 2004), and the influence of anthropogenic activities (Leriche et al. 2006). Aerial photographs for mapping the area covered by *P. oceanica*, dead *P. oceanica* rhizome, rocks, and sand up to 11 m depth were used. Aerial color photographs were taken in August of 2002 with a resolution of 0.4 m. Polygons were drawn around the different areas with Arc/GIS software (Arc/Info and Arc/Map v9.0, ESRI) and classified by bottom types. In those areas where bottom recognition was not possible from the aerial photographs, field surveys were carried out to identify the typology of the substratum (some areas tend to accumulate seagrass leaves which can lead to false interpretation of aerial images). Image classification was validated with bathymetric filtered echo-soundings and field observations.

During 2005, an acoustic survey was carried out to determine the bathymetry of the inner mesh and to test the classification of the seagrass coverage from the aerial photographs. Acoustic mapping of *Posidonia oceanica* was performed with a shipmounted Biosonics DE-4000 echo sounder (BioSonics, Inc., Seattle, USA) equipped with a 200 KHz transducer. The draught of the boat allowed sampling up to depths of approximately 0.5 m. Inshore-offshore echo-sounding transects were sampled perpendicularly to the bathymetric gradient, with a separation of 50 m between transects. Acoustic pulse rate was set to  $25 \text{ s}^{-1}$  and the sampling speed was set to 3 knots, which allowed for a horizontal resolution of 1 m (Orfila et al. 2005). Bottom typology was estimated as the most probable after echogram examination using the first to second bottom echo ratio technique (Orlowski 1984, Chivers et al. 1990). The resulting echo sounding points were filtered, averaged (1 output equals 20 pings) and clustered into three groups (*P. oceanica* meadows, sandy, and hard bottoms) taking into consideration calibrations performed for previously classified bottoms. Hard bottoms include rocks, *P. oceanica* rhizome mats, and zones with poor seagrass coverage (Fig. 2.3). Afterwards, this map was verified by direct observation at random points, also distinguishing those bottom types that the algorithm was not able to identify

---

(i.e., dead rhizome and rocks). The map of bottom typology in Fig. 2.3 represents the final classification (aerial photograph verified with echo-sounding and direct SCUBA observations).

Bathymetric data were interpolated using the kriging technique to create 1-m scale depth contours that were overlaid with bottom typology. Similarly, maximum near-bottom orbital velocity data were interpolated to create 5 cm  $s^{-1}$  scale  $u_b$  contours that were overlaid with bottom typology. Percent coverage of rocks, sand, dead rhizomes of *P. oceanica*, and *P. oceanica* were calculated for each depth and near-bottom orbital velocity interval. A total of 400 points were randomly selected throughout the study area, and the corresponding bottom type and near-bottom orbital velocity interval were used to calculate the average near-bottom orbital velocity for each bottom type. Additionally, 400 points along the upper limit of the *P. oceanica* meadow were randomly selected and the corresponding near-bottom orbital velocities were used to estimate an average along that edge. Differences in near-bottom orbital velocity between each bottom type and the upper limit of *P. oceanica* were evaluated using Kruskal-Wallis non-parametric analysis of variance (due to heterogeneity of data variance).

## 2.3 Results

The study site has a total area of 121.44 ha wherein sand and *Posidonia oceanica* meadow are the most abundant substrata. Shallow bottoms in Cala Millor (depths between 0 and 6 m) are mostly sandy, with some patches of rock, particularly in the center and south parts of the beach (Table 2.1). The upper depth limit of *P. oceanica* is located between 5 and 6 m and the meadow continues down to 30 - 35 m depth (acoustic survey data not shown). The limit between seagrass and sand is irregular and has several areas of hard substratum between 4 and 7 m that correspond to dead rhizomes of *P. oceanica* partly covered by sand and algae, which can be indicative of meadow regression (Fig. 2.3). *P. oceanica* reaches the highest percentage cover at depths greater than 8 m, and no stands are found in depths shallower than 4 m. Most of the rocky bottom is in the shallowest water, between 0 and 2 m. Two large sand fingers cross the seagrass meadow at the center of the study area; these may have resulted from sand transport from the exposed beach after storm events.

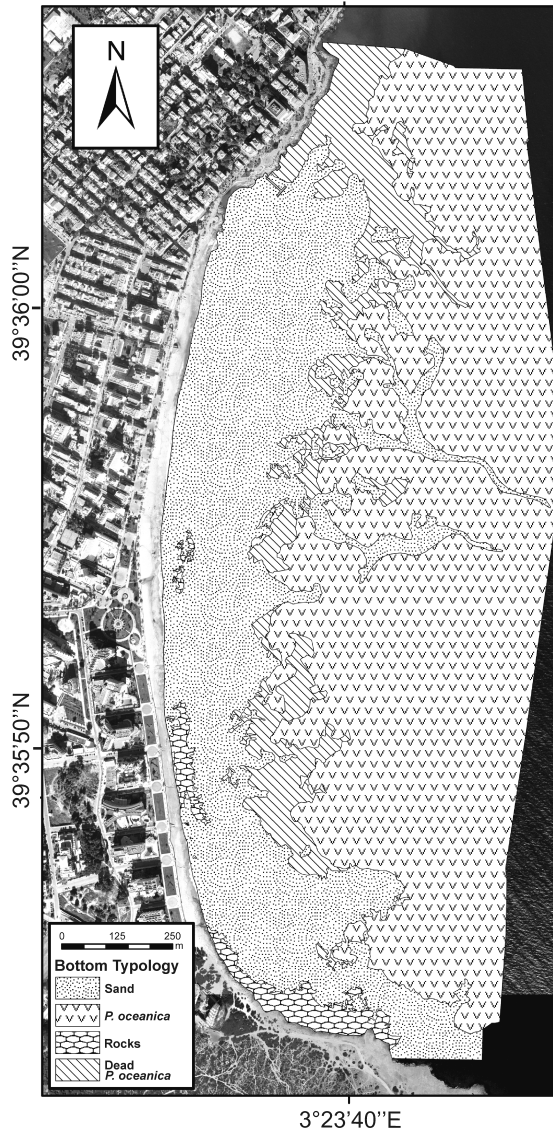


Figure 2.3: Bottom typology off Cala Millor (Mallorca, western Mediterranean Sea).

Mean wave conditions propagated over the beach resulted in wave heights between 0.2 and 0.4 m, with significant wave breaking in the shallow sandy area (between 0.5 and 1 m) (Fig. 2.4a) and near-bottom orbital velocities up to 110 cm s<sup>-1</sup>. The highest velocities occurred in the shallow sandy part of the beach (between 1 and 3 m) (Fig. 2.4b).

Depth (m)	<i>P. oceanica</i>	Sand	Rock	Dead <i>P. oceanica</i>
1 – 2	0	96.63	3.24	0.13
2 – 3	0	97.73	1.75	0.52
3 – 4	0	97.31	0	2.69
4 – 5	0.46	83.36	0	16.17
5 – 6	11.55	51.03	0	37.42
6 – 7	42.34	25.27	0	32.39
7 – 8	73.87	21.10	0	5.03
8 – 9	83.82	14.64	0	1.54
9 – 10	94.40	5.59	0	0
10 – 11	97.98	2.02	0	0
Total area (m <sup>2</sup> )	565,349.42	528,241.5	25,192.7	95,632.92

Table 2.1: Percent cover of bottom type at different depths. The total area of coverage of each bottom type is presented in the last row.

Sandy areas are associated with high values of near-bottom orbital velocities, while *P. oceanica* is associated with lower velocities (Fig. 2.5). *P. oceanica* is not present in areas with velocities higher than 38 - 42 cm s<sup>-1</sup>. This velocity interval might be considered a first estimate of the threshold near-bottom orbital velocity that allows the *P. oceanica* to occur in Cala Millor.

Variance of near-bottom orbital velocity was higher in sand, rock, and dead *P. oceanica* than in the *P. oceanica* meadow (Fig. 2.6). Kruskal-Wallis non-parametric analysis of variance detected significant differences in the average near-bottom orbital velocity between bottom types [ $H(4, n = 800) = 310.34, p < 0.001$ ], and post-hoc multiple comparisons of mean ranks showed that velocities were lower in *P. oceanica* stands and at the *P. oceanica* upper limit than in rock, sand, and dead *P. oceanica* (Fig. 2.6).

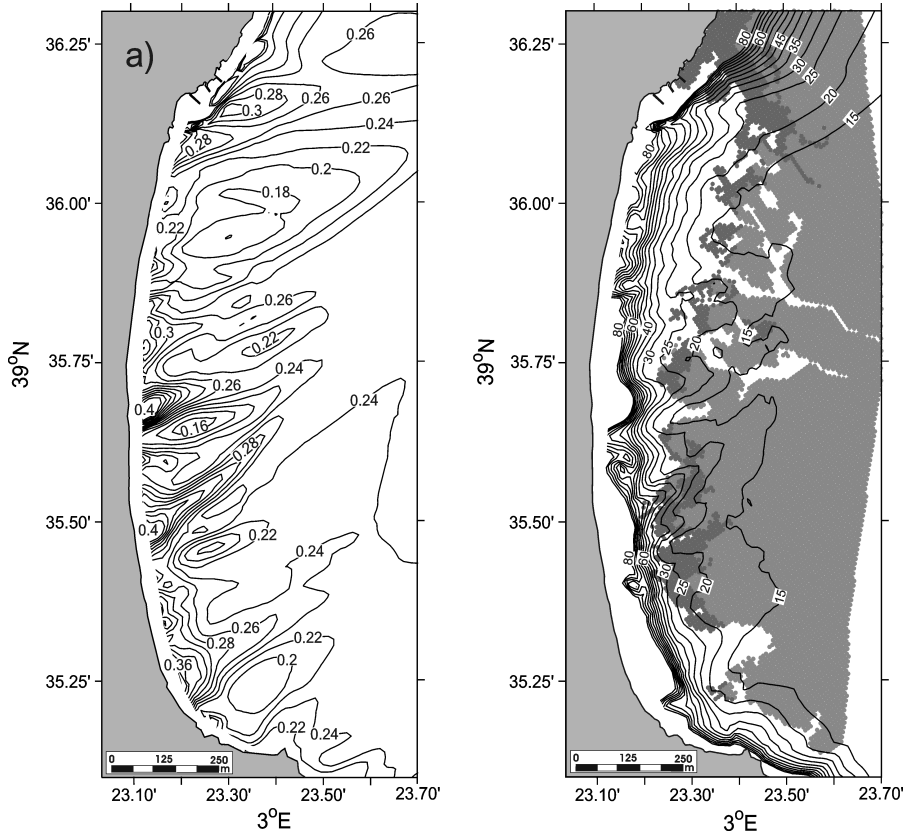


Figure 2.4: (a) Distribution of wave heights (m) at the beach derived from mean wave conditions ( $11.25^\circ$ ,  $H_m = 1.53$  m,  $T_p = 7.30$  s). (b) Distribution of near-bottom orbital velocities ( $u_b$ ,  $\text{m s}^{-1}$ ) at the beach and cover of the *P. oceanica* meadow (gray) and dead rhizomes (dark gray).

## 2.4 Discussion

In this Chapter, a methodology to estimate the wave energy that determines the upper depth limit of *Posidonia oceanica* is presented. Data show that an increase in wave energy is related to a decrease of *P. oceanica* cover, and that above a threshold level of wave energy seagrass is not present. It is important to emphasize that the evidence provided in this study is correlative and applies to this study site only. Other locations, with different sediment characteristics and wave climates might provide different threshold values. Additional sources of disturbance (both natural and anthropogenic) will also introduce variability

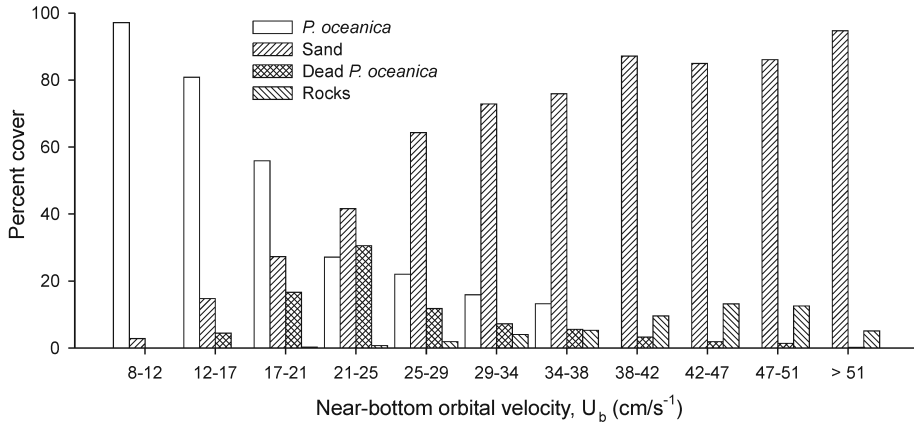


Figure 2.5: Percent coverage of the different bottom types in each of the near-bottom orbital velocity ( $u_b$ ) intervals established in Cala Millor.

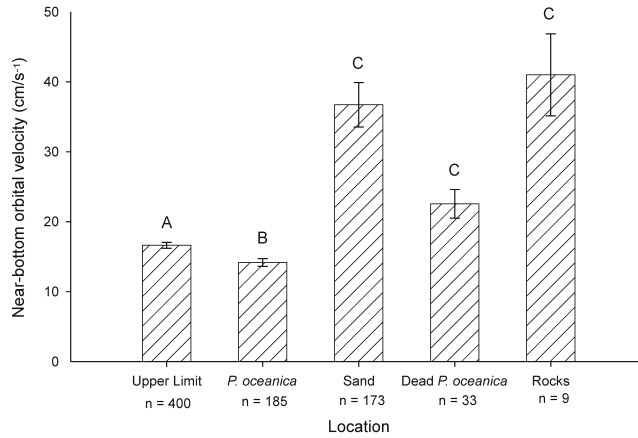


Figure 2.6: Mean near-bottom orbital velocity above each bottom type in Cala Millor. Different capital letters indicate significant differences between bottom types (post-hoc multiple pairwise comparison of mean ranks,  $p < 0.05$ ). Error bars show 95 % confidence intervals. n-values indicate the number of points selected randomly in each bottom type. Differences in n-values between bottom types are driven by the differences in percentage covers of each bottom type in the study area.

in the threshold estimates. The near-bottom orbital velocities are computed from numerical model predictions and real velocities within the meadow could be lower due to wave attenuation by the seagrass meadow and wave-current interactions. However, the predicted velocities where *P. oceanica* is not present provide an estimate of the threshold velocities that would impede the persistence of this seagrass species. The usefulness of this methodology is that it provides quantitative estimates of wave energy that sets the upper depth limit of *P. oceanica* and, therefore, these can be compared to those obtained in other locations.

An estimate of the threshold value of near-bottom orbital velocity that allows the long-term persistence of *Posidonia oceanica* (38 - 42 cm s<sup>-1</sup>) is estimated. It has been suggested that *Zostera marina* L. can tolerate unidirectional current velocities up to 120-150 cm s<sup>-1</sup> and that the meadows formed by this species become spatially fragmented at tidal current velocities of 53 cm s<sup>-1</sup> (Fonseca et al. 1983). Shallow mixed meadows of *Z. marina* and *Halodule wrightii* Asch. seem to remain spatially fragmented at tidal current speeds above 25 cm s<sup>-1</sup> (Fonseca and Bell 1998). Experimental transplantations of *Z. marina* along depth gradients in intertidal zones indicate that this species cannot persist at sites where the maximum bottom orbital velocity during the tidal cycle reaches 53 - 63 cm s<sup>-1</sup>. Furthermore, this species can survive when exposed to waves for less than 60 % of the time and maximum orbital velocity is less than 40 cm s<sup>-1</sup> (van Katwijk and Harmus 2000). Hence, this estimate of the threshold value of near-bottom orbital velocity that allows the persistence of *P. oceanica* is within the range of values of current velocity proposed for other seagrass species.

Frederiksen et al. (2004) used aerial photographs to follow changes in the distribution of *Z. marina* from 1954 to 1999 and showed that seagrass landscapes can change extensively over long periods of time, especially in the more wave-exposed areas. Comparison of aerial photographs taken in 1956 and 2004 indicates that the upper depth limit of *P. oceanica* in Cala Millor has regressed in the south part of the beach (IMEDEA 2005), which is a sector of the beach well exposed to the most energetic waves (those from the N-NNE). However, that other processes may determine the upper depth limit of *P. oceanica* are not rule out. This seagrass species is able to grow in certain locations, usually sheltered, almost to sea level (Ribera et al. 1997), which suggests that neither photo-inhibition nor temperature fluctuations associated with shallow

---



depths are important in setting the upper depth limit. Except for the desiccation effects associated with exposure to air at low tides (negligible in the Mediterranean Sea), the consensus is that the upper depth limit of seagrasses is set by the energy of currents and waves (Koch et al. 2006). Wave breaking might have a role in establishing the upper limit, but the position at which waves break will change depending on wave height, wave period, and presence of submerged sandbars. In addition, the effect of waves of certain energy may depend on the amount of time the plants are exposed to different levels of wave energy. Average wave conditions have been used to estimate the average field of near-bottom orbital velocities, but other wave statistics could be used, such as extreme events (De Falco et al. 2008), and elaborate a prediction of those velocities that allow the long-term persistence of *P. oceanica*. 44 years of data are used, as this would be an adequate period of time over which to average the effects of waves on the slow-growing *P. oceanica* (Marbà and Duarte 1998).

Sediment density and grain size characteristics have not been considered in this study. These granulometric characteristics may play an important role in determining the location of seagrasses, because wave energy will move and resuspend the sediment, which might bury or erode a seagrass meadow. Differences in sediment characteristics between locations will then contribute to the variability of the estimate of the threshold wave energy that sets the upper depth limit of *P. oceanica*.

I conclude that the methodology presented here is a useful tool to estimate wave energy on the bottom and to identify the level that sets the upper depth limit of *Posidonia oceanica* meadows. This approach provides testable estimates of the threshold level of wave energy that allows this species to persist and indicates a research program to validate them. This Chapter also highlights the importance of interdisciplinary and multidisciplinary research in ecological modeling and, in particular, the need for hydrodynamical studies to elucidate the distribution of seagrasses at shallow depths.

---



## Chapter 3

# *Posidonia oceanica* and *Cymodocea nodosa* seedling tolerance to wave exposure

Part of this Chapter has been published as an article on *Limnology and Oceanography*<sup>1</sup>

### 3.1 Summary

In this Chapter the role of hydrodynamics in the establishment of seagrass seedlings for two Mediterranean seagrass species, *Posidonia oceanica* and *Cymodocea nodosa* is studied, by combining flume and field experiments. Flume measurements under both unidirectional and oscillatory flow showed that *P. oceanica* seedlings experienced higher drag forces than *C. nodosa*, which could be related to the larger total leaf area. Drag coefficients were between 0.01 and 0.1, for Reynolds numbers of  $10^3$  and  $10^5$ . As a result, *P. oceanica* seedlings required 40 - 50 % of root length anchored to the sediment before being dislodged while *C. nodosa* required  $\approx 20$  %. To validate the flume results, seedling survival in sandy beds was evaluated for two depths (12 and 18 m) at two field locations. To calculate near-bottom orbital velocities at the planting sites, deep

---

<sup>1</sup>Infantes E, Orfila A, Bouma TJ, Simarro G, Terrados J. *Posidonia oceanica* and *Cymodocea nodosa* seedling tolerance to wave exposure. *Limnology and Oceanography* 56(6) (*In Press*). doi: 10.4319/lo.2011.56.6.0000.

water waves were propagated to shallow water using a numerical model. Results showed that *P. oceanica* seedlings experienced high losses after the first autumn storms when near-bottom orbital velocities exceeded  $18 \text{ cm s}^{-1}$ . The loss of *C. nodosa* seedlings was much lower and some seedlings survived velocities as high as  $39 \text{ cm s}^{-1}$ . Thus, flume and field results are consistent in explaining relative higher losses of *P. oceanica* seedlings than for *C. nodosa*.

## 3.2 Methods

*Posidonia oceanica* and *Cymodocea nodosa* seedlings used in the flume and field studies were obtained from fruits collected at sea. *P. oceanica* fruits were collected from drift material on several beaches of Mallorca and Ibiza Islands (Western Mediterranean Sea) during April-May 2009. Fruits were manually opened and seeds were placed in natural salinity seawater. Seed germination took place within a week or two after collection. *C. nodosa* seeds were collected during February-April 2009 in a shallow (3 m) meadow in Mallorca Island. Seeds were kept in aquariums until May 2009, the month when *C. nodosa* seeds germinate at sea (Buia and Mazzella 1991). Germination of *C. nodosa* was induced by reducing the salinity to 10 (Caye and Meinesz 1986). Both *P. oceanica* and *C. nodosa* germinated seeds were kept in aquariums with natural seawater during early seedling development. Aquariums were in a temperature-controlled room at  $20^\circ\text{C}$  with a 14 h photoperiod and a photon irradiance of  $60 \mu\text{mol m}^{-2} \text{ s}^{-1}$ . Seedlings were haphazardly distributed into two groups, one for flume experiments and another for field experiments.

### 3.2.1 Drag forces and drag coefficient

Drag measurements were carried out to obtain the effective drag forces acting on individual seedlings and to calculate the drag coefficients of both species under unidirectional and oscillatory flows. Experiments were carried out in the NIOO racetrack-shaped channel at Yerseke, Netherlands. The channel is 17.55 m long, 0.6 m wide and 0.45 m deep (Hendricks et al. 2006). In all experiments, water depth was 0.32 m, water temperature was  $20 \pm 0.5^\circ\text{C}$  and salinity 36. The flume allows running both unidirectional and oscillatory flows. Currents in the flume were generated by a conveyor belt. Waves were generated by a vertical wave maker driven by a piston. At the end of the test section waves were damped by

---

a porous gentle slope. Flow was characterised by measuring vertical profiles of the velocity at 5 cm intervals along the water column using an Acoustic Doppler Velocimeter (ADV Vectrino, Nortek) at the same cross section where seedlings were tested. The ADV sampling rate was 25 Hz and measurements were taken for 5 minutes, sampling volume of 7 mm and a nominal velocity range of  $1 \text{ m s}^{-1}$ .

Drag was measured on individual *P. oceanica* and *C. nodosa* seedlings fixed to a force transducer inside the flume. Seedlings were exposed to 7 different wave conditions that include wave heights ( $H$ ) ranging from 1 to 7 cm and periods ( $T$ ) from 1.5 to 4 seconds. These waves gave near-bottom orbital velocities between 4 and  $16 \text{ cm s}^{-1}$ . Seedlings were also exposed to 6 different current velocities ranging between 5 and  $36 \text{ cm s}^{-1}$ . Hereafter,  $u$  represents the near-bottom orbital velocity (for waves) or the mean velocity (currents). Each wave and current flow conditions was repeated for 5 seedlings. Seedlings were attached to a 2 cm long metal screw by the stem using a small cable tie removing the roots and seed. The metal screw was then fixed into the drag sensor. The drag force of the metal screw with cable ties alone is a constant, and was subtracted from the drag force measured on the seedlings. No breaking of leaves or plant fragments was observed during the drag experiments. Drag forces and wave heights were measured at 20 Hz during 3 min. Drag forces were measured using a drag transducer developed by WL-Delft Hydraulics (Bouma et al. 2005) and calibrated as Stewart (2004). Waves were measured with a pressure sensor (Druck, PT1830). Drag measurements were performed on *P. oceanica* in October 2009 and February 2010, but drag in *C. nodosa* was only measured in October 2009 since seedlings did not survive until February 2010.

The force acting over individual plants measured by the transducer can be expressed as,

$$F_D = \frac{1}{2} \rho C_D a_v u |u| \quad (3.1)$$

where  $\rho$  is the density of water,  $a_v$  is the total leaf area of the plant and  $u$  the flow velocity (either unidirectional or oscillatory). The drag coefficient,  $C_D$ , which depends on the Reynolds number, can be readily obtained from the experiments using Eq. A.9. Defining the characteristic length as (Martone and Denny 2008):

$$l_* = \sqrt{a_v} \quad (3.2)$$

the corresponding Reynolds number is defined as,

$$Re = \frac{ul_*}{\nu} \quad (3.3)$$

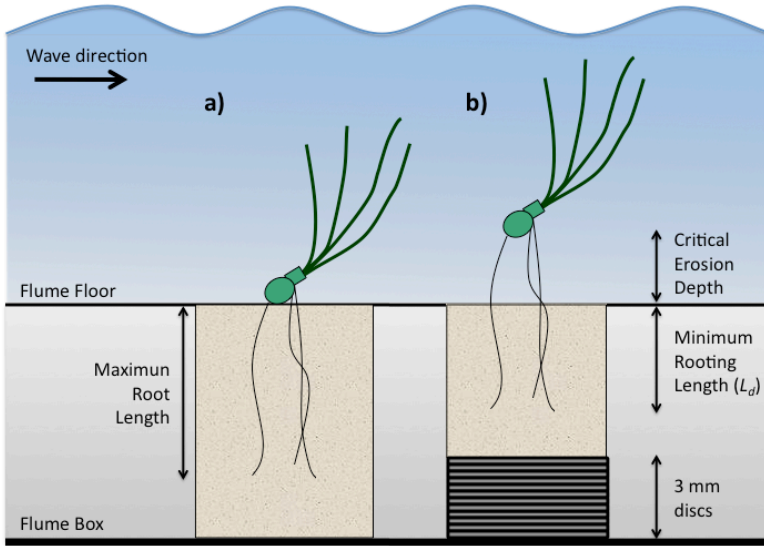


Figure 3.1: Sketch of the flume experimental set-up showing the critical erosion depth and minimum rooting length ( $L_d$ ) of seedlings. (a) Seedling in the flume, (b) seedling before dislodging from the sediment after the discs addition. Critical erosion depth is equivalent to the total height of discs added when the seedling is dislodged. Not drawn to scale

being  $\nu$  the molecular kinematic viscosity of seawater. Most aquatic vegetation is flexible and becomes streamlined with increasing flow velocities and it is very difficult to measure accurately the frontal area under waves and currents (Sand-Jensen 2003, 2005). For this reason, the total surface area was used as the frontal area as it can be accurately measured.

### 3.2.2 Critical erosion depth and minimum rooting length

Once the drag force was measured for the seedlings the next step was to analyze the capacity of both species to withstand dislodgement by sediment disturbances via root anchoring. Individual *P. oceanica* and *C. nodosa* seedlings were planted in cylindrical pots (height x diameter: 12 x 12 cm) over sand with a diameter ( $d_{50}$ ) of  $592 \pm 23 \mu\text{m}$ . Pots were placed in the flume under two sets of experiments: i) periodic waves of  $H = 2.5$  cm and  $T = 2.6$  s ( $u = 5$  cm

s<sup>-1</sup>) and ii) periodic waves of  $H = 5.1$  cm and  $T = 1.9$  s ( $u = 10$  cm s<sup>-1</sup>) during 15 minutes (Fig. 3.1a). Seedlings were repeatedly exposed to 15 minutes of wave action, while in between wave treatments, sediment erosion was mimicked. This was repeated until the critical erosion depth at which seedlings dislodged was found. Sediment erosion was simulated by progressively adding discs of 3 mm thickness underneath the pots removing carefully the pushed-up top layer of sediment. This process was repeated until the waves dislodged the seedling from the sediment. A total of 18 plants were used for *P. oceanica* and 9 for *C. nodosa*. For each seedling, root lengths and total leaf area were measured. The critical erosion depth was measured as the thickness of disks added before the plant became dislodged. The minimum rooting length ( $L_d$ ) or length of the root inside the sediment before the plant become dislodged was obtained by the difference of the maximum root length and the critical erosion depth. The length of the longest root was used for all calculations since in the end, regardless of the number of roots, seedlings remained anchored to the substrata with only one root, even when the rest were dislodged.

### 3.2.3 Field study

Seedlings were planted at sea to assess their survival and to validate the principles observed in the flume. The field study was performed from August 2009 to February 2010 in Mallorca Island, Spain, Western Mediterranean Sea (Fig. 3.2a,b). In this area, tides are almost negligible, e.g., less than 25 cm (Orfila et al. 2005). *P. oceanica* and *C. nodosa* seedlings were planted at two locations in the Natural Reserve of Cap de Enderrocat (Fig. 3.2c). The first location, Cap Enderrocat is a sandy area between the upper limit of *P. oceanica* and the coastline exposed to Southwest and Southeast waves (triangles in Fig. 3.2c). The second location, Cala Blava is located in a large *P. oceanica* meadow with sand gaps (circles in 3.2c), which is only exposed to Southwest waves. The upper depth limit of *P. oceanica* in Cap Enderrocat is at 19 m while that in Cala Blava is at 12 m. The upper depth limit of *C. nodosa* in Cap Enderrocat and Cala Blava is at 12 m. Within each location two depths were selected at 18 m and 12 m depth for the short-term experiment.

Six plots (three for each species) separated by 3 m intervals were established at the four sites. Twelve seedlings were planted on each plot directly on the sediment without any artificial supporting aid, in order to mimic natural condi-

---

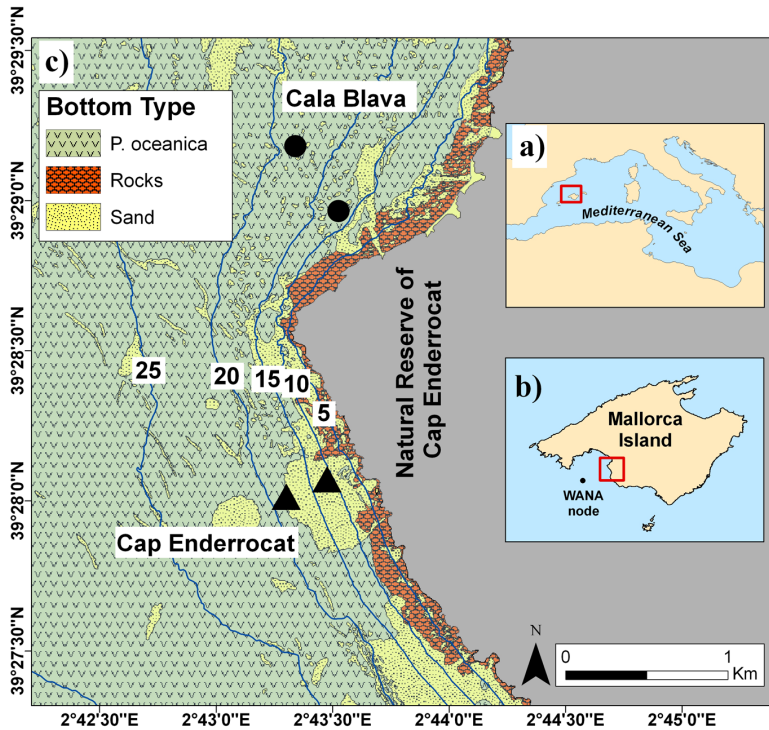


Figure 3.2: (a) Location of Mallorca Island in the Mediterranean Sea. (b) Location of study area and WANA node. (c) Location of the experimental sites, Cap Enderrocat (triangles) and Cala Blava (circles). Bathymetric contours in meters.

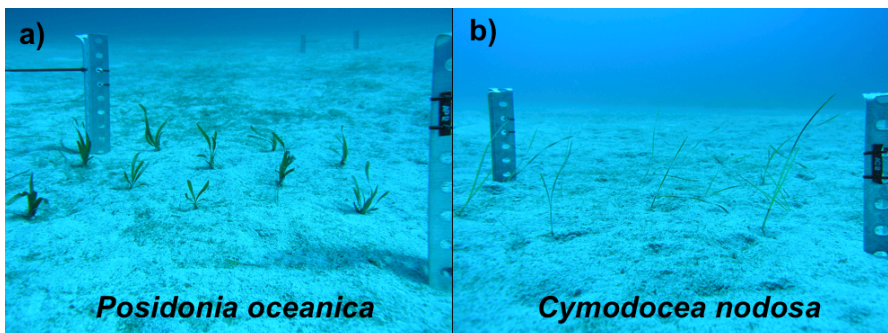


Figure 3.3: Experimental plots with a) *Posidonia oceanica* and b) *Cymodocea nodosa* seedlings at the beginning of the field experiment.



tions where the roots are the only attachment structure to the substrata (Fig. 3.3a,b). A total of 144 seedlings of each species were planted after measuring the number of roots, root lengths and root diameter in the laboratory. Additionally, the number of leaves of each seedling and the length and width of each leaf were measured once planted in the field. The number of seedlings in each plot was counted in September, October, and November 2009 and in February 2010. Whenever seedlings were no longer observed in the plots, it was determined that the loss was not caused by burial.

Survival rate was related to wave conditions as well as to averaged near-bottom orbital velocities between sampling dates at the four experimental sites. Significant wave height ( $H_s$ ), peak period ( $T_p$ ), and direction ( $\Theta$ ) were acquired at deep waters approximately 15 km from the study sites (Fig. 3.2b). These wave conditions were propagated to the study sites using a numerical model based on the mild-slope parabolic approximation (Kirby and Dalrymple 1983, Alvarez-Ellacuria 2010, Infantes et al. 2011). Wave conditions in the study area ranged between a  $H_s$  of 0.5 - 4 m,  $T_p$  of 2 - 12 s and  $\Theta$  of 130 - 270 degrees. Near-bottom orbital velocities at the four locations where *P. oceanica* and *C. nodosa* seedlings were transplanted were computed from the model output between sampling periods using linear wave theory (Dean and Dalrymple 1991).

### 3.2.4 Statistical analysis

Differences in drag forces under currents and waves of both species were tested using a Student t-test. Differences among drag coefficients were evaluated using species (*P. oceanica*, *C. nodosa*) and flow (unidirectional, oscillatory) as fixed factors and Reynolds number as the covariate in the analysis of covariance (ANCOVA) model  $C_D = \text{species} + \text{flow} + \text{Reynolds} + (\text{species} \times \text{flow}) + (\text{species} + \text{Reynolds}) + (\text{flow} \times \text{Reynolds}) + (\text{species} \times \text{flow} \times \text{Reynolds})$  (Quinn and Keough 2002). Critical erosion depths and minimum rooting lengths in the sediment were evaluated using univariate test of significance ANOVA. “Wave velocity” (orbital velocities of  $5 \text{ cm s}^{-1}$  and  $10 \text{ cm s}^{-1}$ ), “Species” (*P. oceanica* and *C. nodosa*) were the between-subjects factors (fixed). Differences of seedling survivorship in the field experiment were also evaluated using univariate test of significance ANOVA. The test was performed only in October 2009 because we observed differences between sites on that date. After October 2009 no plants were left in most of the plots (see Results). “Sites” (Cap Enderrocat and Cala

---

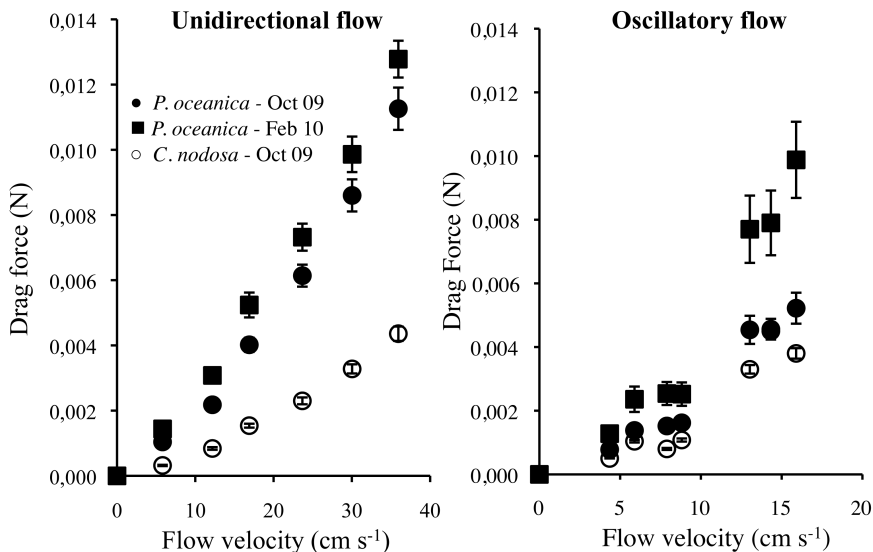


Figure 3.4: Drag forces acting on seedlings in (a) unidirectional flow and (b) oscillatory flow. (mean, SE,  $n = 5$ ).

Blava), “Depth” (18 m and 12 m), “Species” (*P. oceanica* and *C. nodosa*) were the factors (fixed). A Cochran’s C-test was used to test for heterogeneity of variances. All data were normally distributed.

### 3.3 Results

*Posidonia oceanica* and *Cymodocea nodosa* have flexible leaves which easily bend with the currents or waves. Drag forces acting on individual seedlings increased with current and wave velocities (see Fig. 3.4a,b). Drag forces also increased with foliar surface area for both seagrass species (Fig. 3.5). Drag forces were higher ( $t$ -test:  $t = 7.08$ ,  $df = 14$ ,  $p < 0.01$ ) for *P. oceanica* ( $0.006 \pm 4 \times 10^{-4}$  N, mean  $\pm$  SE) than for *C. nodosa* ( $0.003 \pm 3 \times 10^{-4}$  N) at  $u = 16$  cm s<sup>-1</sup> in unidirectional flow (see Fig. 3.5a). Similarly, drag forces were also higher ( $t$ -test:  $t = 3.2$ ,  $df = 14$ ,  $p < 0.01$ ) for *P. oceanica* ( $0.011 \pm 1 \times 10^{-3}$  N) than for *C. nodosa* ( $0.005 \pm 6 \times 10^{-4}$  N) at  $u = 16$  cm s<sup>-1</sup> in oscillatory flow (see Fig. 3.5b).

ANCOVA shows that drag coefficient ( $C_D$ ) depends on Reynolds number

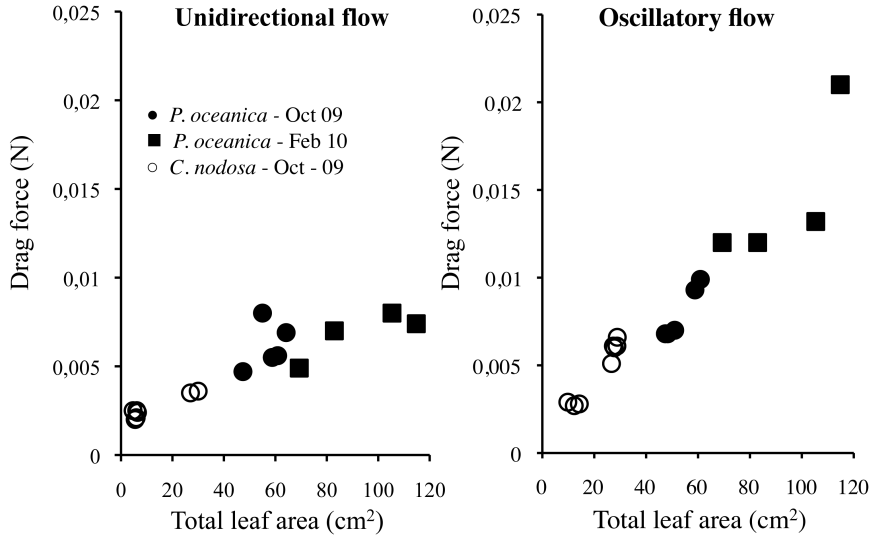


Figure 3.5: Drag forces acting on individual seedlings of different surface area in (a) unidirectional flow and (b) oscillatory flow. Flow velocity of  $16 \text{ cm s}^{-1}$ .

( $Re$ ), ( $F = 298.7$ ,  $p < 0.001$ ) and that it is also influenced by the type of flow ( $C_D$  currents  $>$   $C_D$  waves,  $F = 4.8$ ,  $p < 0.05$ ), but not by the species ( $F = 1.4$ ,  $p = 0.24$ ) (Fig. 3.6). A linear fitting of the drag coefficient for both species under oscillatory motion is,

$$\log_{10}C_D = -0.6653 * \log_{10}Re + 1.1886, (R^2 = 0.77, r = -0.87) \quad (3.4)$$

and similarly for unidirectional flow

$$\log_{10}C_D = -0.7269 * \log_{10}Re + 1.6253, (R^2 = 0.92, r = -0.95) \quad (3.5)$$

The experiments in the flume have shown that there are significant differences in the minimum rooting length that each species tolerates (Table 3.1). *P. oceanica* seedlings require 40 - 50 % ( $2 \pm 0.2 \text{ cm}$ , mean  $\pm$  SE) of root length anchored into the sediment while *C. nodosa* requires only 20 % ( $2.8 \pm 0.2 \text{ cm}$ , mean  $\pm$  SE) of root length anchored into the sediment (Fig. 3.7). *P. oceanica* seedlings tolerate less sediment erosion ( $2.7 \pm 0.3 \text{ cm}$ , mean  $\pm$  SE) to become dislodged than *C. nodosa* ( $5.6 \pm 0.4 \text{ cm}$ , mean  $\pm$  SE) under waves.

The capacity of a plant to remain anchored depends on the force that the roots can manage (which mainly depends on their length  $L_d$ ), and on the force

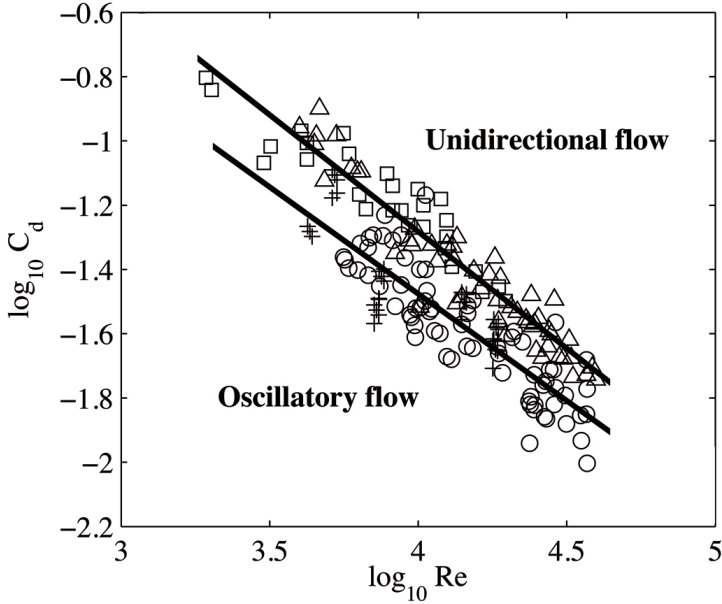


Figure 3.6: Drag coefficient versus Reynolds number for *Posidonia oceanica* and *Cymodocea nodosa* under unidirectional and oscillatory flow. Experimental data under uniform flow for *P. oceanica* seedlings (triangles) and for *C. nodosa* (squares). For oscillatory flow *P. oceanica* seedlings (circles), and *C. nodosa* (crosses). Solid lines are the linear fitting for the different flow conditions.

that the exposed leaves receive from the ambient (which is highly dependent on the total leaf area  $a_v$ ). The above suggests that an important dimensionless coefficient in the problem is the ratio  $L_d/\sqrt{a_v}$ . Since other variables could play a role in the problem, the ratio  $L_d/\sqrt{a_v}$  will not be constant in general, and it could depend on other dimensionless groups representing the plant species, flow velocity, type of flow (wave or current), etc.

From the experimental results, only the influence of the species on  $L_d/\sqrt{a_v}$  has been clearly identified as a measure of the dislodgment risk, which can be termed as the dislodgement safety factor. Results presented in this Chapter indicate that under periodic flows, seedlings of *P. oceanica* will remain anchored as long as  $P. oceanica \approx 0.35$ , i.e., if their root lengths are on average 0.35 times the square root of the leaves area. In the case of *C. nodosa* the condition for the seedlings to remain anchored is  $L_d/\sqrt{a_v} \approx 1.6$ .

	df	MS	<i>F</i>
	1	6828	52.9 ***
<b>Minimum rooting</b>	1	63	0.5 ns
<b>Length</b>	1	196	1.5 ns
	34	129	

Table 3.1: Two-factor way ANOVA testing differences between species and orbital velocities and minimum rooting length. Significant differences are expressed in bold as, \*\*\* $p < 0.001$ , and ns = not significant. Cochran's C-test no significant. df = degrees of freedom and MS = mean square.

The foliar surface of *P. oceanica* seedlings at the beginning of the field experiment was 4 times larger than that of *C. nodosa* seedlings (Table 3.2). As seedlings develop the difference in foliar surface increases. In contrast, *C. nodosa* maximum root lengths are higher than *P. oceanica*. Root diameters are higher for *P. oceanica* than for *C. nodosa*. Survival was related to wave conditions as well as to averaged near-bottom orbital velocities between sampling dates (Fig. 3.8; Table 3.3). No loss of seedlings occurred from August to September 2009. During this period no storms affected the study area and the computed near-bottom orbital velocities were below  $5 \text{ cm s}^{-1}$ .

	<i>P. oceanica</i>	<i>C. nodosa</i>
Total foliar surface ( $\text{cm}^2$ )	$12.9 \pm 1.6$	$3.2 \pm 0.4$
Number of leaves	$6.1 \pm 0.6$	$2.3 \pm 0.2$
Number of roots	$5.2 \pm 0.2$	$4.8 \pm 0.2$
Total root length (cm)	$15.8 \pm 0.2$	$26.1 \pm 0.4$
Max. root length (cm)	$5.5 \pm 0.2$	$6.8 \pm 0.4$
Root diameter (cm)	$1.78 \pm 0.1$	$0.51 \pm 0.03$

Table 3.2: Morphological characteristics of seedlings at the beginning of the field experiment (mean  $\pm$  SE,  $n = 144$ ).

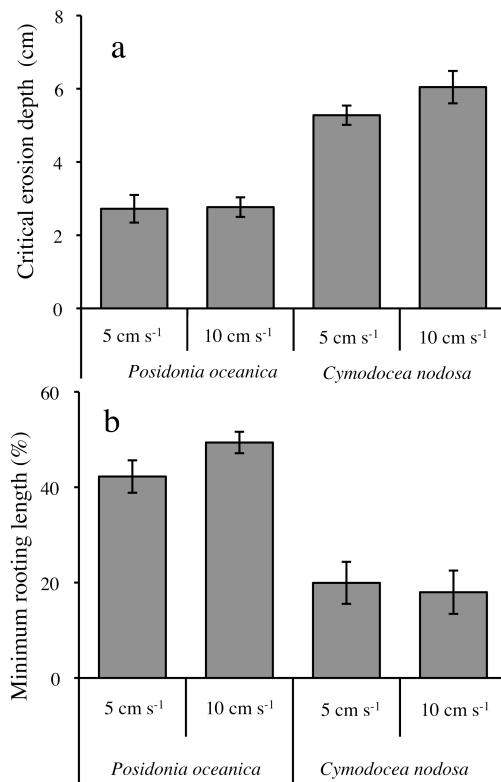


Figure 3.7: (a) Critical erosion depth and (b) Minimum rooting length of *Posidonia oceanica* and *Cymodocea nodosa* exposed to two orbital velocities ( $u = 5$  and  $10 \text{ cm s}^{-1}$ ).

Between September and October 2009, a storm with  $H_s$  of 1.5 m and  $T_p$  of 7 s was measured at deep waters. During this period, the first losses of *P. oceanica* seedlings were observed. Computed  $u$  for this period in Cap Enderrocot was  $8.6 \text{ cm s}^{-1}$  at 18 m depth and  $28 \text{ cm s}^{-1}$  at 12 m depth while in Cala Blava was  $7.3 \text{ cm s}^{-1}$  at 18 m depth and  $14.7 \text{ cm s}^{-1}$  at 12 m depth (Table 3.3). The percentage of *P. oceanica* seedlings surviving in Cala Blava was significantly higher than that in Cap Enderrocot (3.8a; Table 3.4). Moreover, the percentage was significantly higher in the deeper (18 m) than in the shallow (12 m) sites. The loss for *C. nodosa* was also significant but no differences in the percentage of survivorship among sites and depths was detected.

---

	Cap Enderrocat		Cala Blava	
	12 m	18 m	12 m	18 m
Aug-Sep	< 5	< 5	< 5	< 5
Sep-Oct	18.0 ± 1.1	8.6 ± 0.3	14.7 ± 0.9	7.3 ± 0.2
Oct-Nov	34.4 ± 2.2	18.2 ± 1.2	29.4 ± 1.9	17.0 ± 1.1
Nov-Feb	46.0 ± 2.3	25.5 ± 1.2	39.1 ± 1.5	23.4 ± 1.1

---

Table 3.3: Computed near-bottom orbital velocities ( $\text{cm s}^{-1}$ ) at the experimental locations during the sampling periods (mean  $\pm$  SD).

From October to November 2009, two storms from the southwest with  $H_s$  of 4 and 2.5 m and  $T_p$  of 10 and 8 s respectively were recorded at deep waters. After these storms, all *P. oceanica* seedlings disappeared in both Cap Enderrocat and Cala Blava sites while *C. nodosa* seedlings persisted in Cala Blava at both depths (Fig. 3.8b). Computed  $u$  at the experimental sites varied between 17 to 34  $\text{cm s}^{-1}$  (Table 3.3).

From November 2009 to February 2010 several storms were recorded with maximum  $H_s$  of 5 m and  $T_p$  of 11 s at deep waters (Fig. 3.8c). Remaining seedlings of *C. nodosa* persisted during this period. Computed  $u$  in this site varied between 23 and 39  $\text{cm s}^{-1}$  during that period of time.

### 3.4 Discussion

This Chapter offers a mechanistic insight into how the combination of drag and erosion may cause seedling dislodgement from the substrata. Results showed that drag forces were higher in *P. oceanica* seedlings than in *C. nodosa* under both current and waves, and that *P. oceanica* seedlings are earlier dislodged than *C. nodosa* seedlings. Thus flume results predict survival of *C. nodosa* seedlings to exceed that of *P. oceanica* seedlings. Field experiments confirmed this, by showing that seedlings were dislodged during storms, and that *C. nodosa* seedlings survived longer than *P. oceanica*.

Measured drag force per unit total leaf surface area is on average ( $3 \pm 1.2$   $\text{N/m}^2$  mean  $\pm$  SE) for both the *P. oceanica* and *C. nodosa* seedlings at  $u =$

---

---

	df	MS	<i>F</i>
Location	1	9401	40.1 ***
Depth	1	350	1.5 ns
Species	1	3151	13.5 **
Location x Depth	1	651	2.8 ns
Location x species	1	2109	9.1 **
Depth x species	1	2433	10.3 **
Location x depth x species	1	2109	9.2 **
Error	16	234	

---

Table 3.4: Results of three-factor way ANOVA of seedling survival percentage in October 2009. Significant differences are expressed in bold as \*\*  $p < 0.01$  , \*\*\*  $p < 0.001$ , and (ns) not significant. Cochran's C-test no significant. df = degrees of freedom and MS = mean square

16 cm s<sup>-1</sup>, which was in the same order of magnitude as earlier measurements for seagrass model plants with flexible shoots (5.5 - 7.8 N/m<sup>2</sup>) at 37 cm s<sup>-1</sup> (Bouma et al. 2005). For seedling survival, it is however the absolute drag force rather than the drag per unit surface area that matters. Present flume experiments show that drag coefficient,  $C_D$ , depends on Reynolds number but not on the species and that this relationship is different for current and waves (Fig. 3.6). The computed drag coefficients for the individual seedlings of *P. oceanica* and *C. nodosa* are between 0.01 and 0.1 for Reynolds numbers between 10<sup>3</sup> and 10<sup>5</sup>, which is in accordance with those provided for flexible macrophytes (Sand-Jensen 2003, Martone and Denny 2008). It should be noted that drag coefficients for meadows can depend on many factors such as the height and density of the plants, the distance travelled by waves, etc. and that drag coefficient for meadows thus may differ from the values presented for single plants.

Sediment mobilisation is related to hydrodynamics (wave and currents) which can bury or dislodge seagrasses (Madsen et al. 2001, Teeter et al. 2001, Cabaco et al. 2008). Previous studies have shown that 2 cm of sediment erosion caused 75 % of mortality in *C. nodosa* seedlings in stagnant water (Marbà and Duarte 1994), but to my knowledge there are no data about the effect of sediment erosion on *P. oceanica* seedlings. In this Chapter is shown that *P. oceanica* seedlings under waves tolerate less sediment erosion (2 - 3 cm) to become dis-

---



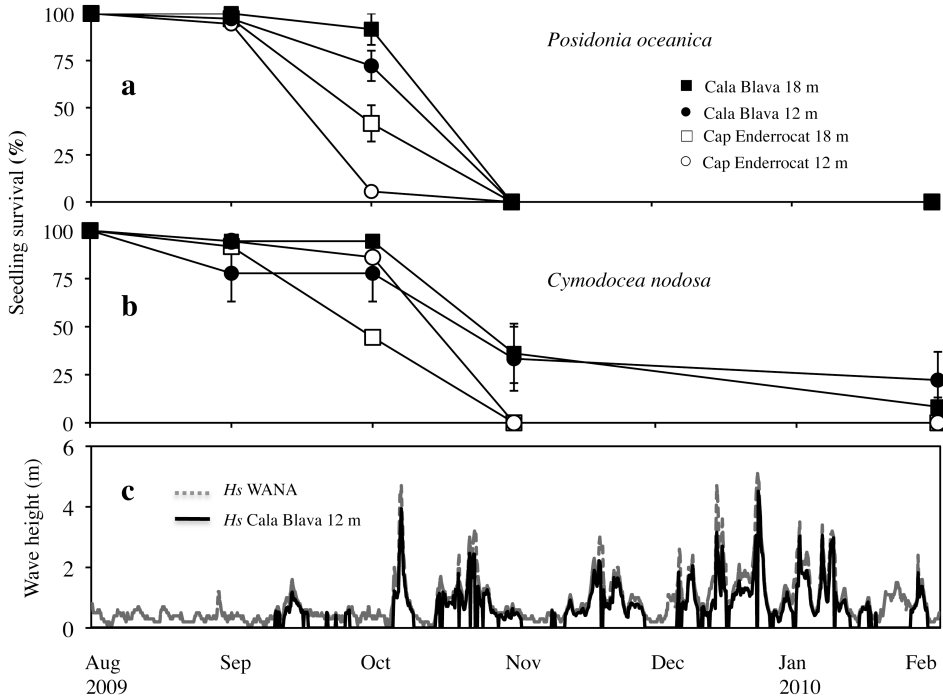


Figure 3.8: Seedling survival on the experimental plots in Mallorca, August 2009 to February 2010. (a) *Posidonia oceanica*, (b) *Cymodocea nodosa*, and (c) wave heights in deep water (WANA node) shown in grey line and propagated wave heights in Cala Blava at 12 m depth shown in black line. Gaps in propagated  $H_s$  corresponds to wave directions other than Southwest to Southeast no affecting the study area.

lodged than *C. nodosa* (5 - 6 cm). *P. oceanica* seedlings need a root length of 0.35 times the square root of the total leaf area to remain anchored while in *C. nodosa* this condition is increased up to 1.6 times the square root of leaf area. However, seedlings of *P. oceanica* in the flume have a foliar area that is on average 20 times higher than those of *C. nodosa* and therefore the seedling capacity to remain anchored is much more limited for *P. oceanica* than *C. nodosa*. This suggests that *P. oceanica* seedlings are adapted to grow at ambients less energetic than *C. nodosa*. This may also be inferred from the proportionally higher root biomass and lower leaf biomass that *C. nodosa* allocates compared to *P. oceanica* (Guidetti et al. 2002). Anderson et al. (2006) described the dislodgement of coenocytic green algae from soft sediments by waves measuring

the mean force to dislodge the algae (4.9 - 12.7 N) which increased as the leaf surface area increased.

The seedling survival in the field also showed that *P. oceanica* and *C. nodosa* seedlings behave differently under the same hydrodynamic conditions. *C. nodosa* seedlings survived longer than *P. oceanica* in Cala Blava during the field experiment. *P. oceanica* seedlings survived at a higher proportion in the deep than in the shallow sites at both locations during October 2009. In November 2009, all *P. oceanica* seedlings disappeared in the plots while *C. nodosa* seedlings persisted at both depths in Cala Blava. Two storms took place before the complete loss of *P. oceanica* seedlings in November 2009. It can not be determined which of these two events caused seedling loss but it can conclude that these storms had a deleterious effect on the survival of *P. oceanica* seedlings. The presence of a large *P. oceanica* meadow from the shallow areas to 30 - 35 m depths demonstrates that the seagrass is not light limited at the study site (Fig. 3.2c). Herbivory is not considered to be a cause of seedling loss because bite scars on the leaves were not observed. Different environmental conditions between sites associated with hydrodynamics such as sediment resuspension and turbidity could have an effect on the seedling survival, although, these are indirect effects to wave exposure. Some studies have shown high mortality of seedlings in the field after storms. A mortality of 75 % to 100 % natural and transplanted *P. oceanica* seedlings on pebbles occurred during the first winter after planting, associated to storms (Balestri et al. 1998). Individual seedlings of four different *Posidonia* spp. planted in a blow out area did not succeed after 1 year (Kirkman 1998).

Water depth had an effect on seedling survival, as wave induced orbital velocities attenuate with depth, near-bottom orbital velocities will be higher at 12 m than at 18 m. In October 2009, a significantly lower survival was observed for *P. oceanica* at 12 m than at 18 m (Fig. 3.8a; Table 3.4). Piazzi et al. (1999) observed lower survival rates of *P. oceanica* seedlings at 2 m depth than at 10 m depth. A correlative study in a *P. oceanica* meadow (Infantes et al. 2009) suggested that at depths between 0 to 5 m near-bottom orbital velocities were too high for *P. oceanica* to be present while at depths deeper than 7 m velocities were lower and a dense meadow was present.

---

Infantes et al. (2009) estimated a threshold in near-bottom orbital velocities of 38 - 42 cm s<sup>-1</sup> for a *P. oceanica* meadow to be present in a shallow bay. In this study, *P. oceanica* seedlings had a 100 % survivorship at near-bottom orbital velocities below 5 cm s<sup>-1</sup>, but for velocities between 7 - 18 cm s<sup>-1</sup> the percentage of seedlings surviving decreased and all seedlings disappeared at velocities above 18 cm s<sup>-1</sup>. Some *C. nodosa* seedlings survived at velocities of 39 cm s<sup>-1</sup>. Thus, these results suggest that seedlings tolerate lower orbital velocities than mature plants. This is not surprising, because mature plants develop a network of roots and rhizomes that penetrate deeper into the substrata than seedlings. Other studies showed that transplanted *Zostera marina* survived at orbital velocities of 40 cm s<sup>-1</sup> but not at 60 cm s<sup>-1</sup> (van Katwijk and Hermus 2000). For meadows, Cabaco et al. (2010) estimated that the decline of *C. nodosa* occurs at velocities over 60 cm s<sup>-1</sup>.

Flow velocity is an important factor determining the size of the marine organisms that inhabit benthic ecosystems (Denny et al. 1985). Present results suggest that the higher drag of large species may make small species relatively more successful in the colonisation of exposed sites. This agrees with the convention (based on size-related differences of growth rates) that large seagrass species generally occupy low energy or sheltered habitats while small seagrass species are able to colonize more energetic habitats because the capacity of small species to recover from disturbance through growth is higher than that of large species (Duarte 1991, Idestam-Almquist and Kautsky 1995, Laugier et al. 1999). Results presented in this Chapter that seedlings of *C. nodosa* are able to persist under higher wave energies than those of *P. oceanica*, are also in agreement with the old but untested assumption that *C. nodosa* is a pioneer species that stabilises the substrata and facilitates the establishment of *P. oceanica* (Den Hartog 1970).

The findings presented in this Chapter provide the basis for understanding seedling survivorship of two Mediterranean seagrass species in sandy substratum under different hydrodynamic conditions. Morphological characteristics of each species such as foliar surface and root length are key factors in colonisation processes. Moreover, drag and sediment erosion play an important role in seedling survival, a crucial stage of seagrass life. Habitat degradation and fragmentation caused by anthropogenic effects around the world's coastal zones raises the need to manage and restore seagrass beds (Short and Wyllie-Echeverria 1996, Orth

---

et al. 2006). Seedling plantings could be more effective in seagrass restoration if more quantitative knowledge on the hydrodynamic effects that limit the survival of seagrass seedlings is gathered.

## Chapter 4

# Assessment of substratum effect on the distribution of two invasive *Caulerpa* (Chlorophyta) species

Part of this Chapter has been published as an article on *Estuarine, Coastal and Shelf Science*<sup>1</sup>

### 4.1 Summary

Two-year monitoring of the invasive marine Chlorophyta *Caulerpa taxifolia* and *Caulerpa racemosa* var. *cylindracea* shows the great influence of substratum on their spatial distribution. The cover of *C. taxifolia* and *C. racemosa* was measured in shallow (< 8 m) areas indicating that these species are more abundant in rocks with photophilic algae and in the dead matte of the seagrass *Posidonia oceanica* than in sand or inside the *P. oceanica* meadow. A short-term experiment comparing the persistence of *C. taxifolia* and *C. racemosa* planted either in a model of dead matte of *P. oceanica* or in sand shows that the persistence of these species was higher in the dead matte model than in sand. Correlative

---

<sup>1</sup>Infantes E, Terrados J, Orfila A (2011) Assessment of substratum effect on the distribution of two invasive *Caulerpa* (Chlorophyta) species. *Estuar. Coast. and Shelf Sci.* 91: 434-441.

evidence suggests that *C. taxifolia* and *C. racemosa* tolerate near-bottom orbital velocities below  $15 \text{ cm s}^{-1}$  and that *C. taxifolia* cover declines at velocities above that value. These results contribute to understand the process of invasion of these *Caulerpa* species predicting which substrata would be more susceptible to be invaded and to the adoption of appropriate management strategies.

## 4.2 Methods

### 4.2.1 Study Sites

The study was carried out in four shallow (depth less than 8 m) locations on the South coast of Mallorca Island, Western Mediterranean sea (Fig. 4.1a). Cala D'Or was chosen for this study because it is the only location in the Balearic Islands where *Caulerpa taxifolia* is present. *Caulerpa racemosa* is mainly found in the South of Mallorca, and the locations of Sant Elm, Cala Estancia and Portals Vells where chosen (Fig. 4.1b). Sand patches, rocky reefs covered by an erect stratum of photophilous macroalgae and meadows of the seagrass *Posidonia oceanica* are the main components of the undersea landscape at the study sites.

### 4.2.2 Presence of *Caulerpa* over different substrata

The cover of *Caulerpa taxifolia* in Cala D'Or and that of *Caulerpa racemosa* in Cala Estancia and Portals Vells was measured during two consecutive summers and winters (years 2007 and 2008) which represent the periods of maximum and minimum vegetative development of these species in the Western Mediterranean (Piazzini and Cinelli 1999). Four to eight 20 m long transects were laid haphazardly at each location and the percentage of substratum covered by *Caulerpa* was estimated at 1 m intervals along the transects by placing two 20 cm x 20 cm quadrats divided in 25 cells of 4 cm<sup>2</sup>. The number of cells corresponding to each type of substratum in each quadrat was counted as well as the number of cells of each substratum type colonized by *Caulerpa*. Substrata were classified either as sand, rocks (always covered by photophilic algae), *Posidonia oceanica* meadow or dead matte of *P. oceanica*. The matte of *P. oceanica* is formed by the accumulation of sediment, rhizomes and/or roots of this seagrass species over time, building a terraced structure that retains the sediment even after seagrass death and that may last hundreds of years (Mateo et al. 1997).

---

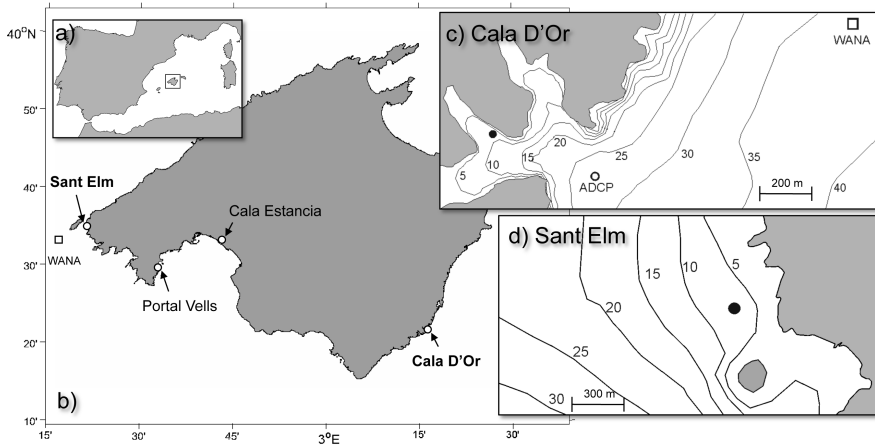


Figure 4.1: Location of the study areas. (a) Mallorca Island in the Mediterranean Sea. (b) Location of the four study areas and deep water wave data (WANA nodes). (c) Bathymetry of Cala D'Or with location of WANA node. (d) Bathymetry of Sant Elm. Experimental plots, WANA nodes and ADCP location in Cala D'Or.

### 4.2.3 Short-term experiment evaluating substratum effect on *Caulerpa* persistence

The experiment evaluated the persistence of *Caulerpa* fragments planted in sand plots (Fig. 4.2a) and in plots of a model of *Posidonia oceanica* dead matte (Fig. 4.2b). The experiment was performed in two locations: Cala D'Or for *Caulerpa taxifolia* and Sant Elm for *Caulerpa racemosa* (Fig.4.1b). These two locations were selected because *C. racemosa* is not present in Cala D'Or, which is the only place where *C. taxifolia* is present in the Balearic Islands, and it was not consider appropriate to contribute to the dispersion of these invasive species by transplanting them to other locations. Besides, the *C. racemosa* experiment was not perform in Cala Estancia or Portals Vells because these sites are highly visited by swimmers and snorkelers and the risk of disturbance to experimental plots was high. A sand patch large enough to hold all the experimental plots at a depth of 7 - 8 m was selected at each location. These sand patches were surrounded by *P. oceanica* meadows.

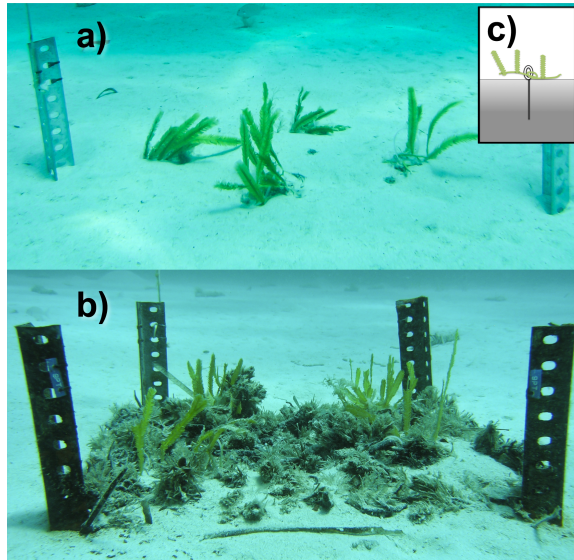


Figure 4.2: Photographs of the experimental set up for *Caulerpa taxifolia* in (a) natural sandy bottom and (b) the model of dead matte of the seagrass *Posidonia oceanica*. (c) Illustration of *Caulerpa* fragments fixed to the plots using pickets.

Six 50 cm x 50 cm plots were established in each location separated every 5 m. Plots were delimited at the corners with galvanized iron bars. The model of dead matte of *Posidonia oceanica* was constructed by attaching fragments of dead *P. oceanica* rhizomes collected from fresh beach-cast plants after a storm to 50 cm x 50 cm squares of plastic gardening mesh, using plastic cable ties (Fig. 4.2b). A density of around 500 vertical rhizomes per m<sup>2</sup> was used as this is a typical *P. oceanica* shoot density found at 8 m depth in clear Mediterranean waters (Marbà et al 2002, Gobert et al. 2003, Terrados and Medina-Pons 2008). A model of dead matte of *P. oceanica* was used instead of natural occurring dead matte to standardize the methodology having the same substratum types in both locations. The dead matte models were attached to the bars delimiting the randomly assigned plots (n = 3) with cable ties and using four pickets to anchor it firmly to the sediment (Fig. 4.2b). The sand plots (n = 3) were made of the naturally occurring sand and placement of the galvanized iron bars delimiting plot corners was the only manipulation performed.

Fragments of *Caulerpa* including at least one stolon apex and 3-4 fronds each were manually collected from the same area and depth where the experimental



plots were located and held in aerated seawater at sea surface until planting. Sixteen *Caulerpa* fragments were fixed to each plot within 2h after collection by threading them in groups of four into four cable-tie loops anchored in each plot using galvanized iron pickets (see Fig. 4.2c). The experiment started in July of 2007 as previous studies on biomass seasonality of *Caulerpa taxifolia* in shallow waters (6 - 10 m) have shown that maximum biomass occurs in summer and autumn (Thibaut et al. 2004). Monitoring of *Caulerpa* cover in each plot was carried out approximately every 30 days for *C. taxifolia* and 15 days for *Caulerpa racemosa* as the latter species has a higher growth rate (Piazzi et al. 2001) using underwater digital photography.

Photographic sampling techniques have been previously used to measure *C. racemosa* cover (Piazzi et al. 2003). In this study, underwater photographs were taken to evaluate the persistence of *Caulerpa* in the plots by analyzing the area covered by the algae over time. This method allowed taking many samples in the field as diving time is limited. Each plot was divided on 4 sub-plots of 25 x 25 cm to improve the delineation of the algae on the photographic images. As algae can swing with wave orbital movements that could affect the area facing up on the images, three images of each sub-plot were taken on calm days. A scale was placed on each sub-plot next to the algae when taking the underwater photographs. Open software (ImageJ, NIH) was used to measure the area of *Caulerpa* on each photograph. To determine the absolute area on the images a relationship between image pixels and real dimensions ratio was established on each image using the scale. In order to test the method, photographs were taken in the laboratory and in the sea before the experiment began. A set of figures of known areas was used to test the output of the image processing analysis, providing an error around 6 %.

#### 4.2.4 Wave climate and modelling at the short-term experimental sites

The propagation of the deep water mean wave climate between sampling dates was performed using a numerical model which allows the calculation of the wave induced near-bottom orbital velocity at the study sites. Significant wave height ( $H_s$ ), peak period ( $T_p$ ) and direction were acquired from July 2007 to March 2008 at deep water which corresponds to the duration of the short-term experiment (see 4.1b, c, for the location of these points). The deep water data have

---

been obtained from the WANA system, a reanalysis with real data of a third generation spectral WAM model and was provided by the Spanish harbour authority operational system. These deep water wave conditions were propagated to the study sites using a numerical model based on the mild slope parabolic approximation (Kirby and Dalrymple, 1983) and near-bottom orbital velocities ( $u_b$ ) at the experimental locations were obtained from the model outputs using linear wave theory (Infantes et al. 2009). These models are widely used in engineering and scientific approaches in order to obtain the accurate wave field in coastal areas from open sea conditions since refraction and diffraction are well captured (Alvarez-Ellacuria et al. 2010).

#### 4.2.5 Field wave measurements and velocity profiles

To test the results of deep water wave propagations, field measurements were performed on the 8th of November of 2007 in Cala D'Or measuring wave conditions ( $H_s$  and  $T_p$ ) at deep and shallow water as well as near-bottom velocities in shallow water on both substrata. An Acoustic Doppler Current Profiler (ADCP) RDI, Sentinel 600 kHz, was deployed at approximately 400 m from the experimental site at a depth of 26 m. The ADCP was set to record 20 min burst intervals every 60 min with a 2 Hz frequency. It was mounted on a tripod at 0.5 m above the bed.  $H_s$  obtained by propagating the deep water conditions to shallow waters, are within a 15 % error to those measured in situ at deep and shallow waters, showing the accuracy of modelled wave conditions. Table 4.1 shows the data provided by the numerical model and those measured by the ADCP at deep water (26 m) and with the ADV at shallow water (7.5 m) on the 8th of November of 2007.

---

	Model outputs	Field measurements
$H_s$ Deep water (26 m)	$0.53 \pm 0.02$ m	$0.47 \pm 0.03$ m
Shallow water (7.5 m)	$0.26 \pm 0.02$ m	$0.21 \pm 0.02$ m

---

Table 4.1: Wave heights from model outputs and field measurements in Cala D'Or (means  $\pm$  95 % CL).

Additionally, vertical profiles of velocity were measured on the *P. oceanica*

---

dead matte model and on sand using Acoustic Doppler Velocimeters (ADV), Vector, Nortek. Simultaneous measurements on both substrata were performed using two ADVs at seven positions (2.5, 5, 10, 20, 40, 60 and 100 cm above the bottom). The instruments were set to measure during 25 min with a frequency of 32 Hz, a nominal velocity range of  $0.1 \text{ m s}^{-1}$  and a sampling volume of 11.8 mm. The ADVs were mounted in a down-looking position on stainless steel bottom fixed structures. Stability of the equipment was verified with the compass, tilt and roll sensors. Raw data were processed by first filtering for low beam correlation ( $< 70 \%$ ). Velocity data were then filtered with a low pass filter to remove high frequency Doppler noise (Lane et al. 1998). Horizontal velocity was calculated as the root mean square (rms). From the velocity profiles, friction coefficients  $C_f$  over sand and dead matte substrata were computed following Simarro et al. (2008).

$$C_f = \frac{\tau_b}{\rho u_c^2} \quad (4.1)$$

where  $\tau_b$  is the bottom shear stress,  $\rho$  the density of seawater and  $u_c$  a characteristic velocity outside the boundary layer. The bed shear stress can be found from,

$$\tau_b = \rho(\nu_T \frac{du}{dz})_{z=\delta} \quad (4.2)$$

where  $\nu_T$  is the eddy viscosity and  $du/dz$  the vertical variation of the velocity evaluated at the outside of the boundary layer  $\delta$ .

Temperature HOBO<sup>®</sup> StowAway Tidbit loggers were moored next to the plots in Cala D'Or and Sant Elm during the experiment. Temperature was recorded every 2 h and averages of water temperature between sampling dates were calculated. The numbers of daylight hours were obtained from the US Naval Observatory (<http://aa.usno.navy.mil/>) for the study areas and averages of daylight hours between sampling dates were also calculated.

#### 4.2.6 Statistical Analysis

A Chi-squared test ( $\chi^2$ ) was used to evaluate if the colonization of benthic communities by *Caulerpa* species depends on the type of substratum, that is, if some substrata are more favourable/unfavourable than others for the colonization of these species. The null hypothesis of the test assumes substratum-independent, random colonization and allows the calculation of expected cover

of *Caulerpa* species in the different substrata that is compared with the cover observed. Changes in cover of *Caulerpa* species through time in the short-term experiments were evaluated using univariate repeated-measures ANOVA. “Substratum” (sand versus model of dead matte of *P. oceanica*) was the between-subjects factors (fixed) and “Time” was the within-subjects factor (random) for both *Caulerpa* experiments. A significant Time x Substratum interaction was to be expected if the type of substratum has an effect on the persistence of *Caulerpa* in the plots. A Cochran’s C-test was used to test for heterogeneity of variances.

### 4.3 Results

*Caulerpa taxifolia* was more abundant in the dead matte of *Posidonia oceanica* than in the rest of substratum types available in Cala D’Or (Fig. 4.3a). *C. racemosa* was also more abundant in the dead matte of *P. oceanica* but it additionally colonized other substrata such as rocks with photophilic algae and sand (Fig. 4.3b). The percent cover of *C. taxifolia* over dead matte showed small changes between summer and winter (Fig. 4.3a). In contrast, the percent cover of *C. racemosa* was highly seasonal since large differences between summer and winter were observed (Fig. 4.3b).

The relative frequencies of the different types of substratum in the total surface of sea bottom surveyed and of the presence of *Caulerpa* on each substratum are shown in Fig. 4.4 for each sampling event. Different distribution of frequencies indicates that *Caulerpa* species do not distribute randomly in the substrata (Table 4.2). Results from the  $\chi^2$  test show that both *Caulerpa* species are found in the dead matte of *P. oceanica* and in rock on a higher proportion than expected in relation to the amount of substratum type available at the study sites. In contrast, *Caulerpa* species are found in a lower proportion than expected in sand and inside the *P. oceanica* meadow. Experimental  $\chi^2$  were largely above critical values (Table 4.2).

The significant “Time x Substratum” interaction in both species (Table 4.3) indicates that substratum type affected the persistence of the two *Caulerpa* species. The temporal evolution of *Caulerpa* cover in the plots (Figs. 4.5a and 4.6a) shows that the persistence of *Caulerpa* was higher in the model of dead

---

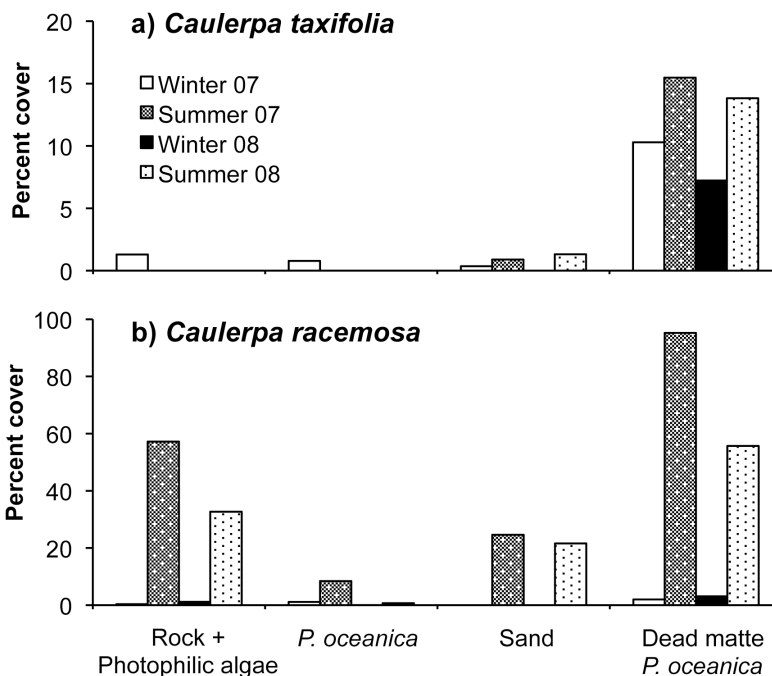


Figure 4.3: Percent cover of (a) *Caulerpa taxifolia* and (b) *Caulerpa racemosa* in the different types of substratum during two consecutive years.

matte of *P. oceanica* than in sand. *C. taxifolia* cover on dead matte increased until the 28th of September while *C. taxifolia* cover on sand did not change during the same period of time (Fig. 4.5a). After the 28th of September, *C. taxifolia* cover decreased with time in both substrata and by the end of winter no *C. taxifolia* was present in the plots. The cover of *C. racemosa* in the model of dead matte increased during the first five weeks of the experiment while on sand was roughly maintained (Fig. 4.6a). After August 30th, the *C. racemosa* experiment was disturbed by a storm that buried the plots with a 30 - 70 cm thick layer of drifting macroalgae and *P. oceanica* leaves causing the death of all *C. racemosa* fragments in the plots.

Seawater temperature in Cala D'Or (*Caulerpa taxifolia* site) changed from 26°C in July to 14°C in March, while the number of daylight hours was reduced from 14.5 h to 9 h (Fig. 4.5b). Conditions in Sant Elm (*Caulerpa racemosa* site) during the experiment were rather constant with a seawater temperature

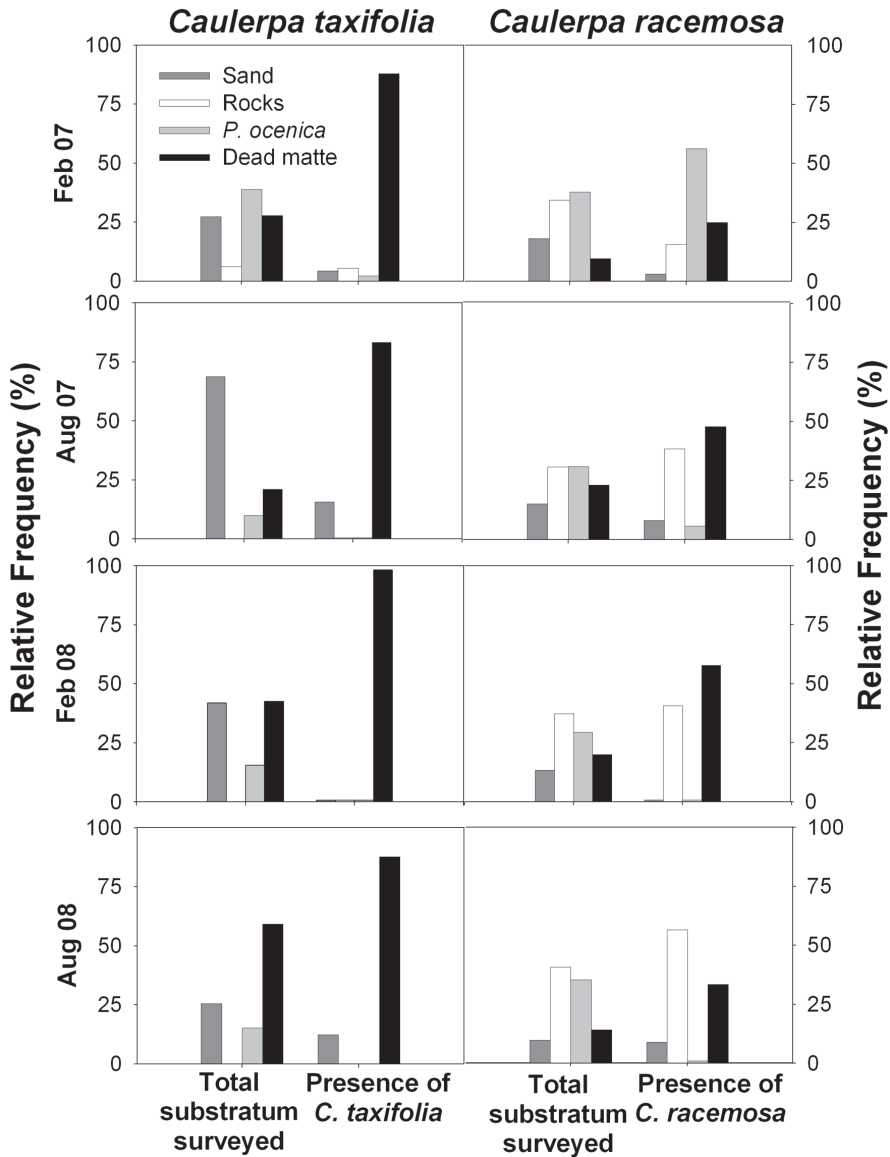


Figure 4.4: Relative frequency of total substratum surveyed and of the presence of *Caulerpa taxifolia* and *Caulerpa racemosa* on each substratum. Low presence of rocks was recorded at the *C. taxifolia* site. Rocky bottom with photophilic algae is indicated as Rocks.

		Rock	<i>P. oceanica</i>	Sand	Dead matte <i>P. oceanica</i>	$\chi^2$
<i>C. taxifolia</i>	Winter 07	–	64 L	36 L	240 M	340***
	Summer 07	–	20 L	79 L	336 M	465***
	Winter 08	–	23 L	65 L	121 M	208***
	Summer 08	–	77 L	32 L	69 M	178***
<i>C. racemosa</i>	Winter 07	3 –	3 –	7 M	7 M	20***
	Summer 07	80 M	879 L	142 L	1153 M	2272***
	Winter 08	1 M	34 L	16 L	91 M	142***
	Summer 08	146 M	796 L	2 L	629 M	1573***

Table 4.2: Chi-square ( $\chi^2$ ) test of observed *Caulerpa* cover on different substrata. *Caulerpa taxifolia* has a critical  $\chi^2$   $p=0.001^{***}$ ,  $2df = 13.81$  and *Caulerpa racemosa* has a critical  $\chi^2$   $p=0.001^{***}$ ,  $3df = 16.26$ . *C. taxifolia* was not found on rock substratum in enough quantities for the test. The type of contribution was classified as more than expected (M) or less than expected (L).

of 26°C and the number of daylight hours between 14 and 13 h (Fig. 6b).

*Caulerpa taxifolia* cover was maintained or increased with estimated near-bottom orbital velocities below 15 cm s<sup>-1</sup> and declined above that value (Fig. 4.5b). *Caulerpa racemosa* was also able to maintain or increase its cover at the same velocity values (Fig. 4.6b). The vertical profiles of velocity indicate that the width of the boundary layer is around 10 cm (Fig. 4.7) showing also a significantly higher reduction of the horizontal rms velocity in the model of dead matte of *P. oceanica* ( $1.5 \pm 0.2$  cm s<sup>-1</sup>, mean  $\pm$  95 % CL) than in sand ( $2.2 \pm 0.2$  cm s<sup>-1</sup>, mean  $\pm$  95 % CL), ( $t$ -test:  $t = 115$ ,  $df = 103598$ ,  $p < 0.01$ ).

The friction coefficient computed for the dead matte model was higher ( $1.04 \times 10^{-1}$ ) than for sand ( $2.33 \times 10^{-2}$ ). Increased friction by the dead matte model would reduce the magnitude of the velocities compared to sand. Wave data from the ADCP showed that wave conditions did not change during the ADV profile measurements, with  $H_s$  of  $0.5 \pm 0.1$  m,  $T_p$  of  $9.5 \pm 0.5$  s and South East direction.

	df	MS	F	p
<i>C. taxifolia</i>				
Intercept	1	469997	293	0.000***
Substratum	1	17685	11	0.029 ns
Error	4	1600		
Time	3	5580	2.9	0.075 ns
Time x Substratum	3	7086	3.7	0.041*
Residual	12	1884		
<i>C. taxifolia</i>				
Intercept	1	41205	36	0.003***
Substratum	1	8321	7	0.053 ns
Error	4	1128		
Time	3	1790	4.6	0.023*
Time x Substratum	3	1929	4.9	0.018*
Residual	12	390		

Table 4.3: Results of repeated measures of ANOVA performed to evaluate if the cover of *Caulerpa taxifolia* and *Caulerpa racemosa* was different between a model of dead matte of *Posidonia oceanica* and a sandy substratum. \* $p < 0.05$ , \*\*\* $p < 0.001$ , ns = not significant. Cochran tests were not significant.

## 4.4 Discussion

The results of this Chapter indicate that substratum plays an important role in the distribution of these invasive *Caulerpa* species. Field measurements show that the presence of *Caulerpa taxifolia* and *Caulerpa racemosa* on the substrata is not at random. Dead matte of the seagrass *Posidonia oceanica* and rock covered with photophilic algae are more favourable than sand to the presence of *Caulerpa* species. Experimental results show that substratum has a significant effect on the persistence of both *Caulerpa* species and confirm that is higher in the model of dead matte of *P. oceanica* than in sand. Hence, the results of both analyses are consistent to each other and suggest that the type of substratum influences the abundance of these invasive *Caulerpa* species.



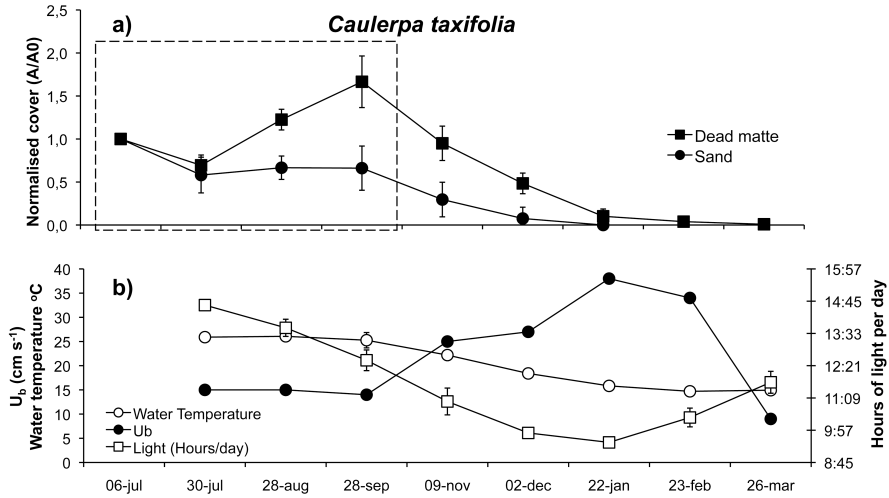


Figure 4.5: (a) *Caulerpa taxifolia* cover (normalised means  $\pm$  SE,  $n = 3$ ). (b) Water temperature at the experimental site, hours of light per day and near-bottom orbital velocities,  $u_b$  (means  $\pm$  SD). Cover area on each sampling date (A) in cm<sup>2</sup> normalised by initial cover area (A0). Dotted square indicates the period used for the statistical analysis ANOVA, Table 4.3.

Understanding the factors that regulate the establishment and spread of introduced *Caulerpa* species is important to predict future pathways of invasion as well as the susceptible areas to be invaded (Carlton and Geller 1993, Bax et al. 2003, Cebrian and Ballesteros 2009). Previous studies mainly based on direct observation indicated that favourable substrata for the establishment of *Caulerpa* spp. are dead matte of *Posidonia oceanica* (Piazzi and Cinelli 1999, Piazzi et al. 2001, Ruitton et al. 2005) and rocky bottoms covered by turf algae (Ceccherelli et al. 2002, Piazzi et al. 2003, Bulleri and Benedetti-Cecchi 2008). A propagation model of *Caulerpa taxifolia* assumed that the settlement probabilities of this species were high for dead matte, harbour mud, and rocks with photophilic algae and low for *P. oceanica* and unstable sand (Hill et al. 1998) but no explanation of how these probabilities were set is given. This Chapter provides the first quantitative evaluation of previous descriptions of dead matte of *P. oceanica* as being a favourable substratum for the colonization of invasive *Caulerpa* species. It also provides quantitative evidence that rocks covered with photophilic algae are also a favourable substratum for *Caulerpa racemosa* colonization. Sand and *P. oceanica* meadows are less favourable than

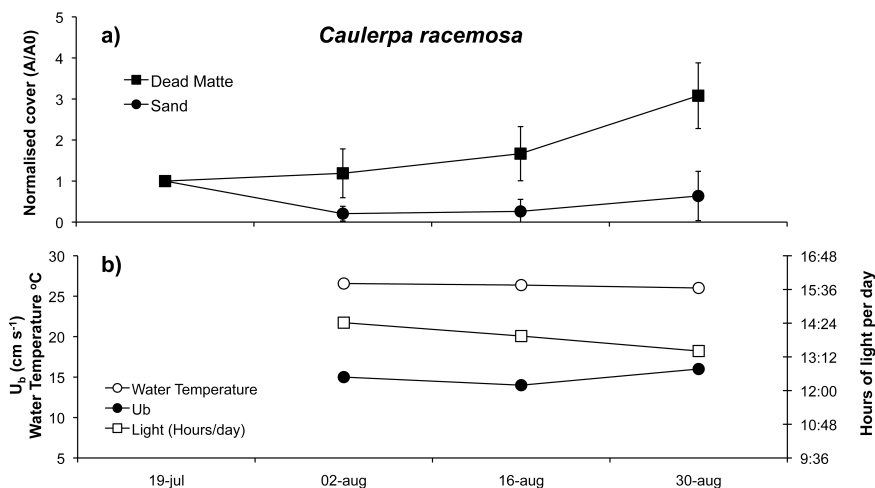


Figure 4.6: (a) *Caulerpa racemosa* cover (normalised means  $\pm$  SE,  $n$  3). (b) Water temperature at the experimental site, hours of light per day and near-bottom orbital velocities,  $u_b$  (means  $\pm$  SD). Cover area on each sampling date (A) in  $\text{cm}^2$  normalised by initial cover area (A0).

the dead matte of *P. oceanica* and rocks covered with photophilic algae for the colonization of *C. taxifolia* and *C. racemosa*.

The positive association between consolidated substrata (rocks and dead matte) and the presence of invasive *Caulerpa* species suggests that near-bottom orbital velocity may be an important determinant of the spatial distribution of these species at shallow depths. The capacity of *Caulerpa* to acquire nutrients from the sediment through the rhizoids (Williams 1984, Chisholm et al. 1996) might be invoked to explain the preferential distribution of invasive *Caulerpa* on dead matte of *P. oceanica* but not over rocky substrata where the amount of sediment is much lower than in dead matte. The structural complexity of the substratum facilitates the retention of *Caulerpa taxifolia* fragments (Davis et al. 2009) and could be a factor to explain why rocky substrata covered by an erect layer of photophilous macroalgae and the *P. oceanica* dead matte are favourable substrata for the establishment of *Caulerpa*. The calculated friction coefficients for the dead matte model and sand indicate that the surface of the dead matte is structurally more complex than sand and that *Caulerpa* fragments established on it will experience lower flow velocities than in sand.

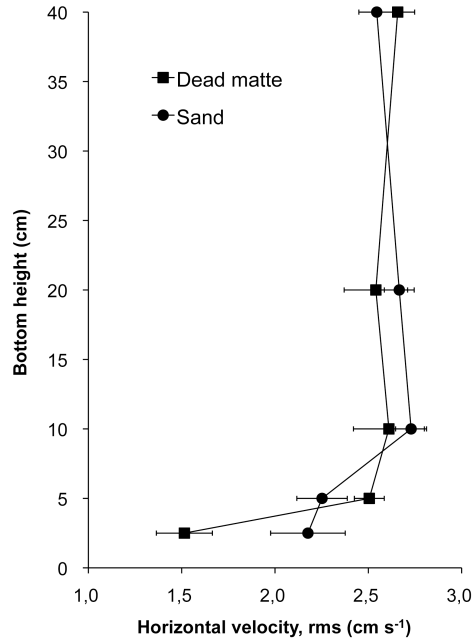


Figure 4.7: Vertical profiles of velocity (means  $\pm$  95 % CL). For convenience only the 40 cm above the bottom is shown.

*Caulerpa taxifolia* and *Caulerpa racemosa* were rarely observed inside the *P. oceanica* meadow in this study and the  $\chi^2$  test shows that *P. oceanica* is not a favourable substratum for the establishment of the introduced *Caulerpa* species even though the matte of the *P. oceanica* meadow is a favourable substratum. Previous studies have also described that dense *P. oceanica* meadows are not invaded by *C. taxifolia* and *C. racemosa* in the short-term (Ceccherelli and Cinelli 1999, Ceccherelli et al. 2000). Dense *P. oceanica* meadows appear to resist the invasion of *C. taxifolia* for more than eight years (Jaubert et al. 1999). Results presented in this Chapter suggest that degraded, low-density *P. oceanica* meadows would be suitable locations for the settlement and growth of invasive *Caulerpa* species if shading by the leaf canopy was the main constraint of *Caulerpa* invasion (Ceccherelli and Cinelli 1999, Ceccherelli et al. 2000), and thus protecting existing meadows would likely reduce the spread of these species in the Mediterranean Sea.

There has been little effort to correlate wave and current energy with the spatial distribution and growth of invasive algae. The effects of wave exposure, morphology and drag forces of the invasive *Codium fragile* were studied under field and flume conditions by D'Amours and Scheibling (2007). These authors suggest that the *C. fragile* became dislodged at flow velocities exceeding 50 cm s<sup>-1</sup>. Moreover, Scheibling and Melady (2008) found that a sheltered location was a more suitable habitat than an exposed location for this species. The effect of wave exposure on *C. racemosa* is not clear since it can be found in both exposed and sheltered locations (Thibaut et al. 2004, Klein and Verlaque 2008). To date, there are no available data on near-bottom orbital velocities that allow the establishment and development of invasive *Caulerpa* species. Results in this Chapter show that *C. taxifolia* and *C. racemosa* do only occur at near-bottom orbital velocities below 15 cm s<sup>-1</sup> and that *C. taxifolia* cover could decline at velocities above that value. This value, however, should not be considered as a velocity threshold for the persistence of *C. taxifolia* because the evidence provided in this Chapter is correlative only and other factors such as seawater temperature and light availability declined as velocities increased in the experimental site (see Figs. 4.5b and 4.6b).

*C. racemosa* was able to colonize sand in summer but disappeared in winter, a season with higher wave energy. One of the potential problems for aquatic macrophytes growing on unconsolidated substrata is sediment movement and deposition that causes uprooting and burial (Fonseca and Kenworthy 1987, Williams 1988, Cabaco et al. 2008). Previous works described that *C. racemosa* was not colonizing fine sand with large ripple marks (Ruitton et al. 2005). Sand with large ripples indicates that orbital velocities are or have been high enough to mobilize the sediment suggesting that only those macrophytes with high anchoring capacity could survive in that location.

Results presented in this Chapter provide novel quantitative evidence highlighting the importance of substratum for the distribution of invasive *Caulerpa* species at shallow depths. It is shown that the two introduced species of *Caulerpa* in the Mediterranean Sea are more abundant in dead mat of *P. oceanica* or rock than inside the *P. oceanica* meadow or sand. These results also suggest the quantitative hydrodynamic conditions that shape colonization as their cover started to decline at near-bottom orbital velocities over 15 cm s<sup>-1</sup>. Further studies should be done to elucidate the validity of this velocity

---

threshold of the colonization of introduced *Caulerpa*.

---



## Chapter 5

# Effect of a seagrass (*Posidonia oceanica*) meadow on wave propagation

Part of this Chapter has been submitted for publication as an article on Marine Ecology Progress Series<sup>1</sup>

### 5.1 Summary

Wave damping induced by the seagrass *Posidonia oceanica* is evaluated using field data from bottom mounted acoustic doppler velocimeters (ADV). Using the data from one storm event, the bottom roughness is calculated for the meadow as  $k_s = 0.42$  m. This roughness length is then used to predict the wave friction factor  $f_w$ , the drag coefficient on the plant,  $C_D$ , and ultimately the wave damping for two other storms. Values for  $C_D$  ranged from 0.1 to 0.4 during both storms. The expected wave decay coefficient for seagrass shoot densities of 200 - 800 shoots  $m^{-2}$  is also predicted. The utility of the bottom roughness for calculating the friction factor and the drag coefficient of a seagrass meadow for conditions in which the meadow height is small compared to the water depth is

---

<sup>1</sup>Infantes E, Orfila A, Terrados J, Luhar M, Simarro G, Nepf H. Effect of a seagrass (*P. oceanica*) meadow on wave propagation (*Under review in Marine Ecology Progress Series*)

demonstrated.

## 5.2 Theory

The bottom boundary layer is a region adjacent to the bottom where the velocity field drops from the value in the core of the fluid to zero at the bed. When seagrasses are present near the bottom, the boundary layer is modified by the seagrass canopy, which influences the mean velocity, turbulence and mass transport (Nepf & Vivoni 2000, Ghisalberti & Nepf 2002, Luhar et al. 2010). A good understanding of the physics of the boundary layer is important because the damping of the waves is mainly due to the friction in the boundary layer where the seagrass is present. *P. oceanica* leaves occupy only a small fraction of the water column and under these conditions the drag associated with the meadow into the bed friction formulation are merged.

The main question to be solved in the analysis of the boundary layer under oscillatory flow is the relationship between the near bed velocity,  $u_b$ , and the bed shear stress transmitted to the combined seagrass and bottom,  $\tau_b$ . The dimensionless parameter relating both quantities is the wave friction factor defined as  $f_w \equiv 2|\tau_b|/\rho u_b^2$ , where  $\rho$  is the fluid density. The friction factor  $f_w$  depends on the Reynolds number and the relative roughness, defined respectively as

$$\text{Re} \equiv \frac{u_b^2}{\nu\omega}, \quad \text{and} \quad \varepsilon \equiv \frac{k_s\omega}{u_b}.$$

Above,  $\nu$  is the kinematic viscosity of the water,  $\omega$  is the wave angular frequency ( $\omega = 2\pi/T$ ) with  $T$  being wave period and  $k_s$  is a length characterizing the bottom roughness, or Nikuradse length. In this approach,  $k_s$  includes both the characteristics of the bottom and of the meadow. If the boundary layer is smooth ( $k_s u_b/\nu < 5$ ), then  $f_w$  becomes a function of the Reynolds number only. If the boundary layer is rough ( $k_s u_b/\nu > 70$ ), the friction factor depends mainly on the relative roughness  $\varepsilon$  (Schlichting 1979).

The friction factor proposed by Nielsen (1992) as a modification of the semiempirical formula of Swart (1974) for sandy bottoms is,

$$f_w = \exp \left\{ 5.5 \left( \frac{k_s\omega}{u_b} \right)^{0.2} - 6.3 \right\}. \quad (5.1)$$



Accounting for signs, the definition of  $f_w$  implies  $\tau_b = \rho f_w u_b |u_b| / 2$ . This is known to be an oversimplification of the problem for oscillatory motions. For instance, it is known that the shear under monochromatic waves is not in phase with velocity. This has led to modifications of the friction factor to introduce the phase lag (Nielsen 1992), and to redefine the friction factor as (Jonsson 1966)

$$f_w \equiv \frac{2\tau_{b,\max}}{\rho u_{b,\max}^2}, \quad (5.2)$$

where the subindex refers to the maximum value of the variable within a wave period. In fact, the expression Eq. (5.1) is actually valid for  $f_w$  defined as in Eq. (5.2). More serious problems regarding the use of the friction factor appear for saw-tooth shaped waves or for wave-current interactions. In general, for oscillatory flows the use of the friction factor  $f_w$  is recommended as a first order approximation of time averaged values.

Assuming that linear wave theory is valid and assuming straight and parallel bathymetric contours, the conservation of wave energy may be written as

$$\frac{\partial(Ec_g)}{\partial x} = -\epsilon_D, \quad (5.3)$$

with  $E \equiv \rho g H_s^2 / 8$  being  $g$  the acceleration of gravity,  $H_s$  the significant wave height,  $\epsilon_D$  the energy dissipation and  $c_g$  the group velocity given by

$$c_g = \frac{\omega}{2k} \left\{ 1 + \frac{2kh}{\sinh 2kh} \right\}, \quad (5.4)$$

with  $k$  being the wave number ( $k = 2\pi/L$ ), where  $L$  is the wave length and  $h$  the local water depth.

Assuming a meadow composed by a set of  $N$  plants per unit of horizontal area where each plant has a leaf length given by  $l_v$  and neglecting the swaying by blades, the energy dissipation  $\epsilon_D$  due to seagrass can be written (Dalrymple et al. 1984) as,

$$\epsilon_D \equiv \overline{\int_{-h}^{-h+l_v} \frac{1}{2} \rho C_D a'_v N |u| u^2 dz}. \quad (5.5)$$

where  $a'_v$  is the plant area per unit height,  $u$  is the orbital velocity and  $C_D$  is the drag coefficient for the forces exerted by the fluid on the plant. In Eq. (5.5)

the integral is evaluated from the bed ( $z = -h$ ) to the vegetation height  $l_v$  and the overbar indicates the time average over a wave period.

Previous theoretical, numerical and observational works on wave propagation over vegetated fields have dealt with the question of obtaining the dissipation term in order to integrate Eq. (5.3) (Kobayashi et al. 1993, Méndez & Losada 2004, Bradley & Houser 2009). Some authors have suggested that the morphology of the *P. oceanica* leaf can be simulated by a vertical cylinder (Méndez & Losada 2004). By doing so, an analytical expression for the dissipation term can be obtained under the hypothesis of linear wave theory (Dalrymple et al. 1984) as,

$$\epsilon_D = \frac{2\rho}{9\pi k} C_D a'_v N \left( \frac{gkH_s}{2\omega} \right)^3 \frac{\sinh^3 kl_v + 3 \sinh kl_v}{\cosh^3 kh}. \quad (5.6)$$

Since one could alternatively approximate  $\epsilon_D$  as  $\overline{\tau_b u_b}$ , assuming that the velocity distribution is nearly uniform within the plant height  $l_v$ , it follows that,

$$C_D = \frac{f_w}{a'_v l_v N}. \quad (5.7)$$

However, the main problem in the determination of the rate of energy dissipation arises from the ignorance of the value of the drag coefficient  $C_D$  in Eq.(5.6). Here, it is proposed to estimate  $C_D$  from  $f_w$ .

If wave propagation is studied over constant depth, an analytical solution can be found for the wave damping as,

$$\frac{H_s}{H_{s,0}} = \frac{1}{1 + K_d H_{s,0} x} \quad (5.8)$$

where  $K_d$  is a decay coefficient given by,

$$K_d = \frac{4}{9\pi} C_D a'_v N k \frac{\sinh^3 kl_v + 3 \sinh kl_v}{(\sinh 2kh + 2kh) \sinh kh} \quad (5.9)$$

In this work the wave damping induced by a *Posidonia oceanica* meadow is evaluated. Data from bottom mounted acoustic doppler velocimeters for one of the three storms measured are used to obtain the roughness length  $k_s$  for the meadow. The friction factor for two other storms are then calculated using Eq. (5.1) and the value of  $C_D$  related with  $f_w$  through the meadow parameters.

This approach assumes that  $l_v/h \ll 1$ , so that the roughness length formulation accounts for the effects of both the bottom and the meadow. Finally, the wave damping is evaluated along a transect by numerical integration of Eq.(5.3).

## 5.3 Material and Methods

Measurements were carried out in Cala Millor, located on the northeast coast of Mallorca Island, Mediterranean Sea (Fig. 5.1, top). Cala Millor is an intermediate barred sandy beach formed by biogenic sediments with median grain values ranging between 0.28 and 0.38 mm at the beach front (Gómez-Pujol et al. 2007). The beach is in an open bay with an area of around 14 km<sup>2</sup>. At depths from 6 m to 35 m, the seabed is covered by a meadow of *Posidonia oceanica* (Infantes et al. 2009). The tidal regime is microtidal, with a spring range of less than 0.25 m (Orfila et al. 2005). The bay is located on the East coast of the island, and it is therefore exposed to incoming wind and waves from NE to ESE directions.

From July 7th to July 23rd 2009, four self-contained Acoustic Doppler Velocimeters, ADVs (Nortek, Vector) with pressure sensors were deployed in a transect perpendicular to the coast at depths of 6.5, 10, 12.5 and 16.5 m and total length of 942 m (see Fig. 5.1, bottom). ADVs were mounted over galvanized iron structures taking care that pressure sensors were placed at 80 - 100 cm above the bottom, just above the seagrass canopy (Fig. 5.2). Stability of the equipment was verified with the compass, tilt and roll sensors (Infantes et al. 2011). Velocity data were collected in bursts of 15 minutes every two hours at 80 cm above the bottom at a sampling rate of 4 Hz, sampling volume of 14.9 mm and a nominal velocity range of 1 m s<sup>-1</sup>.

Wave data was processed using Nortek software (QuickWave v.2.04) that uses the ADV pressure and velocity (PUV method) to estimate from pressure data the wave height ( $H_s$ ), peak period ( $T_p$ ) and the combination of the horizontal components and pressure to calculate wave direction (Nortek AS, 2002). Wave data were filtered to remove waves not approaching perpendicular to the beach. To exclude wave energy lost by white capping, wave records when mean wind velocities higher than 10 m s<sup>-1</sup> were not used (Puertos del Estado wind data).

---

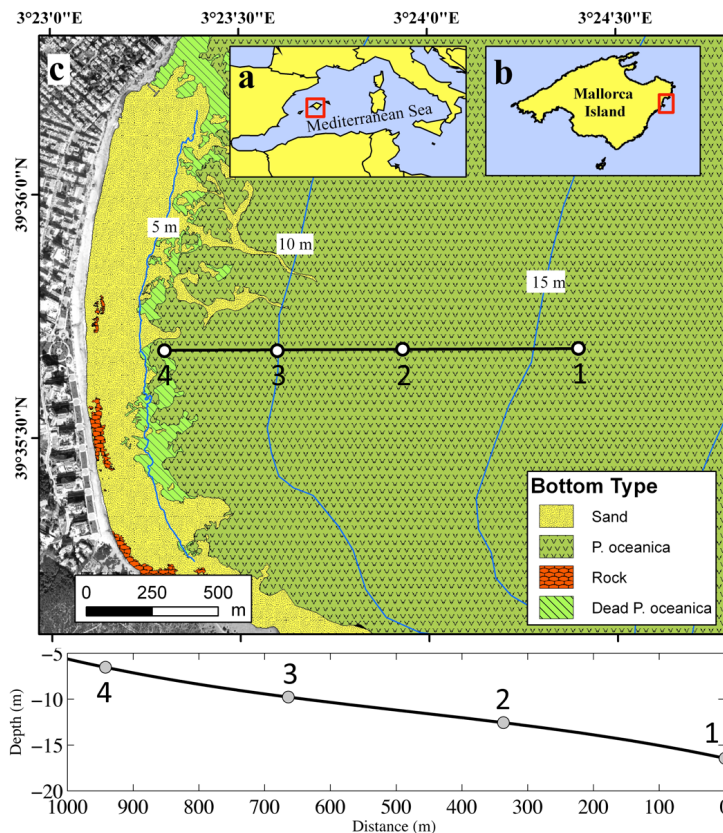


Figure 5.1: (a) Location of Mallorca Island in the Mediterranean Sea. (b) Location of the study area. (c) Location of the transect and deployment sites in Cala Millor. (d) Bathymetric profile and distance between the deployment sites.

The area is under cyclogenetic activity throughout the year (Cañellas et al. 2007). Indeed, during the instrument deployment, three storms affected the area with significant wave heights ( $H_s$ ) larger than 1 m at the deeper location (Fig. 5.3, top). The first storm began on the 13th July with a duration of 2 days and with a maximum  $H_s$  of 1.85 m. The second storm began on the 18th July with a duration of 16 hours reached  $H_s$  of 1.58 m. The third storm began on the 21st July with a duration of 24 hours reached  $H_s$  of 1.1 m. The roughness length  $k_s$ , was calculated independently from the third storm and then used to



Figure 5.2: Acoustic doppler velocimeter (ADV) deployed in the *Posidonia oceanica* seagrass meadow.

compute  $f_w$  and the corresponding  $C_D$  for the first and second storms.

### 5.3.1 Determination of Nikuradse roughness length

As stated, roughness length  $k_s$  is a critical parameter for the characterization of the friction factor in rough turbulent flows.  $k_s$  is assumed to be a property of the meadow morphology (number of shoots, shoot height and leaf width mainly), which in turn is assumed to be constant in time. This is a fair assumption since measurements were done in summer during a short period of time (16 days). *P. oceanica* leaf number, leaf lengths and leaf widths were measured in ten vertical shoots collected at the locations 1, 2, 3 and 4 (Fig. 5.1, top). The mean shoot length was set as  $l_v = 0.8 \pm 0.1$  m (mean  $\pm$  SE) and mean leaf surface area as  $211 \pm 23$  cm<sup>2</sup> (mean  $\pm$  SE). This is the averaged maximum leaf length of individual shoots measured randomly at field. Shoot density was also measured at the same locations and the mean shoot density as  $615 \pm 34$  shoots m<sup>-2</sup> (mean  $\pm$  SE).

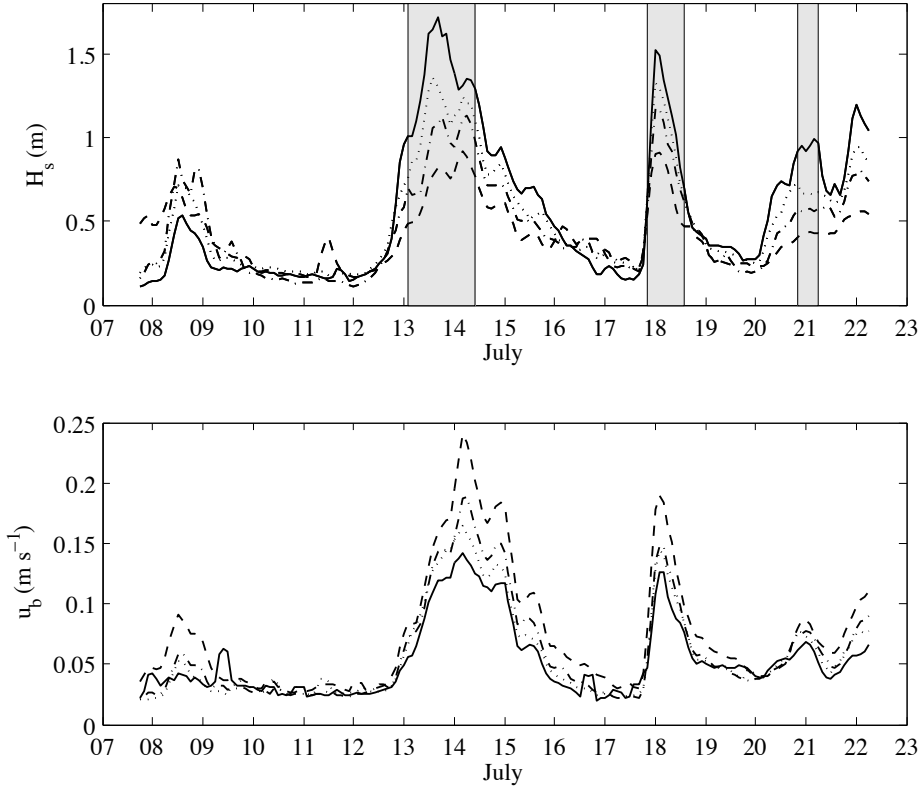


Figure 5.3: Top panel: Significant wave height at 16.5 m depth (solid), at 12.5 m depth (dotted), at 10 m depth (dash-dotted) and at 6.5 m depth (dashed). Grey areas indicate the three storms. Bottom panel: near bottom orbital velocities at the same locations (depths and lines are the same as the top panel).

Measured field velocities and wave heights along the transect during the third storm (July 21st) are used to obtain  $k_s$  in the following procedure. A set of  $C_D$  ranging from 0.01 to 2 are provided to compute the wave damping by numerical integration of Eqs. (5.3)-(5.6). Departing from the wave height measured at location 1, the corresponding  $H_{s,i}$  at locations  $i = 2, 3, 4$  ( $x = 337$  m,  $x = 664$  m and  $x = 942$  m respectively) is computed obtaining the error

between modeled and measured wave as,

$$\epsilon = \sqrt{\sum_{i=2}^4 |H_{s,i}^{computed} - H_{s,i}^{measured}|^2}, \quad (5.10)$$

The value of  $C_D$  that minimizes the error is selected to compute  $f_w$  and its corresponding  $k_s$  through Eq. (5.1).  $k_s$  is computed for a total of 20 hours (10 records) and the average for all records is calculated. The drag coefficient is related with the friction factor through the measured plant characteristics  $a'_v$  and  $l_v$  and  $N$ , Eq. (5.7). Therefore and for the sake of simplicity hereinafter the value of  $C_D$  will be used.

### 5.3.2 Determination of drag coefficient

Once  $k_s$  is determined for the *Posidonia oceanica* meadow,  $f_w(k_s/a_b)$  is computed for the other two storms. A total of 24 hours have been analyzed for the July 13th storm (12 records) and 18 hours for the July 18th storm (9 records). For these events, near-bottom orbital velocities ranged between 12 and 25 cm s<sup>-1</sup> (Fig. 5.3, bottom) with wave periods between 4.5 and 5.5 s during both storms. To obtain the friction factor from Eq. (5.1) it is assumed purely oscillatory motion. This is a fair assumption from the experimental data since mean velocities are one order of magnitude lower than the oscillatory component.

In order to study the energy dissipation within the *P. oceanica* meadow, the energy conservation Eqs. (5.3)-(5.6) are solved. Bathymetry is adjusted by fitting a third order polynomial to the depths at the four moorings (Fig. 5.1, bottom).

## 5.4 Results

During the three storms the significant wave heights  $H_s$  decreases between the depths 16.5 m to 6.5 m (Fig. 5.3, top). In contrast, but as expected by linear wave theory, near-bottom orbital velocities  $u_b$  increase at shallower depths (Fig. 5.3, bottom). The roughness length obtained during July 21st is  $k_s = 0.42 \pm 0.05$ , which is the mean and the standard deviation of the values estimated for stations 2, 3 and 4.

On July 13th at 4am significant wave heights of  $H_s = 0.86$  m were measured at mooring 1 (16.5 m depth). Waves heights above 1 m were recorded for 24 hours with maximum  $H_s = 1.85$  m. Measured significant wave height normalized by incident wave height ( $H_{s,0}$ ) at the four moorings are displayed for this period in Fig. (5.4). Numerical integration of of Eq. (5.3) are plotted as black lines, and the uncertainty in the predictions, based on a 15 % error in the measurement of the initial wave height at period are displayed as dashed lines. For each set of data the apriori estimate of  $C_D$ , based on  $k_s$  and Eq. (5.1), is presented for completeness. Values of  $C_D$  ranged from 0.12 to 0.43. As seen, fairly good agreement is obtained between the measured and predicted  $H_s$ . The second storm lasted 18 hours starting on July 18th at 12am. Fig. (5.5) present this event at a 2 hours interval. Similarly, the measured data (dots) are well represented by the predictions (lines) although some discrepancies appear at the shallow moorings.  $H_s/H_{s,0}$  between the deepest (16.5 m) and shallowest (6.5 m) measurement locations is reduced by  $50\% \pm 4\%$  (mean  $\pm$  SD) during the first storm and by  $39\% \pm 9\%$  during the second storm.

As *P. oceanica* shoot density varies between locations (Marbà et al. 1996), the effect of this variation on wave damping is assessed by computing the wave decay ( $H_s/H_{s,0}$ ) over the bathymetry depicted in Fig. (5.1, bottom), but for different shoot densities. The wave decay for an incident wave of  $H_{s,0} = 1.56$  m and  $T_p = 4.6$  s ( $C_D = 0.41$ ) for shoot densities ranging between 200 to 800 shoots  $\text{m}^{-2}$  is shown in Fig. (5.6). After propagation over 1000 m,  $H_s/H_{s,0}$  is reduced 40 % in a meadow of 200 shoots  $\text{m}^{-2}$ . In a high density meadow of 800 shoots  $\text{m}^{-2}$ , the reduction is  $> 55\%$  over the same distance.

Wave decay over constant depth can be readily obtained from Eq. (5.8). The coefficient  $K_d$  in Eq. (5.9) depends on plant parameters (e.g.,  $a'_v$ ,  $l_v$ ,  $N$  and  $k_s$ ), hydrodynamical conditions (e.g.,  $C_D$ ,  $\omega$ ) and water depth. For a fixed  $\omega = 1.3 \text{ s}^{-1}$  representing a period,  $T \approx 4.8$  s, which is typical condition for the Mediterranean Sea and  $H_{s,0} = 1.1$  m ( $C_D = 0.42$ ) the value of  $K_d(N, h)$  is displayed as a function of the shoot density and the length of the blade in Fig. (5.7) for water depths of  $h = 5$  m (top),  $h = 10$  m (middle) and  $h = 15$  m (bottom). The set of shoot densities were varied from sparse meadows of  $N = 200$  plants/ $\text{m}^{-2}$  to very dense meadows of  $N = 1000$  plants/ $\text{m}^{-2}$ . Blade length was varied from the length of seedlings, around 0.1 m, to blades of 1.4 m. The large values of  $K_d$  obtained at 5 m water depths have to be taken



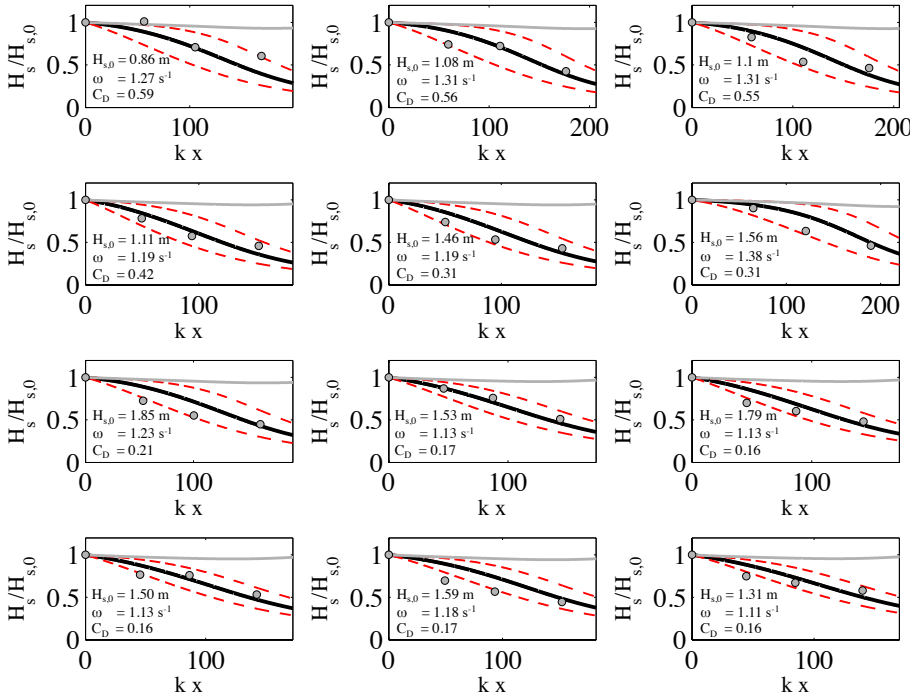


Figure 5.4: Normalized significant wave height (by incident) along nondimensional distance (by wave length) for the first storm. The first panel corresponds to conditions on July 13th at 4am and sequence are elapsed 2 hours. The solid black line displays the computed normalized significant wave height including the dissipation due to *P. oceanica* meadow. The grey line corresponds to the  $H_s$  assuming no dissipation by the seagrass. Dashed lines displays the predictions for wave decay for a 15 % error in the measurement of initial wave height and wave period.

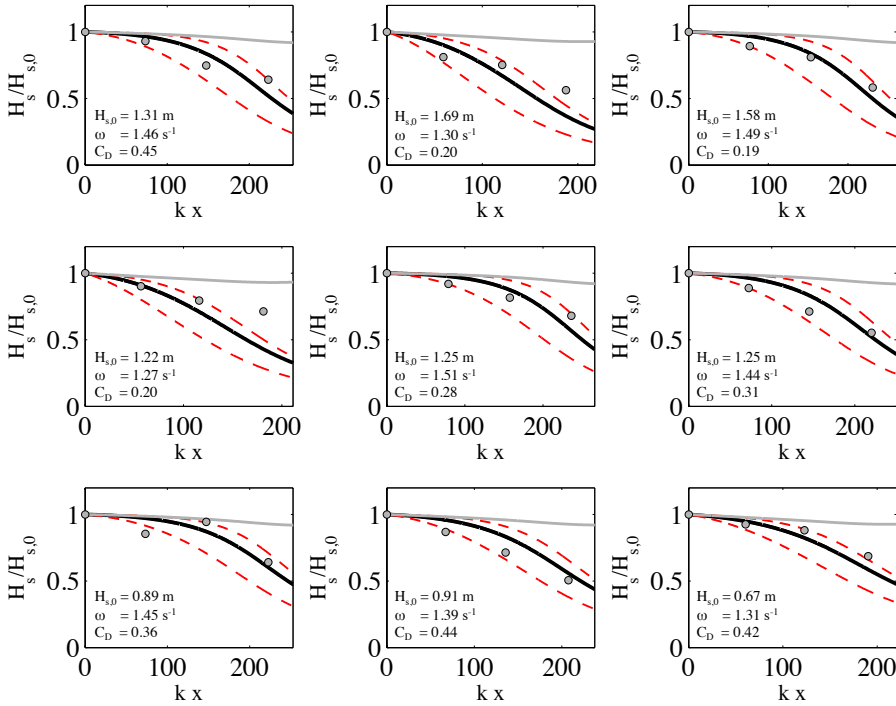


Figure 5.5: Normalized significant wave height (by incident) along nondimensional distance (by wavelength) for the second storm. The first panel correspond to conditions on July 18th at 12am and sequence are elapsed 2 hours. The solid black line displays the computed normalized significant wave height including the dissipation due to *P. oceanica* meadow. The grey line corresponds to the  $H_s$  assuming no dissipation by the seagrass. Dashed lines displays the predictions for wave decay for a 15 % error in the measurement of initial wave height and wave period.

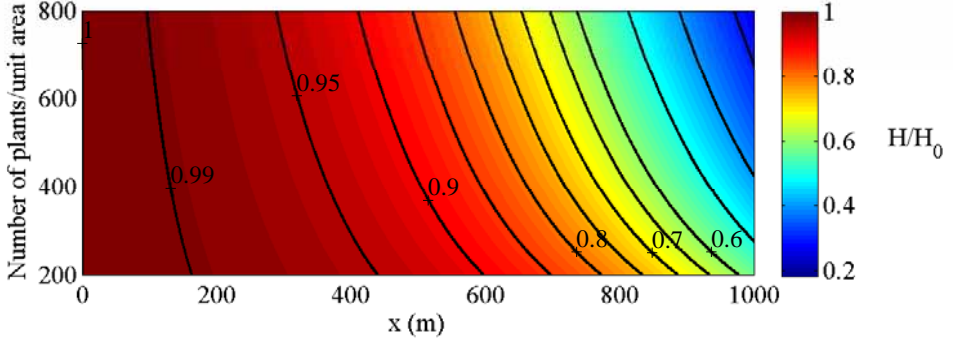


Figure 5.6: Wave damping  $H/H_0$  along the transect for different conditions of shoot density. Initial wave height is  $H_{s,0} = 1.56$  m,  $\omega = 1.38$  s $^{-1}$  and  $C_D = 0.41$ .

with caution. Two conditions are violated for this wave condition at this depth; first, the nonlinearity for the condition presented is  $\epsilon = 0.1$  which is too large to satisfy the hypothesis of linear wave theory, and second, the large values of  $l_v/h$  suggest that the meadow cannot be characterised simply by the roughness length concept to obtain the drag coefficient. Values of  $K_d$  at 10 m depth are between  $5 \cdot 10^{-4}$  m $^{-2}$  for short blades in low density meadow to  $2 \cdot 10^{-3}$  m $^{-2}$  for large blades in high density meadows which gives wave reduction of 20 % to 60 % in 500 m propagation respectively. Values of  $K_d$  at 15 m depth are roughly one order of magnitude smaller.

## 5.5 Discussion

This study suggests that for waves of height  $H_{s,0} = 1.56$  m and period  $T = 4.5$  s, the decay coefficient ranges from  $K_d = 5 \times 10^{-4}$  to  $K_d = 3 \times 10^{-3}$  (Fig. 5.7) for a meadow of density  $N = 200 - 1000$  plants/m $^2$  occupying  $l_v/h = 0.04 - 0.14$  in water depth  $h = 10$  m. In dimensionless terms,  $K_d H_{s,0} L = 0.024 - 0.14$ , which can be interpreted as a 2.4 % to 14 % decay in wave height per wavelength (see Fig. 5.7). Bradley and Houser (2009) measured an exponential decay coefficient that ranged between  $0.004$  m $^{-1}$  to  $0.02$  m $^{-1}$  for waves of peak period 1.5 s in water depth  $\sim 1.0$  m, which equates to approximately a 1.3 % - 6.6 % reduction in wave height per wavelength ( $L \approx 3.3$  m). Further,

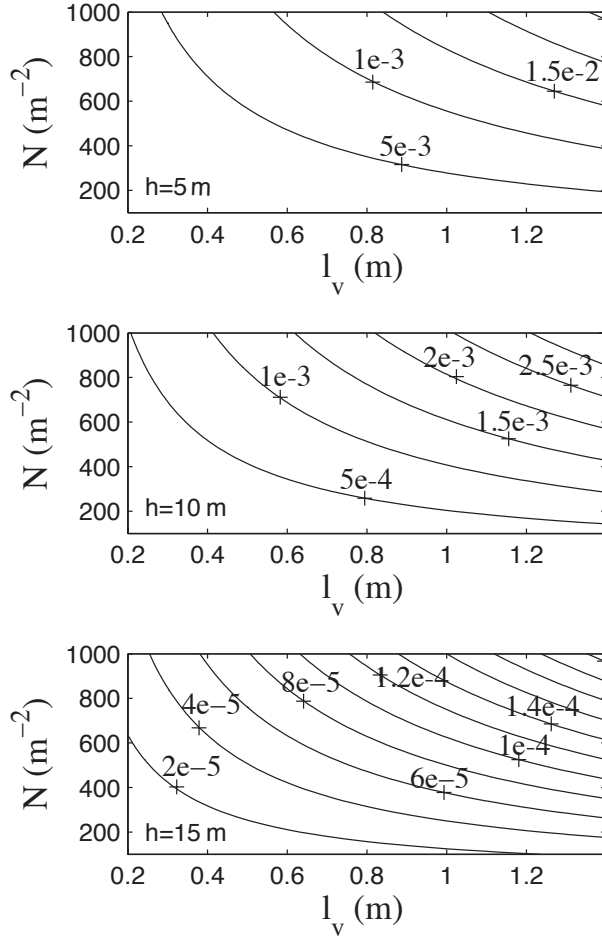


Figure 5.7: Decay coefficient ( $K_d$ ) versus seagrass shoot density ( $N$ ) and leaf length ( $l_v$ ) for an incident wave  $H_{s,0} = 1.56$  m,  $\omega = 1.38$  s $^{-1}$  and  $C_D = 0.41$  propagating over constant depth  $h = 5$  m (top),  $h = 10$  m (middle) and  $h = 15$  m (bottom). Units in  $\text{m}^{-2}$ .

Bradley and Houser (2009) suggest a bottom roughness length of  $k_s = 0.16$  m, which is broadly consistent with the value,  $k_s = 0.42$  m, obtained in this study. The lower roughness length obtained by Bradley and Houser (2009) may be explained by the fact that *T. testudinum* ( $l_v \approx 0.3$  m) is shorter than *P. oceanica* ( $l_v \approx 0.8$  m). Our results are also broadly consistent with Fonseca and Cahalan (1992), who evaluated wave attenuation for four seagrass species (*Zostera marina*, *Halodule wrightii*, *Syringodium filiforme* and *Thalassia testudinum*) in a laboratory study. They found that, on average, wave energy was reduced by  $\sim 40$  % per meter when the length of seagrasses was equal to the water depth. The wavelengths tested by Fonseca and Cahalan were 0.38 m and 0.67 m, leading to a  $\sim 15$  % to  $\sim 27$  % reduction in wave energy per wavelength.

Seasonal changes in the seagrass meadow (shoot density, leaf number and leaf lengths) increases or reduces the degree of wave damping. This work suggests that for a given wave conditions ( $H_{s,0} = 1.56$  m,  $\omega = 1.38$  s $^{-1}$  and  $C_D = 0.41$ )  $H_s/H_{s,0}$  is reduced by  $> 55$  % in a dense meadow (800 shoots m $^{-2}$ ) and a 40 % reduction in a low density meadow (200 shoots m $^{-2}$ ) over the distance of 1000 m (Fig. 5.6). Newell & Koch (2004) observed that wave height reduction was higher during June when the seagrass canopy of *Ruppia maritima* was dense ( $> 1000$  shoots m $^{-2}$ ) and occupied most of the water column than during October. *P. oceanica* shoot densities do not vary along the year, but leave number and length is higher in summer. Instead, *P. oceanica* shoot densities vary between locations and depth (Marbà et al. 1996, Pergent-Martini et al. 1994, Terrados & Medina Pons 2008). Wave damping would be higher in shallow locations with higher shoot densities. Anthropogenic disturbances affecting the shoot density of the meadow could later revert in a change in the upper limit by the increase of wave energy reaching the shallow areas of the beach (Infantes et al. 2009).

The energy dissipation term in Eq. (5.6), obtained by Dalrymple et al. (1984), considers vertical extent of plants as rigid cylinders. As already noted by these authors, a proper characterization of  $C_D$  is crucial in order to cover the ignorance on the plant movement. Since the value of the drag coefficients is estimated directly from wave height measurements, plant motion is accounted for to a certain extent. However it would be desirable to perform specific experiments to characterize the importance of the shoot swaying on the determination of  $C_D$ .

The approach followed in the present study is based on the hypothesis that

hydrodynamics is mainly induced by waves. For the experiments presented in this Chapter, this is a reasonable assumption for the two storms analysed since near-bottom orbital velocities measured by the ADVs are one order of magnitude larger than mean currents. In coastal environments, where the flow is the result of the interaction of waves and currents, the boundary layer interacts directly with the bottom roughness and the turbulence generated near the bottom by the orbital motion increasing the apparent roughness. In those situations, one has to solve explicitly the boundary layer by using a specific model (Grant & Madsen 1979, Simarro et al. 2008).

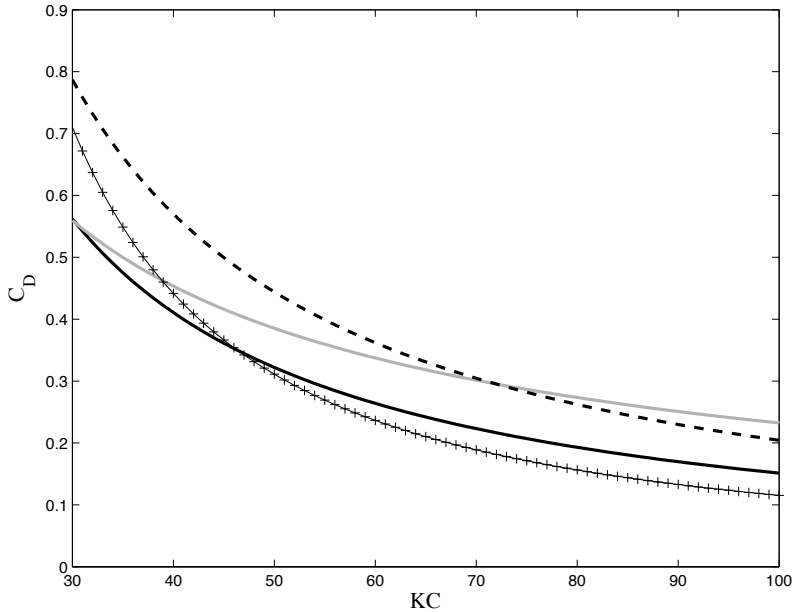


Figure 5.8: Drag coefficient versus Keulegan-Carpenter number for experimental data -crosses-, for Sánchez-González et al. (2011) -black solid-, Kobayashi et al. (1993) -black dashed- and for Méndez and Losada (2004) -grey-.

Méndez & Losada (2004) pointed out that a suitable relation is obtained between the drag coefficient and the Keulegan-Carpenter (KC) number defined as  $K = u_c T_p / l_v$  where  $u_c$  is a characteristic velocity acting over the plant. The term  $a_b / k_s$  used in this Chapter is equivalent to the KC number used by those authors. The data presented in this Chapter and several recent studies show

similar trends in  $C_D$  with KC (Fig. 5.8). Sánchez-González et al. (2011) studied wave attenuation due to seagrass meadows in a scaled flume experiment using artificial models of *P. oceanica* and concluded that  $C_D$  is better related with KC than with Reynolds number. Specifically, these authors found that  $C_D = 22.9/K^{1.09}$  for  $15 \leq K \leq 425$ . Fig. (5.8) shows the drag coefficient predicted for the two storms considered in this study versus the KC number (dots). As seen, good agreement is obtained between the present approach and the expression given by Sánchez-González et al. (2011), shown as a black line in Fig (A.3). Kobayashi et al. (1993) measured  $C_D = 35.5/K^{1.12}$  (black dashed line in Fig. 5.8). Méndez and Losada (2004) measured  $C_D = 6.7/K^{0.73}$  (grey line in Fig. 5.8).

Two aspects should be considered in detail in future research. First, the link between the roughness length and meadow properties has to be explored for different meadow conditions. Second, the limitation of this approach for increasing non-dimensional blade length ( $l_v/h$ ) has to be assessed. Understanding the interaction between waves and bottom canopies such as *P. oceanica* seagrass meadow is crucial for assessing the importance of these communities in coastal protection as well as to determine the final wave parameters which will drive sediments. This work shows that a *P. oceanica* seagrass meadow reduces the wave height that is reaching the beach during two storm events. Parameters such as  $k_s$  and  $C_D$  are necessary in order to run more precise wave propagation models over a seagrass meadows. Moreover, for meadows that occupy a small fraction of the water depth, it may be appropriate to use relations for bare beds, specifically Eq. (5.1), to characterize the drag imparted by the canopy.





## Chapter 6

# General discussion and conclusions

This Ph.D Thesis shows that hydrodynamics and bottom type play an important role on the spatial distribution of a seagrass meadow of *Posidonia oceanica*, the invasive macroalgae *Caulerpa taxifolia* and *Caulerpa racemosa* and seagrass seedlings of *P. oceanica* and *Cymodocea nodosa*. The coastal areas studied in this Thesis are exposed during winter to storm events with wave heights of 3 to 5 m. During these storms near-bottom orbital velocities are elevated and can shape the distribution of macrophytes. Testable estimates of the threshold level of wave energy that allows macrophyte species to persist are provided for two Mediterranean seagrass species and two invasive macroalgae. This Chapter will summarise the various experiments undertaken and link them together.

Previous studies have related the minimum depth of occurrence of macrophytes to wave action. Chambers (1987) calculated the wave conditions from fetch data in lakes obtaining a relationship between minimum depth of macrophyte colonization and wave mixing depth. Vacchi et al. (2010) related the distance of the upper limit of *P. oceanica* meadow from the shoreline and the morphodynamic domain of the beach. Taking into account sedimentological parameters, coastal dynamics was correlated with the position of the *P. oceanica* meadow upper limit and shoot density of its shallow portions. The methodology presented in Chapter 2 allows to estimate the near-bottom orbital velocities that set the upper depth limit of a *Posidonia oceanica* meadow. Mean wave conditions are propagated to the shore using a 2D parabolic model over the detailed

bathymetry. A correlation between hydrodynamics, bottom type and the spatial distribution of *P. oceanica* shows that the percent cover of seagrass over sand is reduced with increasing orbital velocities up to 38 - 42 cm s<sup>-1</sup>. Above these velocities, there is no presence of *P. oceanica* meadow and therefore they set the upper limit of the bathymetric distribution of this species in this location and for the associated wave conditions. These results shows that there is a relation between the wave orbital velocities and the upper limit of seagrass. This has been previously hypothesized (Koch et al. 2006) but it is the first time that near-bottom orbital velocities are quantified, setting a threshold value for the presence of this seagrass species in unconsolidated substratum. *P. oceanica* growing in rocks or dead matte likely supports higher velocities than those when it grows in sand.

Water motion plays an important role in the initial life stages of seagrass (Koch et al. 2010, Rivers et al. 2011) because seedlings are vulnerable to burial or dislodgement. The basis for understanding seedling survivorship of two Mediterranean seagrass species in sandy substratum under different hydrodynamic conditions is provided in this Thesis. Morphological characteristics of each species such as foliar surface and root length are key factors in colonisation processes. *P. oceanica* has larger leaves and shorter roots compared to *C. nodosa*. Drag forces are higher in *P. oceanica* under both unidirectional and oscillatory flow, due to the larger leaf surface area of this species compared to *C. nodosa*. In contrast, *C. nodosa* tolerates larger sediment erosion before becoming dislodged from the sediment than *P. oceanica* due to its longer roots. The drag coefficients of individual seedlings obtained in a biological flume under waves ranged between 0.01 and 0.1. Drag measurements and seedling dislodgement results obtained in the flume agree with those obtained in the field where *C. nodosa* survived longer than *P. oceanica*. These results are important to understand the spatial distribution of these species in sandy substratum.

The strong decline of *P. oceanica* and *C. nodosa* has generated a major interest in restoring both Mediterranean species (Molenaar and Meinesz 1995, Balestri et al 1998). Understanding the habitat requirements of seedlings is necessary before a large-scale seagrass restoration plan is carried out. Results obtained in this Thesis for seagrass seedlings could be applied to restoration purposes. Macrophytes morphology and rooting capacity could determine their success under physical disturbances. This Thesis indicates that seagrass seedlings

---

were dislodged during storms. The disappearance of *P. oceanica* suggests that water dynamics was too severe at these depths for this species. In contrast, *C. nodosa* was better adapted to stand higher orbital velocities. Restoration success in sand will be improved if planting of *P. oceanica* is carried out in a relatively wave sheltered location with low orbital velocities. *P. oceanica* seedlings started to decline at near-bottom orbital velocities between 7 and 18 cm s<sup>-1</sup> and completely disappeared at velocities between 17 and 34 cm s<sup>-1</sup>. *C. nodosa* seedlings started to decline at velocities between 17 and 34 cm s<sup>-1</sup> and some seedlings survived velocities between 23 and 39 cm s<sup>-1</sup>. Anchoring the seedlings to the substratum could improve the rooting capacity and their survivorship in unconsolidated substratum under different hydrodynamic conditions, although this has not been assessed in this Thesis. Planting in consolidated substrata such as dead rhizomes of *P. oceanica* could also increase the seedling rate of success during restoration (Balestri et al. 1998, Infantes et al 2011, Dominguez et al. 2011, Rivers et al. 2011).

Wave exposure determines the morphology of the organisms. Many studies have documented the general trend of decreasing plant size with increasing wave exposure in intertidal systems (Gaylord et al. 1994, Blanchette 1997, Martone and Denny 2008). Hydrodynamic forces are the mechanism responsible for these observed patterns of size with respect to exposure. As seen in Chapter 3, drag forces are related to leaf surface area. The small size of *C. nodosa* will be an advantage over the large size of *P. oceanica* when colonising wave exposed locations. Fast-growing, colonizing species are often small (e.g. *C. nodosa*), whereas slow-growing or climax species are often large (e.g. *P. oceanica*). Results obtained in this Thesis agrees with the general assumption that small seagrass species occupy frequently wave disturbed habitats, while large seagrass species require more stable environments (Marbà et al. 1996), which probably become even more stable when supporting a continuous seagrass cover through current reduction, wave attenuation and sediment trapping.

Assuming that physical dislodgement is the primary mechanism for macrophytes failure, an appropriate area to grow and persist would be one that enhances anchoring ability or reduces physical disturbance. Novel quantitative evidence highlighting the importance of substratum for the distribution of invasive *Caulerpa* species at shallow depths is provided in this Thesis. Observations carried out during two years showed that both *Caulerpa* species are more abun-

---

dant in dead matte of *P. oceanica* or rock than inside the *P. oceanica* meadow or sand. A short time experiment where fragments of both *Caulerpa* species were fixed to sand and dead matte also showed that cover of *Caulerpa* was higher in dead matte than on sand. *C. taxifolia* and *C. racemosa* cover started to decline at velocities above  $15 \text{ cm s}^{-1}$ . The friction coefficient computed for the dead matte model was higher ( $1.04 \times 10^{-1}$ ) than for sand ( $2.33 \times 10^{-2}$ ). The calculated friction coefficients for the dead matte model and sand indicate that the surface of the dead matte is structurally more complex than sand and that *Caulerpa* fragments established on it will experience lower flow velocities than in sand. These results are important because indicate which substrates will be more suitable to be colonised by the invasive *Caulerpa* species.

The importance of hydrodynamics on the spatial distribution of macrophytes ecosystems is clearly shown in Chapters 2 to 4. On the other hand, the presence of macrophytes reduce current velocity and damping wave heights (Nepf and Vivoni 2000, Ghisalberti and Nepf 2002, Fonseca and Cahalan 1992). There is a general agreement that macrophytes can attenuate waves, but little quantitative evidence is available. Field data on wave damping in macrophytes is scarce as most studies have been performed using numerical models (Kobayashi et al. 1993, Méndez et al. 1999, Méndez and Losada 2004, Chen et al. 2007) and flume data (Fonseca and Cahalan 1992, Kobayashi et al. 1993, Méndez and Losada 2004, Augustin et al. 2009, Sánchez-González et al. 2011). This Thesis shows that a *P. oceanica* seagrass meadow attenuates wave height during two storm events. The bottom roughness is calculated for the meadow as  $k_s = 0.42 \text{ m}$  using flow velocities above the seagrass. Wave heights are reduced between 39 and 50 % by a meadow over a distance of 942 m. Computed drag coefficients  $C_D$ , ranged from 0.1 to 0.4 during two storms. These values agree with the  $C_D$  values obtained in a flume using artificial plant models of *P. oceanica* (Sánchez-González et al. 2011). The predicted wave decay coefficient for seagrass shoot densities of 200 - 800 shoots  $\text{m}^{-2}$  ranged between 40 % to 55 % of wave reduction respectively. This Thesis indicates that parameters such as bottom roughness  $k_s$ , wave friction coefficient  $f_w$  and drag coefficient  $C_D$  are necessary in order to run more precise wave propagation models over a seagrass meadows.

In a case scenario of global warming and sea-level rise, the shallow areas will become deeper and orbital velocities reduced. A change in depth due to sea-

---

level rise could modify positively the upper limit as new unoccupied areas would become potentially available for colonization, but findings by Wicks (2005) at the Chincoteague Bay suggest that *Zostera marina* seagrass distribution might be negatively affected by sea level rise as seagrasses would be unable to migrate shoreward due to unsuitable sediments. Another consequence of global warming is an increase in the number and intensity of extreme storm events. These events could have serious implications on the spatial distribution of macrophytes and the upper limit of seagrass. As seen in Chapter 2, the upper depth limit of seagrass is determined by hydrodynamics. An increase in wave energy reaching the shallow areas of a meadow could revert on a deeper position of the upper depth limit.

Hydrodynamics effects operate on several scales from molecules ( $\mu\text{m}$ ) to leaves and shoots (cm), seagrass canopies (m) and seagrass meadows (km), therefore having complex implications for entire macrophyte systems (see review Koch et al. 2006). During this Thesis, hydrodynamic effects have been studied at the scales of individual shoots, seagrass canopies and seagrass meadows. To understand these processes a link between different fields must be build. Quantitative studies on interactions between waves and seagrasses are fairly recent (last  $\sim 10$  years). New, smaller and autonomous wave-current sensors (e.g. Doppler technology) can be easily deployed in shallow coastal areas, providing high quality wave data. The continuous development of new computers with higher computational power can nowadays run complex numerical models that computers made 15 years ago were not able to run.

This Thesis highlights the importance of interdisciplinary and multidisciplinary research in ecological modeling and, in particular, the need for hydrodynamical studies to elucidate the distribution of macrophytes at shallow depths. A relation between fluid dynamics, bottom type and benthic macrophytes is shown. Predicted and measured quantitative results are provided such as near-bottom orbital velocities and drag coefficients that could be tested and compared to other benthic marine macrophytes species on other locations. This Thesis demonstrates that water motion is an important parameter in seagrass ecology and requires serious considerations in seagrass research, conservation and restoration programmes.

---



## Chapter 7

# Recomendations for future work

This Ph.D. Thesis shows that the upper depth limit of a seagrass meadow of *Posidonia oceanica* is related to hydrodynamics. Future work will be devoted to study the near-bottom velocities that determine the upper limit of *Posidonia oceanica* meadows in other locations in the Mediterranean Sea. The relation between hydrodynamics and the upper limit has been applied in a unconsolidated substrata such as sand. This methodology could be also applied to *P. oceanica* colonizing consolidated substrates such as rocks. It can also be applied to other benthics species i.e., seagrass, macroalgae, sponges, bivalves.

There are few numerical models studying flow interactions with sediment and macrophytes. The complexities involved in the calculations involve an understanding of physical, biological and geological parameters (Teeter et al. 2001). One of these limitations in the numerical calculations is the information on the friction coefficient due to the bottom topography and drag caused by the vegetation. In order to improve the accuracy of ecological models, the friction coefficient and bottom roughness must be first determined. Bottom roughness and drag coefficients values obtained for *P. oceanica* meadows can be included in wave propagation models. Additionally, wave induced movement of seagrass canopy and its effects on wave damping remains unknown. Several numerical models have been developed to account for leaf swaying (Méndez et al. 1999, Bradley and Houser 2009) but more effort needs to be made in this topic.

Most studies have dealt with interactions of either current or waves on macrophytes. In nature, both types of flow are usually present in a higher or lower degree. To date, little is known about the interaction of macrophytes with the combination of current and waves. This type of studies will be first carried out in hydraulic flumes where the current flow, wave conditions and meadow parameters can be easily adjusted.

Macrophytes distribution is influenced by both sediment inputs and hydrodynamics (Frederiksen et al. 2004). Studies have been carried out to determine interactions between hydrodynamics and sediment movements such as bars, ripples, sand waves, beach profiles, etc (Álvarez-Ellacuria et al. 2010, Gómez-Pujol et al. 2011). Some studies have carried out on interactions between vegetation and hydrodynamics, but little work has been devoted to study interactions between hydrodynamics, sediment dynamics and macrophytes.

---



# Appendix A

## Background review on fluid dynamics

Fluid dynamics is the study of the movement of fluid. Among other things it addresses velocity, acceleration, and forces exerted by or upon fluids in motion. In this Appendix, a review is made on the basic concepts of fluid dynamics that affect the life of macrophytes. Linear wave theory, wave propagation and benthic boundary layers are summarised.

### A.1 Waves

Water flow in coastal marine ecosystems can be divided into unidirectional and oscillatory flows. Unidirectional flows (also described as currents) are those in which water particles tend to move in the same direction over time. These flows in marine ecosystems are mainly generated by tides. Oscillatory flows (also described as waves) are those in which water particles move in two directions at a periodic interval. These flows are generated by waves. Depending on the dominance of wave periodicity, at marine ecosystem can be characterized as tide-dominated or wave-dominated. Because this Thesis is mainly focused on wave-dominated flows, for simplicity, the currents and tides characteristics will not be reviewed in this Appendix.

Wind generated waves are formed by the frictional stress produced by two fluid layers of different speed which creates a transfer of energy from the wind

to the water surface. Wind generated waves are surface waves that occur on the ocean, sea, lake, rivers, and canals or even on small puddles and ponds. Wave size depends on the wind speed blowing over a distance of sea surface (known as fetch) for a length of time.

Wave data can be obtained by direct measurements of the sea conditions using oceanographic instruments or estimated using numerical models. Several oceanographic instruments are used to measure waves such as pressure sensors, accelerometers, acoustic dopplers, radars or altimeters mounted on satellites. Instruments can be deployed anchored at the sea bottom or fixed at meteorological buoys or at the shore. Wave records are generally very limited in space and time due to the cost of the instruments and measuring platforms. Also, waves are usually recorded on a specific location over a period of time. For these reasons, numerical models are used to estimate the wave conditions in locations where wave measurements are not available. In order to obtain a wave field over larger portions of the sea surface area where wave measurements are not available, numerical models are used. Numerical models are widely used, for example, to estimate wave fields over the Mediterranean Sea (Cañellas et al. 2007), to study a specific coastal area with an ecological, economical or turistic interest (Álvarez-Ellacuria et al. 2009, Álvarez-Ellacuria et al. 2010).

Waves are characterized by a wave height  $H$  (from trough to crest) or wave amplitude  $a$  (half of the wave height), wavelength  $L$ , (from crest to crest), wave period  $T$ , (time interval between arrival of consecutive crests at a stationary point) and wave propagation direction (Fig. 2). Waves in a given area typically have a range of heights. For weather reporting and for scientific analysis of wind wave statistics, their characteristic height over a period of time is usually expressed significant wave height,  $H_s$ , which represents an average height of the highest one-third of the waves in a given time period. The angular frequency is  $\omega = 2\pi/T$ , and the wave number is  $k = 2\pi/L$ .

Airy wave theory or linear wave theory gives a linear system description of the wave propagation of gravity waves on the surface of a homogeneous fluid layer. The theory assumes that the fluid layer has a uniform mean depth, and that the fluid flow is inviscid, incompressible and irrotational. Linear wave theory uses a potential flow approach to describe the motion of gravity waves on a fluid surface. In nature, a combination of waves and currents are present, but

---

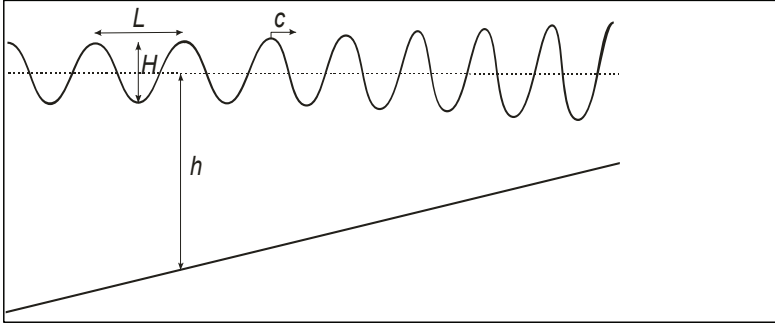


Figure A.1: Diagram of a shoaling wave approaching to shore. Variable names are defined in the text.

for simplicity we have deal with them independently.

Assuming linear wave theory, the dispersion relationship in deep and shallow water describes the field of propagating waves as

$$\omega^2 = gk \tanh(kh), \quad (\text{A.1})$$

where  $g$  is the acceleration of gravity and  $h$  is the water depth. Substituting  $\omega$  and  $k$ , Eq. (A.1) can also be written as:

$$L = \frac{T^2 g}{2\pi} \tanh\left(\frac{2\pi h}{L}\right) \quad (\text{A.2})$$

Waves approaching to the coast travel through different water depths and are classified into three regimes; deep, shallow and intermediate depth waves. The speed of the wave propagating,  $C$ , can be expressed as

$$C^2 = \frac{g}{k} \tanh(kh) \quad (\text{A.3})$$

In deep water,  $kh$  is large and  $\tanh(kh) = 1$ , therefore  $L = T^2 g / 2\pi$  or  $C = \sqrt{g/k}$ . For a water depth larger than half the wavelength,  $h > L/2$ , the orbits are circular and the phase speed of the waves is hardly influenced by depth (this is the case for most wind waves on the sea and ocean surface).

In shallow water,  $kh$  is small and  $\tanh(kh) = kh$ , therefore  $C = \sqrt{gh}$ . For a water depth smaller than the wavelength divided by 20,  $h < L/20$ , the orbits become elliptical or flatter due to the influence of the bottom. The phase speed

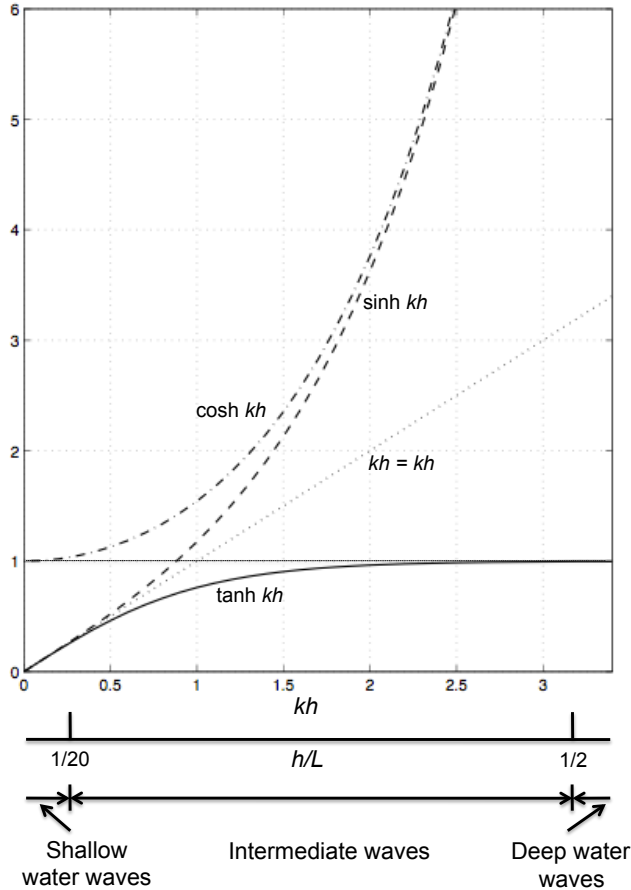


Figure A.2: Relative depth and asymptotes to hyperbolic functions.

of the waves is only dependent on water depth, and no longer a function of periodic function or wavelength. All other cases,  $L/20 < h < L/2$ , are termed intermediate depth waves, where both water depth and period (or wavelength) have a significant influence on the solution of Airy wave theory. In this case waves combine characteristics of deep and shallow water waves and speed is described as Eq. (A.3).

Assuming linear wave theory, deep and shallow waves differ in characteristics other than wave velocity. In deep-water waves, the individual particles describe circles whose radius decreases with depth. In the surface the radius is the same

as the wave amplitude, and the particle velocity is the circumference of the circle divided by the wave period. In shallow-water waves the particles describe ellipses. The radius along the minor axis is equal to the wave amplitude at the surface and decreases linearly with depth. At the bottom the minor axis is zero and the motion is horizontal. The radius of the major axis is a function of water depth, wavelength and amplitude. In this Thesis, near-bottom orbital velocity,  $u_b$ , is given by

$$u_b = 2\pi a_b / T \quad (\text{A.4})$$

where  $a_b$  is the wave orbital amplitude calculated as

$$a_b = \frac{H_s}{2\sinh(2\pi h/L)}, \quad (\text{A.5})$$

where  $L$  is calculated iteratively from Eq A.2.

Orbital velocities can be also measured from instruments deployed in the seafloor. Records from acoustic doppler velocimeters (ADV) provide large datasets to calculate velocity and turbulence. Field records are usually filtered to remove spikes and low beam correlations. Then velocity data can be filtered with a low pass filter to remove high frequency Doppler noise (Lane et al. 1998). Horizontal velocity is calculated as the root mean square (rms).

$$u_{rms} = \sqrt{\frac{1}{N} \sum_{i=1}^N x_i^2 + y_i^2} \quad (\text{A.6})$$

where  $x$  and  $y$  are the two horizontal velocities.

Wave energy possessed by a wave is in two forms, kinetic and potential. Kinetic energy is the energy inherent in the orbital motion of the water particles while potential energy possessed by the particles when they are displaced from their mean position. The total energy  $E$  per unit area of a wave is,

$$E = \frac{1}{8} \rho g H_s^2. \quad (\text{A.7})$$

## A.2 Wave propagation

As water waves propagate from the region where they were generated to the coast, both wave amplitude and wavelength are modified due to refraction (e.g.

---

changes in the bathymetry or interactions with wind induced currents), diffraction (e.g. intense variations of the bottom), the loss of energy due to the shoaling, damping and finally wave breaking. The surf zone is a highly dynamic area where energy from waves is partially dissipated through turbulence in the boundary layer and transformed in short and long waves, mean sea level variations and currents. Therefore, the energy dissipated in the surf zone is used for sediment transport providing a highly variable morphological environment (Dean and Dalrymple 2002).

Early efforts to study wave transformation from deep to shallow water were based on the geometrical ray theory. As a modification to the linear wave theory, the mild slope approach which assumes that the water depth changes slowly in a typical wave length appears as an improvement to the former since it includes wave diffraction. In this approach, the vertical structure of the velocity is the same as that for a progressive wave over a constant depth being the governing partial differential equations of the elliptic type. Moreover, these equations can be easily converted into parabolic type by assuming that the wave amplitude is primarily a function of water depth due to the shoaling. This approach, known as the parabolic approach, can be seen as a modification of the ray theory where wave energy can be diffused along the rays as wave propagate (Liu and Losada 2002).

In this Thesis, deep-water wave conditions were propagated to the study sites using a numerical model (Oluca) based on the mild slope parabolic approximation (Kirby and Dalrymple 1983) and was developed by the University of Cantabria, Spain. The Oluca model is a variation of the REF/DIF model (Kirby and Dalrymple 1983). These models are widely used in engineering and scientific approaches in order to obtain the accurate wave field in coastal areas from open sea conditions since refraction and diffraction are well captured (Álvarez-Ellacuria et al. 2010).

### A.3 Boundary Layers

The boundary layer is that layer of fluid in the immediate vicinity of a bounding surface where effects of viscosity of the fluid are considered in detail. The boundary layer effect occurs at the field region in which all changes occur in the

---

flow pattern. The boundary layer distorts surrounding non-viscous flow. It is a phenomenon of viscous forces. This effect is related to the Reynolds number. The thickness of the boundary layer,  $\delta$ , is normally defined as the distance from the solid body at which the flow velocity is 99 % of the free stream velocity, that is, the velocity that is calculated at the surface of the body in an inviscid flow solution.

When benthic marine macrophytes are present, the boundary layer is modified by the canopy which influences the mean velocity, turbulence and mass transport (Nepf and Vivoni 2000, Ghisalberty and Nepf 2002, Luhar et al. 2010). Macrophytes reduce the flow velocity near the bottom changing the logarithmic velocity profile. The goal of studying benthic boundary layers in ecological studies is to understand the water movement around organisms that live on or near the substratum.

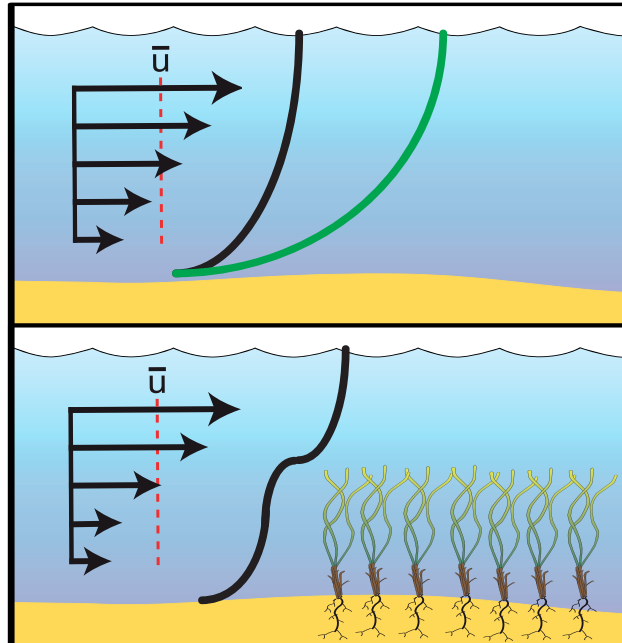


Figure A.3: Vertical profile of velocity. Top, weak currents (black line) and fast currents (dashed line). Bottom, velocity reduction due to benthic macrophytes.

Water flow can either be smooth and regular as the fluid flows in layers (laminar flow) or rough and irregular (turbulent flow). This depends on the velocity and the length scale (temporal and spatial scales respectively) and is defined by the Reynolds number. The Reynolds number  $Re$  is a dimensionless number that gives a measure of the ratio of inertial forces  $\rho\nu^2/l_*$  to viscous forces  $\mu\nu/l_*^2$  and consequently quantifies the relative importance of these two types of forces for given flow conditions and is expressed as

$$Re = \frac{ul_*}{\nu}, \quad (\text{A.8})$$

where  $u$  is the flow velocity,  $l_*$  is the characteristic length and  $\nu$  is the kinematic water viscosity.

Macrophytes are a source of drag, they reduce near-bottom water flow, and dissipate current and wave energy. Drag forces act in a direction opposite to the oncoming flow velocity. Drag on macrophytes increases with water velocity and foliar surface area. In flexible organisms, foliar surface area will change with increasing flow velocity, and this change is encapsulated in the drag coefficient. Drag force is expressed as:

$$F_D = \frac{1}{2}\rho a_f C_D u^2 \quad (\text{A.9})$$

where  $\rho$  is density of the water,  $a_f$  is the frontal area,  $C_D$  is the drag coefficient and  $u$  is the water velocity. The drag coefficient  $C_D$  is a dimensionless parameter used to quantify the drag or resistance of an object in a fluid environment. It is used in the drag equation, where a lower drag coefficient indicates the object will have less hydrodynamic drag. The drag coefficient is always associated with a particular surface area.

---



# Bibliography

- Ackerman JD and Okubo A (1986) Reduced Mixing in a Marine Macrophyte Canopy. *Funct. Ecol.* **7(3)**: 305-309.
- Álvarez-Ellacuria A, Orfila A, Olabarrieta M, Gómez-Pujol L, Medina R, Tintoré J (2009) An Alert System for Beach Hazard Management in the Balearic Islands. *Coast. Manage.* **37**: 569-584
- Álvarez-Ellacuria A, Orfila A, Olabarrieta M, Medina R, Vizoso G, Tintoré J (2010) A nearshore wave and current operational forecasting system. *J. Coast. Res.* **26**: 503-509.
- Anderson K, Close L, DeWreede RE, Lynch BJ, Ormond C, Walker M (2006) Biomechanical properties and holdfast morphology of coenocytic algae (Halimedales, Chlorophyta) in Bocas del Toro, Panama. *J. Exp. Mar. Biol. Ecol.* **328**: 155-167.
- Augustin LN, Irish JL, Lynett P (2009) Laboratory and numerical studies of wave damping by emergent and near-emergent wetland vegetation. *Coast. Eng.* **56**: 332-340.
- Balestri E, Piazzini L, Cinelli F (1998) Survival and growth of transplanted and natural seedlings of *Posidonia oceanica* (L.) Delile in a damaged coastal area. *J. Exp. Mar. Biol. Ecol.* **228**: 209-225.
- Bax N, Williamson A, Agüero M, Gonzalez E, Geeves W (2003) Marine invasive alien species: a threat to global biodiversity. *Mar. Policy* **27**: 313-323.
- Bell SS, Robbins BD, Jensen SL (1999) Gap dynamics in a seagrass landscape. *Ecosystems* **2(6)**: 493-504.
- Blanchette CA (1997) Size and survival of intertidal plants in response to wave action: a case study with *Fucus gardneri*. *Ecology* **78**: 1563-1578.

- Bold HC, Wynne MJ (1978) Introduction to the Algae. Structure and reproduction. Prentice-Hall, Inc., Englewood Cliffs.
- Boudouresque CF and Verlaque M (2002) Biological pollution in the Mediterranean Sea: invasive versus introduced macrophytes. *Mar. Pollut. Bull.* **44**: 32-38.
- Boudouresque CF, Bernard G, Bonhomme P, Charbonnel E, Diviacco G, Meinesz A, Pergent G, Pergent-Martini C, Ruitton S, Tunesi L (2006) Préservation et conservation des herbiers à *Posidonia oceanica*. L' Accord RAMOGE, 202 pp.
- Boudouresque CF, Bernard G, Pergent G, Shili A, Verlaque M (2009) Regression of Mediterranean seagrasses caused by natural processes and anthropogenic disturbances and stress: A critical review. *Bot. Mar.* **52**: 395-418.
- Bouma TJ, de Vries MB, Low E, Peralta G, Tanczos C, van de Koppel J, Herman PMJ (2005) Trade-offs related to ecosystem engineering: A case study on stiffness of emerging macrophytes. *Ecology* **86**: 2187-2199.
- Bouma TJ, de Vries MB, Herman PMJ. (2010) Comparing ecosystem engineering efficiency of two plant species with contrasting growth strategies. *Ecology* **91**(9): 2696-2704
- Bradley K and Houser C. (2009) Relative velocity of seagrass blades: Implications for wave attenuation in low-energy environments. *J. Geophys. Res.* 114: F01004
- Buia MC and Mazzella L (1991) Reproductive phenology of the Mediterranean seagrasses *Posidonia oceanica* (L.) Delile, *Cymodocea nodosa* (Ucria) Aschers, and *Zostera noltii* Hornem. *Aquat. Bot.* **40**: 343-362.
- Bulleri F, Benedetti-Cecchi L (2008) Facilitation of the introduced green alga *Caulerpa racemosa* by resident algal turfs: experimental evaluation of underlying mechanisms. *Mar. Ecol. Prog. Ser.* **364**: 77-86.
- Cabaco S, Santos R, Duarte CM (2008) The impact of sediment burial and erosion on seagrasses: A review. *Estuar. Coast. and Shelf Sci.* **79**: 354-366.
- Cabaco S, Ferreira O, Santos R (2010) Population dynamics of the seagrass *Cymodocea nodosa* in Ria Formosa lagoon following inlet artificial relocation. *Estuar. Coast. and Shelf Sci.* **87**: 510-516.
-

- Carlton JT, Geller JB (1993) Ecological roulette - The global transport of non-indigenous marine organisms. *Science* **261**: 78-82.
- Cañellas B, Orfila A, Méndez FJ, Menéndez M, Tintoré J (2007) Application of POT model to estimate the extreme significant wave height levels around the Balearic Sea (Western Mediterranean). *J. Coast. Res.* **50**: 329-333.
- Castillo MC, Baquerizo A, Losada MA (2005) Temporal and spatial statistical variability of the wave height in the surf zone. 29th International Conference on Coastal Engineering, 2004. Lisbon, Portugal. Vols 1-4: 997-1008.
- Caye G and Meinesz A (1986) Experimental study of seed germination in the seagrass *Cymodocea nodosa*. *Aquat. Bot.* **26**: 79-87.
- Cebrian E and Ballesteros E (2009) Temporal and spatial variability in shallow- and deep-water populations of the invasive *Caulerpa racemosa* var. *cylindracea* in the Western Mediterranean. *Estuar. Coast. and Shelf Sci.* **83**: 469-474.
- Ceccherelli G and Cinelli F (1999) Effects of *Posidonia oceanica* canopy on *Caulerpa taxifolia* size in a north-western Mediterranean bay. *J. Exp. Mar. Biol. Ecol.* **240**: 19-36.
- Ceccherelli G, Piazzzi L, Balata D (2002) Spread of introduced *Caulerpa* species in macroalgal habitats. *J. Exp. Mar. Biol. Ecol.* **280**: 1-11.
- Chambers PA (1987) Nearshore occurrence of submersed aquatic macrophytes in relation to wave action. *Can. J. Fish. Aquat. Sci.* **44**: 1666-1669.
- Chen SN, Sanford LP, Koch EW, Shi F, North EW (2007) A nearshore model to investigate the effects of seagrass bed geometry on wave attenuation and suspended sediment transport. *Estuar. and Coasts* **30**: 296-310
- Chisholm JRM and Moulin P (2003) Stimulation of nitrogen fixation in refractory organic sediments by *Caulerpa taxifolia* (Chlorophyta). *Limnol. Oceanogr.* **48**: 787-794.
- Chisholm JRM, Dauga C, Ageron E, Grimont PAD, Jaubert JM (1996) Roots in mixotrophic algae. *Nature* **381**: 382.
- Chivers R, Emerson N, Burns D (1990) New acoustic processing for underway surveying. *The Hydrographic Journal* **56**: 8-17.
-

- Clarke SM and Kirkman H (1989) Seagrass dynamics. In: Larkum AWD, McComb AJ, Shepherd SA (Eds.) *Biology of Seagrasses: a treatise on the biology of seagrasses with special reference to the Australasian region*. Elsevier, North Holland.
- Costanza R, d'Arge R, de Groot R, Farber S, Grasso M, Hannon B, Limburg K, Naeem S, O'neill RV, Paruelo J, Raskin RG, Sutton P, van den Belt M (1997) The value of the world's ecosystem services and natural capital. *Nature* **387**: 253-260.
- Cornelisen CD and Thomas FIM (2004) Ammonium and nitrate uptake by leaves of the seagrass *Thalassia testudinum*: impact of hydrodynamic regime and epiphyte cover on uptake rates. *J. Mar. Systems* **29**: 177-194.
- Cornelisen CD and Thomas FIM (2006) Water flow enhances ammonium and nitrate uptake in a seagrass community. *Mar. Ecol. Prog. Ser.* **312**: 1-13.
- Dalrymple RA, Kirby JT, Hwang PA. (1984) Wave diffraction due to areas of energy-dissipation. *J. Waterw. Port C-ASCE* **110**: 67-79.
- D'Amours O and Scheibling RE (2007) Effect of wave exposure on morphology, attachment strength and survival of the invasive green alga *Codium fragile* ssp. *tomentosoides*. *J. Exp. Mar. Biol. Ecol.* **351**: 129-142.
- Davis AR, Ferguson AM, Wright JT (2009) Structural complexity facilitates accumulation and retention of fragments of the invasive alga, *Caulerpa taxifolia*. *J. Exp. Mar. Biol. Ecol.* **371**: 163-169.
- Dean RG. and Dalrymple RA (1991) *Water wave mechanics for engineers and scientist*. Advanced series on ocean engineering, volume 2. World Scientific.
- Dean RG. and Dalrymple RA (2002) *Coastal processes with engineering applications*. Cambridge University Press, Cambridge. pp. 475.
- De Falco G, Baroli M, Cucco A, Simeone S (2008) Intrabasinal conditions promoting the development of a biogenic carbonate sedimentary facies associated with the seagrass *Posidonia oceanica*. *Cont. Shelf Res.* **28(6)**: 797-812.
- Den Hartog C (1970) *The seagrasses of the world*. North Holland Publishing Company, Amsterdam.
- Den Hartog C (1971) The dynamic aspect of the ecology of sea-grass communities. Conference paper. *Thalassia Jugoslavica* **7(1)**: 101-112.
-

- Dennison WC and RS Alberte RS (1985) Role of daily light period in the depth distribution of *Zostera marina* (Eelgrass). Mar. Ecol. Prog. Ser. **25(1)**: 51-61.
- Dennison WC (1987) Effects of light on seagrass photosynthesis, growth and depth distribution. Aquat. Bot. **27(1)**: 15-26.
- Denny MW, Daniel TL, Koehl MAR (1985) Mechanical limits to size in wave-swept organisms. Ecol. Monogr. **55**: 69-102.
- Domínguez M, Infantes E, Terrados J (2010) Seed maturity of the Mediterranean seagrass *Cymodocea nodosa*. Vie et Milieu **60**: 1-6.
- Domínguez M, Celdrán-Sabater D, Muñoz-Vera A, Infantes E, Martínez-Baños P, Marín A, Terrados J (2011) Experimental evaluation of the restoration capacity of a fish-farm impacted area with *Posidonia oceanica* (L.) Delile seedlings. Rest. Ecol. 10.1111/j.1526-100X.2010.00762.x
- Duarte CM (1991) Seagrass depth limits. Aquat. Bot. **40(4)**: 363-377.
- Duarte CM, Terrados J, Agawin NSR, Fortes MD, Bach SS, Kenworthy WJ (1997) Response of a mixed Philippine seagrass meadow to experimental burial. Mar. Ecol. Prog. Ser. **147**: 285-294.
- Folkard AM (2005) Hydrodynamics of model *Posidonia oceanica* patches in shallow water. Limnol. Oceanogr. **50(5)**: 1592-1600.
- Fonseca MS, Fisher JS, Zieman JC, Thayer GW (1982) Influence of the seagrass, *Zostera marina* L, on current flow. Estuar. Coast. Shelf Sci. **15(4)**: 351-364.
- Fonseca MS, Zieman JC, Thayer GW, Fisher JS (1983) The role of current velocity in structuring eelgrass (*Zostera marina* L.) meadows. Estuar. Coast. Shelf Sci. **17**: 367-380.
- Fonseca MS and Fisher JS (1986) A comparison of canopy friction and sediment movement between 4 species of seagrass with reference to their ecology and restoration. Mar. Ecol. Prog. Ser. **29(1)**: 15-22.
- Fonseca MS and Kenworthy WJ (1987) Effects of current on photosynthesis and distribution of seagrasses. Aquat. Bot. **27**: 59-78.
- Fonseca MS and Cahalan JA (1992) A preliminary evaluation of wave attenuation by 4 species of seagrass. Estuar. Coast. and Shelf Sci. **35**: 565-576.
-

- Fonseca MS (1996) The role of seagrasses in nearshore sedimentary processes: a review. In: Nordstrom KF, Roman CT (eds) *Estuarine Shores: Evolution, Environments and Human Alterations*. John Wiley & Sons LTD, p 261-281
- Fonseca MS and Bell SS (1998) Influence of physical settings on seagrass landscapes near Beauford, North Carolina, USA. *Mar. Ecol. Prog. Ser.* **171**: 109-121.
- Fonseca MS, Whitfield PE, Kelly NM, Bell SS (2002) Modeling seagrass landscape pattern and associated ecological attributes. *Ecol. Appl.* **12(1)**: 218-237.
- Fornes A, Basterretxea G, Orfila A, Jordi A, Álvarez A, Tintoré J (2006) Mapping *Posidonia oceanica* from IKONOS. *Journal of Photogrammetry and Remote Sensing* **60(5)**: 315-322.
- Frederiksen M, Krause-Jensen D, Holmer M, Laursen JS (2004) Spatial and temporal variation in eelgrass (*Zostera marina*) landscapes: influence of physical setting. *Aquat. Bot.* **78(2)**: 147-165.
- Gacia E and CM Duarte (2001) Sediment retention by a Mediterranean *Posidonia oceanica* meadow: the balance between deposition and resuspension. *Estuar. Coast. Shelf Sci.* **52**: 505-514.
- Gambi MC, Nowell ARM, Jumars PA (1990) Flume observations on flow dynamics in *Zostera marina* (Eelgrass) beds. *Mar. Ecol. Prog. Ser.* **61(1-2)**: 159-169.
- Ghisalberti M and Nepf HM (2002) Mixing layers and coherent structures in vegetated aquatic flows. *J. Geophys. Res.* **107(C2)**, doi:10.1029/2001JC000871.
- GIOC (2003) Spectral wave propagation model (Oluca-SP). State Coastal Office - Spanish Environmental Ministry and University of Cantabria. pp. 170. (in Spanish).
- Glasby TM, Gibson PT, Kay S (2005) Tolerance of the invasive marine alga *Caulerpa taxifolia* to burial by sediment. *Aquat. Bot.* **82**: 71-81.
- Gobert S, Kyramarios M, Lepoint G, Pergent-Martini C, Bouquegneau JM (2003) Variations at different spatial scales of *Posidonia oceanica* (L.) Delile beds; effects on the physico-chemical parameters of the sediment. *Oceanol. Acta* **26**: 199-207.
-

- Gómez-Pujol L, Orfila A, Cañellas B, Álvarez-Ellacuria A, Méndez FJ, Medina R, Tintoré J (2007) Morphodynamic classification of sandy beaches in low energetic marine environment. *Mar. Geol.* **242(4)**: 235-246.
- Gómez-Pujol L, Orfila A, Álvarez-Ellacuria A, Tintoré J (2011) Controls on sediment dynamics and medium-term morphological change in a barred microtidal beach (Cala Millor, Mallorca, Western Mediterranean). *Geomorphology*. doi: 10.1016/j.geomorph.2011.04.026
- Granata TC, Serra T, Colomer J, Casamitjana X, Duarte CM, Gacia E, Petersen JK (2001) Flow and particle distributions in a nearshore seagrass meadow before and after a storm. *Mar. Ecol. Prog. Ser.* **218**: 95-106
- Grant WD and Madsen OS (1979) Combined wave and current interaction with a rough bottom. *J. Geo. Res.* **84**:C4
- Green EP and Short FT (2003) *World atlas of seagrasses*. University of California Press.
- Greve T and Krause-Jensen D (2005) Predictive modelling of eelgrass (*Zostera marina*) depth limits. *Mar. Biol.* **146**: 849-858.
- Guidetti P, Lorenti M, Buia MC, Mazzella L (2002) Temporal dynamics and biomass partitioning in three Adriatic seagrass species: *Posidonia oceanica*, *Cymodocea nodosa*, *Zostera marina*. *Mar. Ecol-P. S. N. I.* **23**: 51-67.
- Hemminga MA and Nieuwenhuize J (1990) Seagrass wrack-induced dune formation on a tropical coast (Banc-Darguin, Mauritania). *Estuar. Coast. and Shelf Sci.* **31**: 499-502.
- Hendriks IE, van Duren LA, Herman PMJ (2006) Turbulence levels in a flume compared to the field: Implications for larval settlement studies. *J. Sea Res.* **55**: 15-29.
- Hill D, Coquillard P, Vaugelas J, Meinesz A (1998) An algorithmic model for invasive species: Application to *Caulerpa taxifolia* (Vahl) C. Agardh development in the North-Western Mediterranean Sea. *Ecol. Model.* **109**: 251-265.
- Hine AC, Evans MW, Davis RA, Belknap DF (1987) Depositional response to seagrass mortality along a low-energy, barrier-island coast: west-central Florida. *J. Sedim. Petrol.* **57**: 431-439.
-

- Hovel KA, Fonseca CR, Myer DL, Kenworthy WJ, Whitfield PE (2002) Effects of seagrass landscape structure, structural complexity and hydrodynamic regime on macrofaunal densities in North Carolina seagrass beds. *Mar. Ecol. Prog. Ser.* **243**: 11-24.
- Idestam-Almquist J and Kautsky L (1995) Plastic responses morphology of *Potamogeton pectinatus* L. to sediment and above-sediment conditions at two sites in the northern Baltic proper. *Aquat. Bot.* **52**: 205-216.
- IMEDEA (2005) Variabilidad y Dinámica Sedimentaria De Las Playas de Cala Millor y Cala Sant Vicent. Volumen 1. Cala Millor. Govern de les Illes Balears. (in Spanish)
- Infantes E, Terrados J, Orfila A, Caëllas A, Álvarez-Ellacuria (2009) Wave energy and the upper depth limit distribution of *Posidonia oceanica*. *Bot. Mar.* **52**: 419-427.
- Infantes E, Terrados J, Orfila A (2011) Assessment of substratum effect on the distribution of two invasive *Caulerpa* (Chlorophyta) species. *Estuar. Coast. and Shelf Sci.* **91**: 434-441
- Jaubert JM, Chisholm JRM, Ducrot D, Ripley HT, Roy L, Passeron-Seitre G (1999) No deleterious alterations in *Posidonia* beds in the bay of menton (France) eight years after *Caulerpa taxifolia* colonization. *J. Phycol.* **35**: 1113-1119.
- Jonsson IG (1967) Wave boundary layers and friction factors. Proc. 10th Int. Conf. Coastal Engineering, ASCE, New York, 127.
- Keddy PA (1984) Quantifying a within-lake gradient of wave energy in Gillfillan Lake, Nova-Scotia. *Can. J. Bot.* **62(2)**: 301-309.
- Kendrick GA and Burt JS (1997) Seasonal changes in epiphyte macro-algae assemblages between offshore exposed and inshore protected *Posidonia sinuosa* seagrass meadows, Western Australia. *Bot. Mar.* **40**: 77-85.
- Kenworthy WJ and Fonseca MS (1996) Light requirements of seagrasses *Halodule wrightii* and *Syringodium filiforme* derived from the relationship between diffuse light attenuation and maximum depth distribution. *Estuaries* **19(3)**: 740-750.
-



- Kirby JT and Dalrymple RA (1983) A parabolic equation for the combined refraction-diffraction of Stokes waves by mildly-varying topography. *J. Fluid Mech.* **136**: 453-466.
- Kirkman H and Kuo J (1990) Pattern and process in southern Western Australian seagrasses. *Aquat. Bot.* **37**: 367-382.
- Kirkman H (1998) Pilot experiments on planting seedlings and small seagrass propagules in western Australia. *Mar. Pollut. Bull.* **37**: 460-467
- Knutson PL, Bronchu RA, Seelig WN (1982) Wave damping in *Spartina alterniflora* marshes. *Wetlands* **2**: 87-104.
- Kobayashi N, Raichle AW, Asano T (1993) Wave Attenuation by Vegetation. *J. Waterw. Port C-ASCE.* **119**: 30-48
- Koch EW and Beer S (1996) Tides, light and the distribution of *Zostera marina* in Long Island Sound, USA. *Aquat. Bot.* **53(1-2)**: 97-107.
- Koch EW and Gust G (1999) Water flow in tide- and wave-dominated beds of the seagrass *Thalassia testudinum*. *Mar. Ecol. Prog. Ser.* **184**: 63-72.
- Koch EW (2001) Beyond light: Physical, geological, and geochemical parameters as possible submersed aquatic vegetation habitat requirements. *Estuaries* **24**: 1-17.
- Koch EW, Ackerman JD, Verduin J, van Keulen M (2006) Fluid Dynamics in Seagrass Ecology - from Molecules to Ecosystems. In: (Larkum, A.W.D., R.J. Orth, C.M. Duarte, eds). *Seagrasses: Biology, Ecology and Conservation*. Springer, Netherlands. pp. 193-224.
- Koch EW, Barbier EB, Silliman BR, Reed DJ, Perillo GME, Hacker SD, Granek EF, Primavera JH, Muthiga N, Polasky S, Halpern BS, Kennedy CJ, Kappel CV, Wolanski E (2009) Non-linearity in ecosystem services: temporal and spatial variability in coastal protection. *Front. Ecol. Environ.* **7**: 29-37.
- Krause-Jensen D, Pedersen MF, Jensen C (2003) Regulation of eelgrass (*Zostera marina*) cover along depth gradients in Danish Coastal Waters. *Estuaries* **26**: 866-877.
- Lacy JR, Sherwood CR, Wilson DJ, Chisholm TA, Gelfenbaum GR (2005) Estimating hydrodynamic roughness in a wave-dominated environment with a high-resolution acoustic Doppler profiler. *J. Geophys. Res.* **110**, C06014, doi:10.1029/2003JC001814
-

- Lane SN, Biron PM, Bradbrook KF, Butler JB, Chandler JH, Crowell MD, McLelland SJ, Richards KS, Roy AG (1998) Three-dimensional measurement of river channel flow processes using acoustic Doppler velocimetry. *Earth Surf. Processes* **23**: 1247-1267.
- Laugier T, Rigollet V, de Casabianca ML (1999) Seasonal dynamics in mixed eelgrass beds, *Zostera marina* L. and *Z. noltii* Hornem., in a Mediterranean coastal lagoon (Thau lagoon, France). *Aquat. Bot.* **63**: 51-69.
- Leriche A, Pasqualini V, Boudouresque CF, Bernard G, Bonhomme P, Clabaut P, Denis J (2006) Spatial, temporal and structural variations of a *Posidonia oceanica* seagrass meadow facing human activities. *Aquat. Bot.* **84(4)**: 287-293.
- Lowe RJ, Koseff JR, Monismith SG, Falter JL (2005) Oscillatory flow through submerged canopies: 1. Velocity structure. *J. Geophys. Res.* **110**, C10016, doi:10.1029/2004JC002788.
- Luque AA, Templado J (Eds.) (2004) Praderas y bosques marinos de Andalucía. Consejería de Medio Ambiente, Junta de Andalucía, Sevilla, 336 pp.
- Luhar M, Rominger J, Nepf H (2008) Interaction between flow, transport and vegetation spatial structure. *Env. Fluid Mech.* **8**: 423-439.
- Luhar M, Coutu S, Infantes E, Fox S, Nepf H (2010) Wave-induced velocities inside a model seagrass bed. *J. Geophys. Res.* **115**, C12005, doi:10.1029/2010JC006345.
- Madsen JD, Chambers PA, James WF, Koch EW, Westlake DF (2001) The interaction between water movement, sediment dynamics and submersed macrophytes. *Hydrobiologia* **444**: 71-84.
- Marbà N and Duarte CM (1994) Growth response of the seagrass *Cymodocea nodosa* to experimental burial and erosion. *Mar. Ecol. Prog. Ser.* **107**: 307-311.
- Marbà N, Duarte CM, Cebrian J, Gallegos ME, Olesen B, Sand-Jensen K (1996) Growth and population dynamics of *Posidonia oceanica* on the Spanish Mediterranean coast: Elucidating seagrass decline. *Mar. Ecol. Prog. Ser.* **137**: 203-213
- Marbà N and Duarte CM (1998) Rhizome elongation and seagrass clonal growth. *Mar. Ecol. Prog. Ser.* **174**: 269-280.
-

- Marbà N, Duarte CM, Holmer M, Martinez R, Basterretxea G, Orfila A, Jordi A, Tintoré J (2002) Effectiveness of protection of seagrass (*Posidonia oceanica*) populations in Cabrera National Park (Spain). *Environment. Conser.* **29**: 509-518.
- Martone PT and Denny MW (2008) To break a coralline: mechanical constraints on the size and survival of a wave-swept seaweed. *J. Exp. Biol.* **211**: 3433-3441.
- Mateo MA, Romero J, Perez M, Littler MM, Littler DS (1997) Dynamics of millenary organic deposits resulting from the growth of the Mediterranean seagrass *Posidonia oceanica*. *Estuar. Coast. Shelf Sci.* **44**: 103-110.
- McKenzie LJ, Finkbeine MA, Kirkman H (2001) Methods for mapping seagrass distribution. In: (Short, F.T. and Coles, R.G. eds). *Global Seagrass Research Methods*. Elsevier, Amsterdam. pp. 101-121.
- Meinesz A and Hesse B (1991) Introduction of the tropical alga *Caulerpa taxifolia* and its invasion of the Northwestern Mediterranean. *Oceanol. Acta* **14**: 415-426.
- Méndez FJ, Losada IJ, Losada MA (1999) Hydrodynamics induced by wind waves in a vegetation field. *J. Geophys. Res.* **104**: 18383-18396
- Méndez FJ, Losada IJ (2004) An empirical model to estimate the propagation of random breaking and nonbreaking waves over vegetation fields. *Coast. Eng.* **51**: 103-118
- Molenaar H and Meinesz A (1995) Vegetative reproduction in *Posidonia oceanica*: survival and development of transplanted cuttings according to different spacings, arrangements and substrates. *Bot. Mar.* **38**: 313-322
- Nepf HM and Vivoni ER (2000) Flow structure in depth-limited, vegetated flow. *J. Geophys. Res.* 105(C12) **28**: 547-557, doi:10.1029/2000JC900145.
- Nielsen P (1992) *Coastal bottom boundary layer and sediment transport*. World Scientific, Singapore
- Nielsen P and Callaghan DP (2003) Shear stress and sediment transport calculations for sheet flow under waves. *Coast. Eng.* **47(3)**: 347-354
- Nortek AS (2002) *Wave measurements using the PUV method, TN-19*. Doc. No. N4000-720
-

- Orfila A, Jordi A, Basterretxea G, Vizoso G, Marbà N, Duarte CM, Werner FE, Tintoré J (2005) Residence time and *Posidonia oceanica* in Cabrera Archipelago National Park, Spain. *Cont. Shelf. Res.* **25**: 1339-1352.
- Orth RJ, Carruthers TJB, Dennison WC, Duarte CM, Fourqurean JW, Heck KL, Hughes AR, Kendrick GA, Kenworthy WJ, Olyarnik S, Short FT, Waycott M, Williams SL (2006) A global crisis for seagrass ecosystems. *Bioscience* **56**: 987-996.
- Orlowski A (1984) Application of multiple echo energy measurements for evaluation of sea bottom type. *Oceanologia* **19**: 61-78.
- Paling EI, van Keulen M, Wheeler KD, Phillips J, Dyhrberg R (2003) Influence of spacing on mechanically transplanted seagrass survival in a high wave energy regime. *Rest. Ecol.* **11**: 56-61.
- Pasqualini V, Pergent-Martini C, Clabaut P, Pergent G (1998) Mapping of *Posidonia oceanica* using aerial photographs and side scan sonar: Application off the Island of Corsica (France). *Estuar. Coast. Shelf Sci.* **47(3)**: 359-367.
- Pergent-Martini C, Rico-Raimondino V, Pergent G (1994) Primary production of *Posidonia oceanica* in the Mediterranean Basin. *Mar Biol* **120**: 9-15
- Piazzzi L, Cinelli F (1999) Developpement et dynamique saisonniere d'un peuplement mediterraneen de l'algue tropicale *Caulerpa racemosa* (Forsskal) J. Agardh. *Crytogamie Algol.* **20**: 295-300. (in French, with English Abstract)
- Piazzzi L, Acunto S, Cinelli F (1999) In situ survival and development of *Posidonia oceanica* (L.) Delile seedlings. *Aquat. Bot.* **63**: 103-112.
- Piazzzi L, Ceccherelli G, Cinelli F (2001) Threat to macroalgal diversity: effects of the introduced green alga *Caulerpa racemosa* in the Mediterranean. *Mar. Ecol. Progr. Ser.* **210**: 149-159.
- Piazzzi L, Ceccherelli G, Balata D, Cinelli F (2003) Early Patterns of *Caulerpa racemosa* recovery in the Mediterranean Sea: the influence of algal turfs. *J. Mar. Biol. Assoc. UK.* **83**: 27-29.
- Piazzzi L, Balata D, Ceccherelli G, Cinelli F (2005) Interactive effect of sedimentation and *Caulerpa racemosa* var. *cylindracea* invasion on macroalgal assemblages in the Mediterranean Sea. *Estuar. Coast. Shelf Sci.* **64**: 467-474.
-

- Preen AR, Lee Long WJ, Coles RG (1995) Flood and cyclone related loss, and partial recovery, of more than 1000 km<sup>2</sup> of seagrass in Hervey Bay, Queensland, Australia. *Aquat. Bot.* **52**: 3-17.
- Procaccini G, Buia MC, Gambi MC, Perez M, Pergent G, Pergent-Martini C, Romero J (2003) The seagrasses of the Western Mediterranean. In: (E.P. Green, F.T. Short, eds), *World Atlas of Seagrasses*, UNEP World Conservation Monitoring Centre. University of California Press, Berkeley, pp. 48-58.
- Quinn GP and Keough MJ (2002) *Experimental design and data analysis for biologists*. Cambridge University Press, pp 357
- Ratsimandresy AW, Sotillo MG, Carretero Albiach JC, Álvarez Fanjul E, Hajji H (2008) A 44-year high-resolution ocean and atmospheric hindcast for the Mediterranean Basin Developer within the HIPOCAS Project. *Coast. Eng.* **55**: 827-842.
- Riedel HP (1972) Direct measurement of bed shear stress under waves. Ph.D. thesis, Queen's University, Ont., Canada
- Ribera G, Coloreu M, Rodríguez-Prieto C, Ballesteros E (1997) Phytobenthic assemblages of Addaia Bay (Menorca, Western Mediterranean): Composition and distribution. *Bot. Mar.* **40**: 523-532.
- Riis T and Hawes I (2003) Effect of wave exposure on vegetation abundance, richness and depth distribution of shallow water plants in a New Zealand lake. *Freshwater Biol.* **48**: 75-87.
- Rivers DO, Kendrick GA, Walker DI (2011) Microsites play an important role for seedling survival in the seagrass *Amphibolis antarctica*. *J. Exp. Mar. Biol. Ecol.* **40**: 29-35
- Robertson AI and Mann KH (1984) Disturbance by ice and life-history adaptations of the seagrass *Zostera marina*. *Mar. Biol.* **80(2)**: 131-141.
- Ruitton S, Javel F, Culioli JM, Meinesz A, Pergent G, Verlaque M (2005) First assessment of the *Caulerpa racemosa* (Caulerpales, Chlorophyta) invasion along the French Mediterranean coast. *Marine Pollution Bulletin* **50**: 1061-1068.
- Ruíz GM, Fofonoff PW, Carlton JT, Wonham MJ, Hines AH (2000) Invasion of coastal marine communities in North America: Apparent patterns, processes, and biases. *Annu. Rev. Ecol. Syst.* **31**: 481-531.
-

- Sánchez-González JF, Sánchez-Rojas V, Memos CD (2011) Wave attenuation due to *Posidonia oceanica* meadows. J. Hydr. Res. In Press. doi:10.1080/00221686.2011.552464
- Scheibling RE and Melady RA (2008) Effect of water movement and substratum type on vegetative recruitment of the invasive green alga *Codium fragile* ssp. *tomentosoides*. Bot. Mar. **51**: 341-349.
- Shepherd SA and Womersley HBS (1981) The algal and seagrass ecology of Waterloo Bay, South-Australia. Aquat. Bot. **11(4)**: 305-371.
- Short FT and Short CA (1984) The seagrass filter: purification of estuarine and coastal waters. In: VC Kennedy (ed.), The Estuary as a Filter, Academic Press.
- Short FT and Wyllie-Echeverria S (1996) Natural and human-induced disturbance of seagrasses. Environ. Conserv. **23**: 17-27.
- Short FT, Davis RC, Kopp BS, Short CA, Burdick DM (2002) Site-selection model for optimal transplantation of eelgrass *Zostera marina* in the north-eastern US. Mar. Ecol. Prog. Ser. **227**: 253-267.
- Simarro G, Orfila A, Liu PLF (2008) Bed-shear stress in turbulent wave-current boundary layers. J. Hydr. Eng. Asce **134**: 225-230.
- Soares CG, Carretero JC, Weisse R, Álvarez E (2002) A 40 years hindcast of wind, sea level and waves in European waters. Proceedings of OMAE 2002: 21st International Conference on Offshore Mechanics and Arctic Engineering. Oslo, Norway.
- Stevens CL and Hurd CL (1997) Boundary-layers around aquatic macrophytes. Hydrobiologia **346**: 199-128.
- Stewart HL (2004) Hydrodynamic consequences of maintaining an upright posture by different magnitudes of stiffness and buoyancy in the tropical alga *Turbinaria ornata*. J. Marine Syst. **49**: 157-167.
- Swart DH (1974) Offshore sediment transport and equilibrium beach profiles. Delft Hydr. Lab. Publ. No 131
- Taylor WR (1960) Marine algae of the Eastern tropical and subtropical coasts of the Americas. University of Michigan Press, Ann Arbor.
-

- Teeter AM, Johnson BH, Berger C, Stelling G, Scheffner NW, Garcia MH, Parchure TM (2001) Hydrodynamic and sediment transport modeling with emphasis on shallow-water, vegetated areas (lakes, reservoirs, estuaries and lagoons). *Hydrobiologia* **444**: 1-24.
- Terrados J (1997) Is light involved in the vertical growth response of seagrasses when buried by sand?. *Mar. Ecol. Prog. Ser.* **152**: 295-299.
- Terrados J and Duarte CM (2000) Experimental evidence of reduced particle resuspension within a seagrass (*Posidonia oceanica*) meadow. *J. Exp. Mar. Biol. Ecol.* **243(1)**: 45-53.
- Terrados J and Medina-Pons FJM (2008) Epiphyte load on the seagrass *Posidonia oceanica* (L.) Delile does not indicate anthropogenic nutrient loading in Cabrera Archipelago National Park (Balearic Islands, western Mediterranean). *Scientia Marina* **72**: 503-510.
- Thibaut T, Meinesz A, Coquillard P (2004) Biomass seasonality of *Caulerpa taxifolia* in the Mediterranean Sea. *Aquat. Bot.* **80**: 291-297.
- Thomas FIM, Cornelisen CD, Zande JM (2000) Effects of water velocity and canopy morphology on ammonium uptake by seagrass communities. *Ecology* **81**: 2704-2713
- Thomas FIM and Cornelisen CD (2003) Ammonium uptake by seagrass communities: effects of oscillatory versus unidirectional flow. *Mar. Ecol. Prog. Ser.* **247**: 51-57
- Vacchi M, Montefalcone M, Bianchi CN, Morri C, Ferrari M (2010) The influence of coastal dynamics on the upper limit of the *Posidonia oceanica* meadow. *Mar. Ecol.* **31**: 546-554.
- van Katwijk MM and Hermus DCR (2000a) Effects of water dynamics on *Zostera marina*: Transplantation experiments in the intertidal Dutch Wadden Sea. *Mar. Ecol. Prog. Ser.* **208**: 107-118.
- van Katwijk MM, Hermus DCR, de Jong DJ, Asmus RM, de Jonge VN (2000b) Habitat suitability of the Wadden Sea for restoration of *Zostera marina* beds. *Helgoland Mar. Res.* **54(2-3)**: 117-128.
- van Katwijk MM, Bos AR, de Jonge VN, Hanssen LSAM, Hermus DCR, de Jong DJ (2009) Guidelines for seagrass restoration: Importance of habitat selection
-

- and donor population, spreading of risks, and ecosystem engineering effects. *Mar. Pollut. Bull.* **58**: 179-188.
- Verduin JJ and Backhaus JO (2000) Dynamics of plant-flow interactions for the seagrass *Amphibolis antarctica*: Field observations and model simulations. *Estuar. Coast. and Shelf Sci.* **50**: 185-204
- Ward LG, Kemp WM, Boynton WR (1984) The influence of waves and seagrass communities on suspended particulates in an estuarine embayment. *Mar. Geol.* **59**: 85-103
- Wicks EC, Koch EW, O'Neil JM, Elliston K (2009) Effects of sediment organic content and hydrodynamic conditions on the growth and distribution of *Zostera marina*. *Mar. Ecol. Prog. Ser.* **378**: 71-80.
- Williams SL (1984) Uptake of sediment ammonium and translocation in a marine green macroalga *Caulerpa cupressoides*. *Limnol. Oceanogr.* **29**: 374-379.
- Williams SL (1988) Disturbance and recovery of a deep-water Caribbean seagrass bed. *Mar. Ecol. Prog. Ser.* **42**: 63-71.
- Worcester SE (1995) Effects of eelgrass beds on advection and turbulent mixing in low current and low shoot density environments. *Mar. Ecol. Prog. Ser.* **126(1-3)**: 223-232.
- Wright LD and Short AD (1983) Morphodynamics of beaches and surf zones in Australia. In: (P.D. Koma, eds). *Handbook of Coastal Processes and Erosion*. CRC Press, Boca Raton, FL. pp. 35-64.
-



# Curriculum Vitae

Eduardo Infantes Oanes was born in Santander, Spain in 1976. He grew up in Lanzarote, in the Canary Islands where the passion for marine life begun. Studied the last year of high school in Denver, CO, USA. BSc (Hons) in Environmental Analysis from the University of Huddersfield, UK in 2002 and a MSc degree in Applied Marine Science from Plymouth University, UK in 2003.

In 2001 he worked for a year in Wimtec Enviromnetal Ltd, London, UK as an environmental analyst and in 2004 for two years in Sidmar Bernard Pack S.L, Alicante, Spain as a marine consultant on Puertos del Estado projects. In 2006 worked for Pharmamar S.A. in Madrid, Spain as a diving expedition member to Madagascar for one month.

In 2006 he obtained a FPI grant from the Ministerio de Educación y Ciencia to do a PhD at the Instituto Mediterráneo de Estudios Avanzados. During the PhD he spent four months at the Massachusetts Institute of Technology, USA working in a hydraulic flume on mass transport and wave attenuation by a seagrass meadow. He spent four months at the Netherlands Institute of Ecology, Netherlands, working on the effects of erosion and drag forces on seagrass seedlings using a biological flume. He also spent three months at the Horn Point Laboratory in Maryland, USA working in collaboration with Proffesor Evamaria Koch.

Eduardo has combined his scientific career with his interest in underwater photography, collecting a large amount photographic material. Winner of several underwater photography competitions in the Balearic Islands during 2008 and 2009. His photographic collection comprises images from the Mediterranean Sea, Canary Islands, East Coast-USA, Red Sea and Galápagos Islands.

## PUBLICATIONS

### Peer-Reviewed Publications

- **Infantes E**, Terrados J, Orfila A, Cañellas B, Álvarez-Ellacuaría A (2009). Wave energy and the upper depth limit distribution of *Posidonia oceanica*. **Botanica Marina** 52: 419-427. Impact Factor: 1.6, Times Cited: 9.
- Luhar M, Coutu S, **Infantes E**, Fox S, Nepf H (2010) Wave-induced velocities inside a model seagrass bed. **Journal of Geophysical Research** 115, C12005. Impact Factor: 3.3, Times Cited: 1.
- Domínguez M, **Infantes E**, Terrados J (2010) Seed maturity of the Mediterranean seagrass *Cymodocea nodosa*. **Vie et Milieu** 60: 1-6. Impact Factor: 0.47, Times Cited: 0.
- Domínguez M, Celdrán-Sabater D, Muñoz-Vera A, **Infantes E**, Martínez-Baños P, Marín A, Terrados J (2010) Experimental evaluation of the restoration capacity of a fish-farm impacted area with *Posidonia oceanica* (L.) Delile seedlings. (In Press: **Restoration Ecology**, doi:10.1111/j.1526-100X.2010.00762.x). Impact Factor: 1.93, Times Cited: 0.
- **Infantes E**, Terrados J, Orfila A (2011). Assessment of substratum effect on the distribution of two invasive *Caulerpa* (Chlorophyta) species. **Estuarine, Coastal and Shelf Science** 91: 434-441. Impact Factor: 1.88, Times Cited: 2.
- **Infantes E**, Orfila A, Bouma TJ, Simarro G, Terrados J (2011). *Posidonia oceanica* and *Cymodocea nodosa* seedling tolerance to wave exposure. **Limnology and Oceanography** 56(6) doi:10.4319/lo.2011.56.6.0000. (In Press). Impact Factor: 3.38, Times Cited: 0.

### Manuscripts under review and preparation

- **Infantes E**, Orfila A, Terrados J, Luhar M, Simarro G, Nepf H. Effect of a seagrass (*P. oceanica*) meadow on wave propagation (Submitted to **Marine Ecology Progress Series**).
- March D, Alós J, Cabanellas M, **Infantes E**, Palmer M. Probabilistic mapping of *Posidonia oceanica* cover: a Bayesian geostatistical model from drop camera system data. (Submitted to **Aquatic Botany**).

- Luhar M, **Infantes E**, Nepf H. Seagrass blade motion under waves and its impact on wave decay. (*In preparation*).
- Klaassen PC, Bouma TJ, Balke T, **Infantes E**, Van Dalen J, Temmerman S, Herman PMJ. Quantifying the critical sediment disturbance depth for seedling survival of coastal vegetations: a method. (*In preparation*).
- Terrados J, Domínguez M, Marín A, Celdrán D, Muñoz-Vera A, **Infantes E**, Martínez-Baños P. Survivorship and leaf development of *Posidonia oceanica* seedlings transplanted in a fish-farm impacted bay. (*In preparation*).

## CONFERENCES

**2009** - **Infantes E**, Terrados J, Orfila A. Substratum affinity of three Caulerpa (Chlorophyta) species. Advancing the Science of Limnology and Oceanography (ASLO). Nice, France. Poster presentation student Award.

**2008** - Terrados J, Asmus R, Herkul K, Asmus H, Box A, **Infantes E**, Kadel P, Kotta J, Crowe T. Experimental evaluation of the role of seagrasses in the resistance and resilience of sediment functioning to organic matter loading. World Conference on Marine Biodiversity. Valencia, Spain.

**2008** - **Infantes E**, Terrados J, Orfila A. Wave energy and the upper depth limit distribution of *Posidonia oceanica*. V Jornades de Medi Ambient de les Illes Balears. Mallorca, Spain.

---